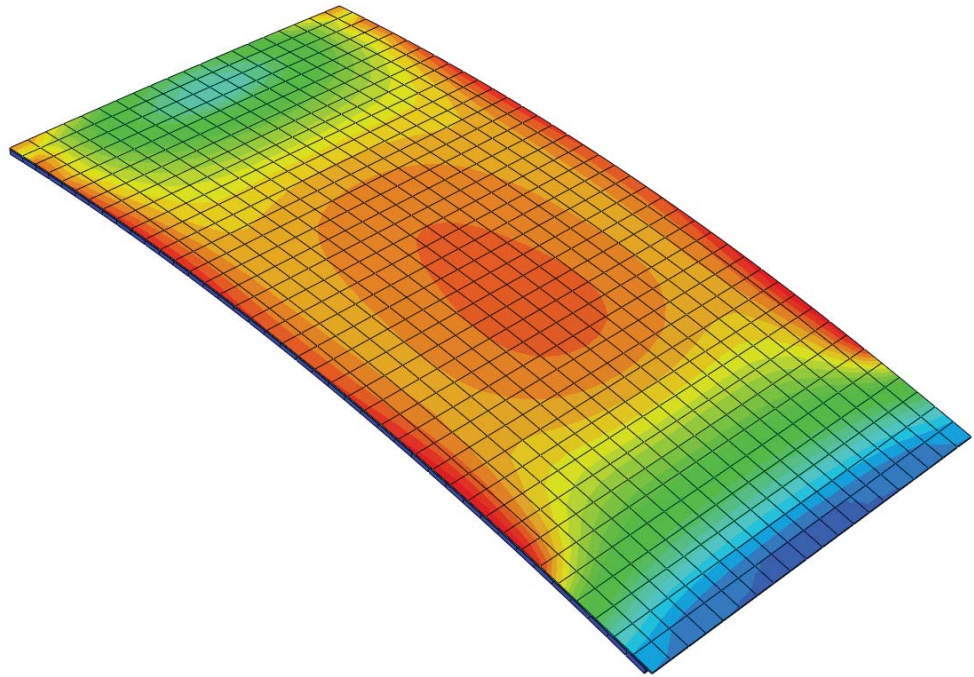




LUND
UNIVERSITY



MODELLING OF CURVED GLASS ELEMENTS

Cold-Bent Glass and Simplified Models

MOHAMAD BARADEY

Structural
Mechanics

Master's Dissertation

DEPARTMENT OF CONSTRUCTION SCIENCES
DIVISION OF STRUCTURAL MECHANICS

ISRN LUTVDG/TVSM--25/5280--SE (1-100) | ISSN 0281-6679

MASTER'S DISSERTATION

MODELLING OF CURVED GLASS ELEMENTS

Cold-Bent Glass and Simplified Models

MOHAMAD BARADEY

Supervisor: Professor **KENT PERSSON**, Division of Structural Mechanics, LTH
Examiner: **SUSANNE HEYDEN**, Associate Professor, Division of Structural Mechanics, LTH.

Copyright © 2025 Division of Structural Mechanics,
Faculty of Engineering LTH, Lund University, Sweden.

Printed by V-husets tryckeri LTH, Lund, Sweden, July 2025 (*PI*).

For information, address:
Division of Structural Mechanics,
Faculty of Engineering LTH, Lund University, Box 118, SE-221 00 Lund, Sweden.
Homepage: www.byggmek.lth.se

Abstract

Glass architecture continues to evolve with increasing demands for aesthetics, functionality, and durability. The use of curved glass elements is becoming increasingly common in modern constructions. Traditionally, curved glass is made of float glass that is heated above the glass transition temperature and formed into a curved shape. This technique is time- and energy-intensive, and consequently, relatively expensive. For this reason, other more efficient alternatives can be used, namely cold-bent glass. This means that the glass elements are bent during assembly on site without any heat treatment.

This thesis investigates the modeling and stress analysis of cold-bent glass elements, which involves elastically deforming flat glass panels on a curved frame substructure without heat, resulting in permanent intrinsic stresses throughout the panel's service life. The aim of this work is to evaluate how cold-bent glass can be modeled under intrinsic bending stresses and in combination with external loads, such as wind, using simplified models suitable for practical use, and to work out which parameters and conditions are crucial.

Both monolithic and laminated glass panels were studied using analytical methods (Euler-Bernoulli beam and Kirchhoff-Love plate theory) and validated against detailed finite element numerical simulations in Abaqus. The study focuses on glass panels with radii between 10–20 meters, and thicknesses between 6–12 millimeters, typical of architectural applications. The results show that thinner plates and larger bending radii significantly reduce internal stresses. Laminated glass with thicker PVB interlayers exhibits improved flexibility and lower peak stresses due to better strain distribution.

The study finds that simplified models can be developed to predict the stresses in glass induced by cold bending while maintaining sufficient accuracy using analytical methods, especially for simple monolithic glass, and although analytical methods have tended to slightly overpredict stresses for laminated panels, they still provide a conservative and useful tool for early design stages. Numerical methods remain essential for capturing complex effects such as edge constraints, nonlinearities, and complex interlayer behavior. Recommendations for optimal panel thickness and interlayer configurations are provided, along with suggestions for future work, including double-curved and insulated glass units.

The principle of stress superposition is found to be approximately valid for glass, which behaves elastically up to failure. Numerically, it has been shown that it is possible to superpose external loads such as stresses induced by wind with cold bending stresses by, for example, simulating a suction load in a direction opposite to the direction of the cold bending, resembling the behavior to that of wind, and then superposing the maximum principal stresses. The challenge was to approximate the wind loads on a curved structure with given constraints from the model using analytical methods,

as simplifying the model by assuming it is a flat, rectangular pane and supported on all edges, did not give the same results. In short, it is possible to superpose cold bending stresses with external load stresses, but finding a simplified analytical method to approximate the external load stresses remains unclear.

Sammanfattning

Glasarkitektur utvecklas ständigt med ökande krav på estetik, funktionalitet, och hållbarhet. Användningen av böjda glaselement blir allt vanligare i modern byggnation. Traditionellt tillverkas krökt glas av floatglas som upphettas över glasets transitions-temperatur och formas till önskad krökning. Denna teknik är tids- och energikrävande och därmed relativt kostsam. Av denna anledning används andra mer effektiva alternativ, nämligen kallböjt glas. Det innebär att glaselementen böjs på plats under monteringen utan någon värmebehandling.

Detta examensarbete undersöker modellering och spänningsanalys av kallböjda glaselement, där plana glastrutor elastiskt deformeras över en böjd ramstruktur utan uppvärmning, vilket leder till permanenta inre (intrinsiska) spänningar genom hela glaspanelens livslängd. Syftet med arbetet är att utvärdera hur kallböjt glas kan modelleras under dessa böjspänningar och i kombination med yttre laster, såsom vind, med hjälp av förenklade modeller som är praktiskt användbara, samt att identifiera vilka parametrar och villkor som är viktiga och avgörande.

Både monolitiska och laminerade glaspaneler studerades med analytiska metoder, nämligen Euler-Bernoulli balkteori och Kirchhoff-Love plattteori, och validerades mot detaljerade finita element numeriska simuleringar i Abaqus. Studien fokuserar på glaspaneler med radier mellan 10–20 meter och tjocklekar mellan 6–12 millimeter, typiska för arkitektoniska tillämpningar. Resultaten visar att tunnare plattor och större böjningsradier minskar de inre spänningarna avsevärt. Laminerat glas med tjockare PVB-folier uppvisar förbättrad flexibilitet och lägre maxspänningar tack vare en bättre fördelning av spänningarna.

Studien visar att förenklade modeller kan utvecklas för att förutsäga spänningarna i glas som uppstår vid kallböjning med tillräcklig noggrannhet, särskilt för enkla monolitiska glas med användning av analytiska metoder. Även om de analytiska metoderna tenderar att överskatta spänningarna i laminerade paneler något, är de ändå användbara som konservativa verktyg i de tidiga skedena av konstruktionen, för att t.ex. utföra preliminära analys. Numeriska metoder är dock avgörande för att fånga komplexa effekter såsom kantförhållanden, icke-linjäriteter och en mer exakt PVB beteendet i laminerade strukturer. Rekommendationer för optimal paneltjocklek och mellanskikt-konfigurationer ges, tillsammans med förslag på framtida arbete, inklusive dubbelkrökta och isolerade glaselement.

Principen om superposition av spänningar visade sig vara giltig för glas, som uppvisar elastiskt beteende fram till brott. Numeriskt har det visats att det är möjligt att superponera yttre laster, såsom spänningar orsakade av vind, med kallböjningsspänningar, till exempel genom att simulera en sugkraft i motsatt riktning mot kallböjningen, vilket efterliknar vindens påverkan, och sedan superponera de maximala huvudspänningarna. Utmaningen låg i att approximerar vindlaster på en krökt struktur med givna randvillkor i modellen med analytiska metoder, eftersom en förenkling där strukturen antas

vara en plan rektangulär ruta med stöd längs alla kanter inte gav samma resultat. Med enkla ord, det är möjligt att superponera kallböjningsspänningar med externa laster, men att hitta en förenklad analytisk metod för att uppskatta de yttre lasterna kvarstår som oklart.

Acknowledgements

First and foremost, I would like to express my sincere gratitude to my supervisor, Professor Kent Persson, for his invaluable guidance and insightful support throughout my master's thesis. I would also like to thank Professor Susanne Heyden, my examiner, for taking the time to review and assess my thesis work.

A special thanks also to the Division of Structural Mechanics for providing me an office, breakfast and many meaningful conversations with student and teacher colleagues during breaks. I would also like to express my appreciation to the teachers for their dedication and efforts, and to my fellow students for their collaboration and mutual support and helping each other out throughout the years.

Finally, I would like to thank my family, friends, and my partner for their unwavering love and support, which has motivated me throughout my entire education, as well as the challenges of this thesis.

Lund, May, 2025 Mohamad Baradey

Notations and Symbols

Latin letters

a	Length of the glass panel
b	Width of the glass panel
D	Elasticity matrix
d_i	Distance from center of each glass layer to the neutral axis
E_g	Elastic modulus of the glass
E_{int}	Elastic modulus of the interlayer
F_d	Design value of an action
f_{bk}	Characteristic value of glass strength after strengthening treatment
f_{gd}	Design value of bending strength of glass
f_{gk}	Characteristic bending strength of pre-stressed glass
G_{int}	Shear modulus of the interlayer
h	Total thickness of the glass panel
h_i	Thickness of each glass layer in laminated glass
h_{int}	Thickness of the interlayer
$h_{\text{ef,w}}$	Effective thickness for deflection calculations
$h_{\text{ef},\sigma}$	Effective thickness for stress calculations
I	Second moment of area
k_1	Coefficient from SS-EN 16612 for rectangular panes
k_e	Edge or hole finishing factor
$k_{e,p}$	Edge or hole prestress factor
k_i	Interference factor
k_{mod}	Modification factor depending on load duration
k_p	Coefficient accounting for the reduction of the process-induced prestress
k_{sp}	Surface treatment factor
L	Panel length used in code examples
M	Bending moment
M_A	Moment in direction A
M_B	Moment in direction B

n	Plies number
q	Distributed load
R	Radius of curvature
V	Shear force
w	Deflection of beam or plate
x, y, z	Cartesian coordinates

Greek letters

α	Coefficient for moment in direction A
α_T	Coefficient of linear thermal expansion
β	Coefficient for moment in direction B
γ_M	Material partial factor
γ_p	Partial factor for prestress on the surface
ε	Strain of beam or plate
η_{p2}	Adjustment factor in EET formulas for a 2-pile laminate
κ	Curvature
λ	Aspect ratio a/b
λ_A	Size-effect factor area
λ_l	Size-effect factor length (edge, hole)
ν_g	Poisson's ratio for glass
ν_{int}	Poisson's ratio for interlayer
ρ_g	Density of glass
σ	Normal stress
σ_1	Maximum principal stress
σ_{xx}	Stress in x-direction
σ_{yy}	Stress in y-direction
$\sigma_{cb,e}$	Cold bending stress from Euler-Bernoulli
$\sigma_{cb,k}$	Cold bending stress from Kirchhoff-Love
ψ	Shape factor used in laminated effective thickness
τ	Angular displacement in cylindrical coordinates

Abbreviations

CPT	Classical Plate Theory
CSG	Chemically Strengthened Glass
CSS8	Continuum Solid Shell
EBBT	Euler Bernoulli beam theory
EET	Enhanced Effective Thickness
ESG	Einscheibensicherheitsglas (Tempered Glass in German)
FEA	Finite Element Analysis
FEM	Finite Element Method
IGU	Insulated Glass Unit
NLGEOM	Nonlinear Geometry
PVB	Polyvinyl Butyral
SG	Sentry Glass
TVG	Teilvorgespanntes Glas (Heat-strengthened Glass in German)
UDL	Uniformly Distributed Load
VSG	Verbundsicherheitsglas (Laminated Safety Glass in German)

Contents

Abstract	I
Sammanfattning	III
Acknowledgements	V
Notations and Symbols	VII
Table of Contents	XII
1 Introduction	1
1.1 Background	1
1.2 Aim and Objective	1
1.3 Method	2
1.4 Limitations and future studies	2
2 Glass	3
2.1 Mechanical properties	4
2.2 Glass Treatments and Prestress	7
2.2.1 Annealed glass	7
2.2.2 Heat-strengthened Glass - TVG	7
2.2.3 Tempered Glass - ESG	8
2.2.4 Chemically strengthened Glass - CSG	9
2.3 Composite Glass Structures	9
2.3.1 Monolithic float glass	10
2.3.2 Laminated glass - VSG	10
2.3.3 Insulated glass unit - IGU	12
2.4 Geometry of Curved Glass	12
2.4.1 Single Curved Glass (Uniaxial)	12
2.4.2 Double Curved Glass (Biaxial)	13
2.4.3 Free-form Glass	15
2.5 Production of Curved Glass	16
2.5.1 Hot-bending	16
2.5.2 Cold-lamination	18
2.5.3 Cold-bending	19
3 Numerical approach	23
3.1 The Finite Element Method	23
3.2 Abaqus	23
3.2.1 Model	24

3.3	Principal Stresses in Cold Bending	32
4	Analytical approach	35
4.1	Assumptions	35
4.2	Euler-Bernoulli Beam Theory	36
4.3	Kirchhoff-Love Plate Theory	39
4.4	Curvature	42
4.5	Stresses due to Cold-bending	46
4.5.1	Euler-Bernoulli Beam Approach	47
4.5.2	Kirchhoff-Love Plate Approach	48
5	Cold Bending of Monolithic Glass	51
5.1	Influence of plate dimensions	51
5.2	Cold-Bending Stresses	54
6	Cold Bending of Laminated Glass	59
6.1	Mechanical Properties of the Interlayer (PVB)	59
6.2	Effective Thickness of Laminated Glass	61
6.3	Cold-Bending Stresses	63
6.3.1	Interlayer thickness 0.76 mm	64
6.3.2	Interlayer thickness 1.52 mm	67
7	Load combinations	71
8	Discussion	79
8.1	Monolithic Glass	79
8.1.1	Analysis of Monolithic glass cold bending behavior	79
8.1.2	Analytical limitations (h/R)	80
8.1.3	Maximum Principal Stress	83
8.2	Laminated Glass	83
8.2.1	Analysis of Laminated glass cold bending behavior	83
8.2.2	Maximum Principal Stress	86
8.3	Load Combinations	87
9	Conclusion	89
9.1	The goal of the study	89
9.2	Additional notes	91
	Bibliography	93
A	Enhanced effective thickness (EET)	97

1 Introduction

1.1 Background

Glass architecture continues to evolve with increasing demands for aesthetics, functionality, and durability. The use of curved glass elements is becoming increasingly common in modern constructions. Traditionally, curved glass is made of float glass that is heated above the glass transition temperature and formed into a curved shape. This technique is time- and energy-intensive and, consequently, relatively expensive, but allows the production of both single- and double-curved glass. For this reason, other more efficient alternatives can be used, namely cold-bent glass. This means that the glass elements are bent during assembly on site without any heat treatment. Most often, tempered float glass is used, which is gradually mounted on a curved frame. Finally, the curved panel is mechanically attached to the frame, which means that the glass is subjected to bending stresses throughout its service life. Cold-bent glass offers a sustainable and cost-effective solution by reducing the energy consumption during processing while maintaining the mechanical properties of the material. However, significant challenges remain related to the modeling and analysis of cold bent glass, as well as in combination with other loads such as wind loads and snow loads. This thesis investigates how cold-bent glass can be designed with respect to other loads and explores important and crucial parameters to develop simplified models to facilitate the design process and improve safety assessments for cold-bent glass elements.

1.2 Aim and Objective

The aim is to evaluate and develop modeling strategies and simple guidelines for cold-bent glass elements, with a particular focus on cold-bent glass, to ensure their function and durability in building applications. The study examines cold bending radii ranging from 10-20 m, and thicknesses 6-12 mm, corresponding to typical architectural applications, with particular attention to stress concentrations caused by pure bending. The possibility of superposing intrinsic and extrinsic stresses on the cold-bent glass using simple calculations is also investigated.

Issues and Research Questions:

- How can cold-bent glass be modeled and what parameters and conditions are crucial?
- Is it possible to develop simplified models that maintain sufficient accuracy for practical use?

- How should other loads be combined with the bending stresses that arise during cold bending of glass?

1.3 Method

In order to create simplified models to estimate cold-bending induced stresses in a glass plate, analytical approaches such as beam and plate theories will be used as a baseline to compare with FEA numerical approaches. The analytical results help by offering a quick, simplified, approximate check against complex numerical models, ensuring that the calculated stresses are within expected ranges.

FEA incorporates material nonlinearities, boundary effects, and interlayer interactions in laminated glass, which can be difficult to capture or predict analytically. By comparing both methods, one can assess whether FEA results deviate significantly due to secondary effects, or if it is good enough.

Once the analytical approaches have been validated, the study will explore implementing these simplified methods for combining cold bending with other loads. This will include investigating superposition techniques for intrinsic and extrinsic stresses, along with any necessary adjustment coefficients.

1.4 Limitations and future studies

In this study, the focus will be on both tempered monolithic and laminated safety glass panels, which are single-curved (monoclastic). Future studies can investigate cold bent double-curved (synclastic/anticlastic) glass panels and possibly look at the behavior of insulated glass panels (IGUs) under cold bending.

2 Glass

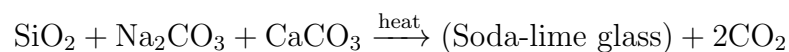
Glass is a transparent solid material that plays a key role in modern architecture by allowing natural light into buildings, offering versatile design possibilities, and enhancing indoor environments. Glass objects have been made for both practical and decorative uses since ancient times. Thanks to advances in manufacturing techniques such as the float process and improvements in large-scale coating technologies, flat glass has become a widely used construction material [1].

This so-called "float" process is where almost all flat glass products are made. The process involves the flotation of molten glass on a bath of liquid tin to create a perfect flat surface on both sides. This method is today the standard method for glass production, over 90%, and does not cause waves or distortions [2].

One of the most prevalent types of float glass is Lime Silicate Glass, which is known as Soda-lime Glass which accounts for about 90% of manufactured glass. Soda-lime glass is transparent glass that is most commonly used for windowpanes and glass containers like bottles and jars or similar. It is made from silica (SiO_2), sodium oxide (Na_2O), and calcium oxide (CaO) [3].

Chemical Reaction for Soda-Lime Glass Formation:

Soda-lime glass is manufactured by heating a mixture of silica (SiO_2), sodium carbonate (Na_2CO_3), and calcium carbonate (CaCO_3). Upon heating, the carbonates decompose into their respective oxides, (Na_2O) and (CaO), releasing carbon dioxide gas, with all the weight percentages presented in table 2.1. The resulting oxides then react to form the amorphous glass structure. The overall chemical reaction can be represented as:



During this process:

- Sodium carbonate decomposes into sodium oxide (Na_2O) and carbon dioxide (CO_2).
- Calcium carbonate decomposes into calcium oxide (CaO) and carbon dioxide (CO_2).
- Silica SiO_2 combines with sodium oxide (Na_2O) and calcium oxide (CaO) to form soda-lime glass.

Table 2.1: Chemical composition of soda lime silicate glass [4]

Chemical Name	Chemical Formula	Weight Percentage
Silica	SiO ₂	69 – 74
Lime	CaO	5 – 14
Soda	Na ₂ O	10 – 16
With small amounts of magnesium, aluminum, iron and other elements		

2.1 Mechanical properties

Glass is a stiff, elastic, and brittle material with unique mechanical properties. A material being elastic means that it can deform slightly and return to its original shape when stress is removed. However, unlike ductile materials such as metals, glass does not exhibit plasticity, which is the ability to undergo permanent deformation after the elastic limit is exceeded. As a result, glass cannot handle large strains and tends to fail suddenly without warning when stressed beyond its limit state, which characterizes its brittle nature, meaning it exhibits no ductility.

In short: materials that exhibit plastic deformation before fracture are classified as ductile, while those that fracture with little to no plastic deformation are considered brittle. The general mechanical properties of Soda Lime Silicate Glass according to EN 1900-1:2023, are presented in table 2.2.

Table 2.2: General Mechanical Properties of Soda Lime Silicate Glass EN 19100-1:2023 [5].

Modulus of elasticity	$E_g = 70\,000\text{ MPa}$
Poisson's ratio	$\nu_g = 0.23$
Coefficient of linear thermal expansion	$\alpha_T = 9 \cdot 10^{-6} 1/K$
Glass density	$\rho_g = 2\,500\text{ kg/m}^3$

Glass is much stronger in compression than in tension. This is because any small surface imperfections or cracks can easily grow under tensile stress, leading to failure. Since it has low resistance to fracture, a crack will spread quickly as soon as it forms, causing the glass to break suddenly. However, certain treatments can help to significantly improve its strength, such as pre-stressing the glass using heat-tempering. Table 2.3 shows the characteristic bending strength values for annealed and prestressed glass.

Table 2.3: Characteristic Bending Strength for Different Glass Materials According to EN 19100-1:2023 [5]

Glass material	Values for characteristic bending strength f_{gk} for annealed glass and f_{bk} for pre-stressed glass:			
	Annealed	thermally toughened safety glass	heat strengthened glass	chemically strengthened glass
float glass or drawn sheet glass	45 MPa	120 MPa	70 MPa	150 MPa

Steel, as a material, demonstrates a typical ductile response. Initially, it behaves elastically, which means that the stress is proportional to the strain, effectively, in a linear matter. After reaching the yield stress f_{yk} , it enters a plastic region where it is no longer linear and continues to deform without a significant increase in stress, eventually reaching its ultimate strength f_{gk} before undergoing ductile failure. The modulus of elasticity (stiffness) for steel is approximately 210 GPa, indicating a relatively high resistance to elastic deformation.

In contrast, glass exhibits brittle behavior. It undergoes linear elastic deformation up to its failure point without yielding. Once its strength f_{gk} is exceeded, it suddenly fractures without significant plastic deformation. Its modulus of elasticity is lower than that of steel, around 70,000 MPa, making it less stiff and more prone to breaking under stress.

This behavior can be visualized using the curves in Figure 2.1, where the glass curve cuts off at its ultimate strength, while the steel curve continues, exhibiting plastic deformation. Additionally, the glass curve has a gentler slope, indicating lower stiffness, which means that less stress is required to produce strain.

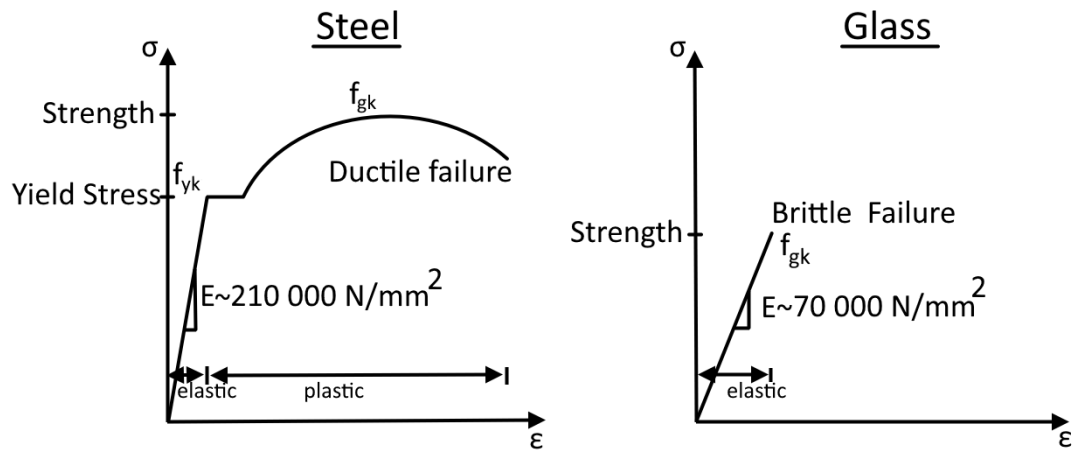


Figure 2.1: Stress-strain curves comparison for glass and steel.

Glass bending strength design value

According to prEN 19100-1:2023 [5], Annex A, Equation (A.1), the design bending strength is calculated as:

$$f_{g,d} = \lambda_A \cdot \lambda_l \cdot k_e \cdot k_{\text{mod}} \cdot \frac{k_{sp} \cdot f_{g,k}}{\gamma_M} + k_p \cdot k_{e,p} \cdot \frac{f_{b,k} - f_{g,k}}{k_i \cdot \gamma_p} \quad (2.1)$$

The term “bending strength” in EN 19100-1:2023 refers to the strength of glass components subjected to bending moments, normal forces or combinations thereof.

The parameters λ_A and λ_l are set to 1, as the glass panes considered in this study do not exceed an area of 18 m² or a side length of 6 m.

According to prEN 19100-1:2023 [5], Table A.1, the edge finishing factor k_e for annealed float glass is taken as 1, assuming polished or smoothly ground edges. Additionally, since the glass surface will remain as produced and will not undergo sandblasting, the surface profile factor k_{sp} is also set to 1 for float glass, in accordance with Table A.2.

This study accounts for stresses induced by cold-bending, snow, and wind. Therefore, the lowest modification factor k_{mod} from Table A.3 is applied, which is 0.29. However, this only applies for annealed glass, whereas in all other cases, k_{mod} is set to 1.

The heat-treatment factor k_p , which accounts for the reduction in process-induced pre-stress is set as 1 for heat treatment with horizontal process and 0.6 for vertical process (table A.4). According to SS-EN-16612-2019-EN [6] ”The presence of tong marks in vertically toughened glass reduces the effectiveness of the pre-stressing locally compared with horizontally toughened glass which has no tong marks”. The use of tongs or other devices to hold the glass during the vertical toughening in the manufacturing process, reduces its efficacy and therefore a reduction factor of 0.6 would have to be applied. As this study considers horizontally toughened glass, k_p is set to 1.

For a thermally toughened glass panel subjected to out-of-plane loading, the edge pre-stressing factor $k_{e,p}$, responsible for verifications near edges and holes and under tension, is set to 1 (table A.5). Furthermore, the interference factor k_i , which accounts for the beneficial statistical interference between the distributions of pristine glass strengths and pre-stress, is taken as 0.9 for thermally toughened glass and consequence class 3 (table A.6).

The partial factors γ_M and γ_P are chosen according to table 8.1. For persistent and transient in consequence class 3, $\gamma_M=2.0$ and $\gamma_P=1.3$.

Finally, the characteristic bending strength $f_{g,k}$ for the design of annealed basic soda-lime silicate glass is 45 N/mm², and characteristic bending strength $f_{b,k}$ for design of prestressed basic soda-lime silicate glass is 120 N/mm²

The design bending strength becomes for thermally toughened lime silicate glasses in CC3:

$$f_{g,d} = 1.0 \cdot 1.0 \cdot 1.0 \cdot 1.0 \cdot \frac{1.0 \cdot 45}{2.0} + 1.0 \cdot 1.0 \cdot \frac{120 - 45}{0.9 \cdot 1.3}$$
$$f_{g,d} = 86.6 \text{ MPa}$$

2.2 Glass Treatments and Prestress

Glass can be categorized based on its processing and treatment. Annealed glass is the most basic form, slowly cooled to relieve internal stress but breaks into sharp shards when shattered. Prestressed glass includes tempered, heat-strengthened, and chemically strengthened glass. Tempered glass is rapidly cooled after heating, making it four to five times stronger than annealed glass and breaking into small, blunt pieces for safety. Heat-strengthened glass is cooled more slowly than tempered glass, making it twice as strong as annealed glass but still breaks into sharp fragments.

2.2.1 Annealed glass

Annealed glass is ordinary float glass that has not been heat-strengthened or tempered. Annealing is the process of controlled cooling to minimize or prevent residual stress in glass. It is characterized by its flat smooth surfaces, transparency, hard wearing and compressive strength. [7].

Annealed glass is widely used in solar panel technology, car windows, building surfaces, and smart device screens, thanks to its anti-reflective and solar control properties [4]. However, annealed glass cannot be classified as "safety" glass because of its failure pattern. Annealed glass is brittle, especially due to its flaws resulting mainly by the way it is produced, e.g. in cutting and handling, and upon failure, it breaks into big sharp shards [7]. This kind of glass can be broken because of the large temperature difference, impact loading or large imposed strain. Then it splits into large pieces which are very dangerous making this type of glass prohibited in some places such as bathroom, door, fire exit or school to avoid the risk of injury [4].

Instead of annealed glass, glass classified as "safety" glass such as laminated or tempered glass comes into play and is strongly recommended for such places because of their small-piece failure pattern.

2.2.2 Heat-strengthened Glass - TVG

Heat-strengthened glass, *Teilvorgespanntes* in German (TVG), also known as semi-tempered glass, is a variety that in terms of strength and treatment lies between annealed glass and fully-tempered glass [8]. It is produced by subjecting annealed glass to a thermal cycle consisting of heating and rapid cooling that induces compressive stresses on the surface of the glass, making it tougher in compression [4]. In heat-strengthened (semi-tempered) glass, the entire glass is heated uniformly and then cooled more slowly than in fully tempered glass. This process does not create as high an internal stress as in fully tempered glass and therefore is not as strong as fully tempered glass but is more durable than annealed float glass.

It has some of the advantages of tempered glass, such as being stronger than ordinary float glass, but not by much, making it still not considered a safety glass, with strength approximately twice that of annealed glass and a similar failure pattern [8].

However, when semi-tempered glass breaks, it generally remains intact without collapsing after breaking, and that is because its cracks radiate from the source of the fracture without causing significant tangential crack propagation, making it less susceptible to spontaneous breakage and shattering into small pieces upon breakage as with fully tempered glass, which can also have poor flatness in some cases [8].

Heat-strengthened glass can not be used as monolithic, because it is not safety glass, therefore, it is often used in laminated glass or insulated glass units (IGU) [8].

2.2.3 Tempered Glass - ESG

Tempered glass, or fully tempered glass, Einscheibensicherheitsglas in German (ESG), is annealed glass that has also undergone a thermal cycle of heating and cooling, more rapidly than semi-tempering however, inducing compressive stresses on the surface of the glass and tensile stresses internally, significantly increasing its mechanical strength to approximately 4-5 times more than that of annealed float glass. [8].

The induced compressive stresses are caused by the glass surfaces contracting due to rapid cooling by air jets, whereas the inner region continues to float a while longer. When the inner region finally contracts, the surfaces subjected to compression will be balanced by tensile stresses in the inner region [9].

Glass is mainly vulnerable to tensile stresses, making it the primary cause of failure in most situations. However, toughened glass can withstand greater bending-induced deformation compared to ordinary annealed float glass. This is because the compressive stresses on its surface enable it to endure higher levels of tensile stress during bending (see Figure 2.15). If toughened glass does break, it fragments into many smaller, less dangerous pieces [9].

Fully tempered glass shatters into small, blunt-edged pieces that are unlikely to cause significant injury, making it qualify as safety glass and possible to be used as monolithic glass or in laminated glass and insulated glass units. However, the disadvantages of tempered glass include a tendency to spontaneously shatter. It is also worth noting that it has reduced flatness compared to semi-tempered and annealed glass [8].

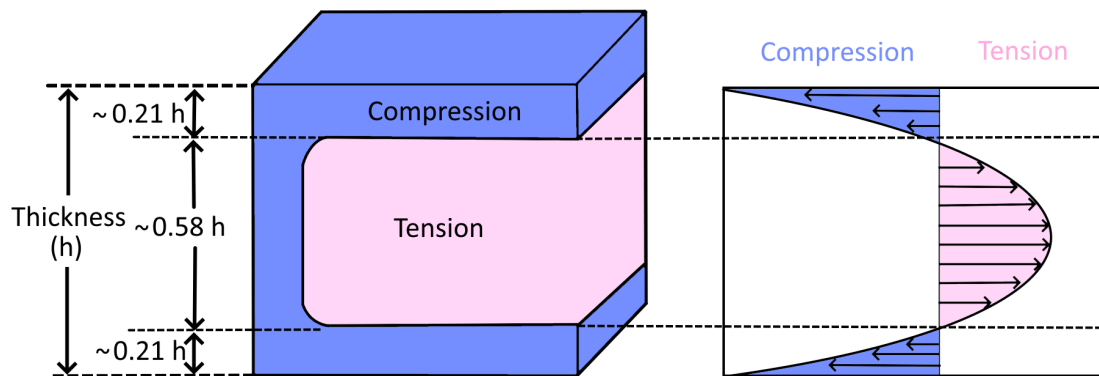


Figure 2.2: Typical through-thickness stress distribution profile in tempered glass [10].

2.2.4 Chemically strengthened Glass - CSG

Prestressing can be induced in glass using thermal methods, as described above, but also using chemical methods by immersing the glass in a chemical bath, changing the chemical composition of its surface, leading to an increase in surface compression.

The process involves immersing Soda-Lime-Silicate glass in a molten bath of potassic salt (e.g. saltpetre) at a temperature of 550°C, causing an exchange of sodium and potassium ions leading to inducing the desired stresses [11].

This occurs because of the difference in the ionic radii between K⁺ ions ($r = 0.144$ m) and Na⁺ ions ($r = 0.096$ m), having K⁺ ions use approximately 30% more room than Na⁺ ions, causes the glass surface to condense and therefore a compression zone is developed, with the maximum compression zone proportional to the maximum ion exchange rate on the glass surface. Naturally, when there is compression on the surface, tension must occur on the inside of the glass to maintain equilibrium [11].

Induced prestress from a chemical bath is superior to thermal prestress. It significantly increases the glass's mechanical strength many times over by correcting the defects on the glass surface, such as micro- or macro-cracks and notches, which could cause breakage leading to failure.

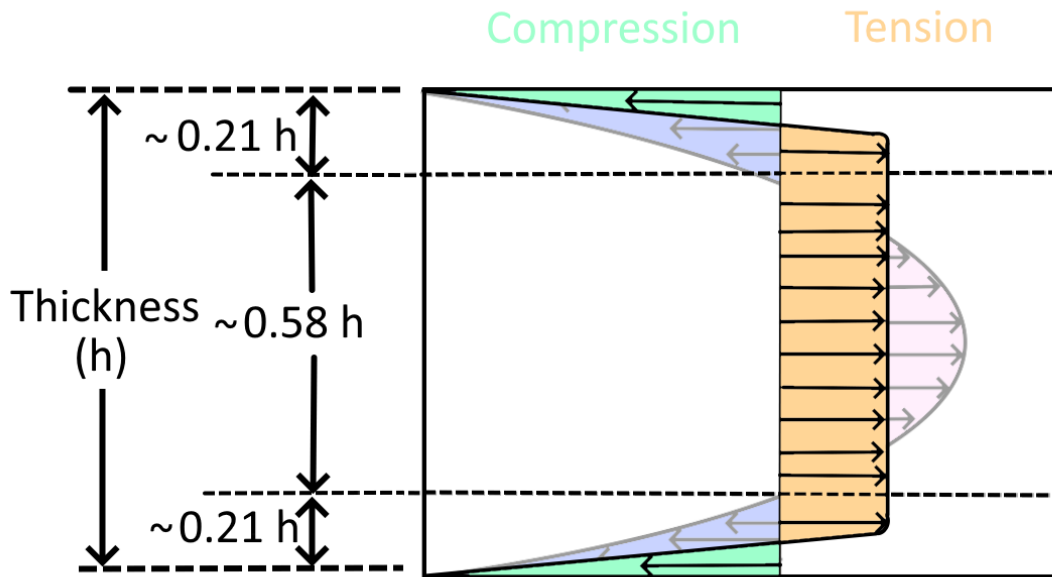


Figure 2.3: Residual stress distribution comparison of thermally and chemically pre-stressed glass [12].

2.3 Composite Glass Structures

Composite glass structures are made by combining two or more layers of glass with interlayers or spacers to enhance performance. Combining materials into these struc-

tures, such as laminated or insulated glass, offer improved safety, thermal insulation, sound reduction, durability and other benefits compared to single-pane glass.

2.3.1 Monolithic float glass

Monolithic Glass is a single solid piece of glass, as opposed to laminated or insulated glass, that consists of multiple layers. Monolithic glass is a single solid pane of glass without any lamination or layering. It can be annealed or prestressed depending on the processing. Monolithic glass is commonly used in windows, doors, and architectural applications where a single sheet of glass is sufficient. Laminated and insulated glass differs from monolithic glass in that they involve multiple layers for a purpose such as added strength, safety, or insulation.

2.3.2 Laminated glass - VSG

Laminated glass (VSG), Verbund-Sicherheits-Glas in German, is a layered glass configuration consisting of two or more glass panes that are bonded together by thin plastic interlayers, such as Polyvinyl Butyral (PVB), Ethylene-Vinyl Acetate (EVA), and Ionoplast polymers (like SentryGlass Plus) and Thermoplastic Polyurethane (TPU). Laminated glass is regarded as a safety glass, that is because laminated glass does not shatter during failure and holds itself together, reducing risk of injury. This happens because the pieces stick to the interlayer.

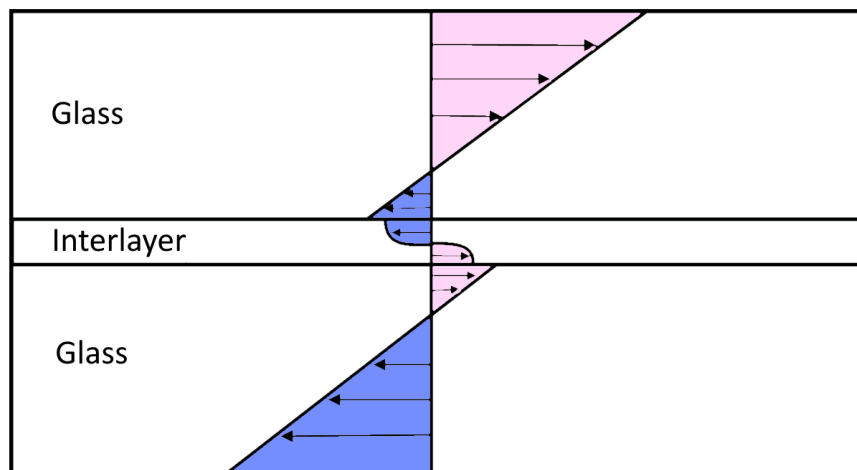


Figure 2.4: Stress distribution of a laminated glass panel.

Laminated glass was invented in 1903 or, rather, accidentally discovered by a French chemist, Édouard Bénédictus, inspired by a laboratory accident, where a glass flask had become coated with plastic cellulose nitrate, and when it fell, it shattered, but did not break into pieces [13]. This accident is what inspired today's laminated safety glass. Today, it can be made from regular annealed (float) glass and semi- or fully tempered glass for increased safety.

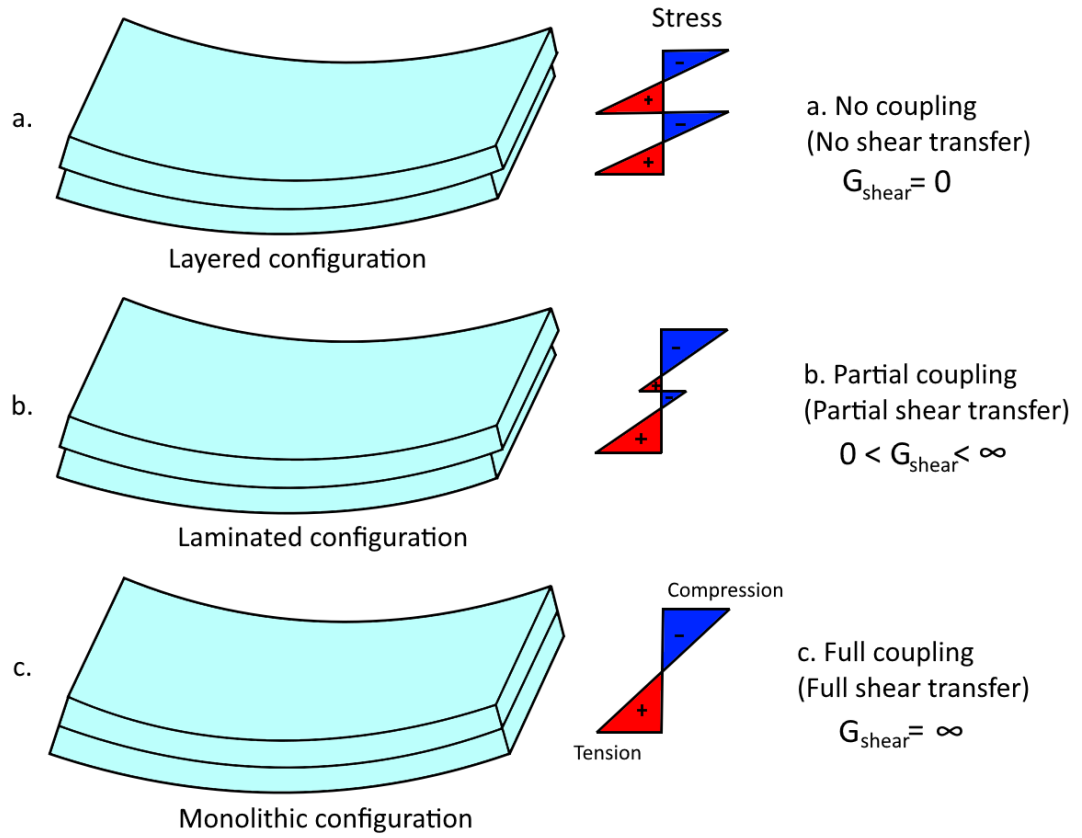


Figure 2.5: Stress profile for (a) layered configuration, (b) Laminated configuration, (c) Monolithic configuration.

Interlayer

There are many types of interlayer, with the most common one being the PVB interlayer. The plastic interlayers exhibit time- and temperature-dependent viscoelastic properties. The stiffness highly depends on the load duration and the temperature. It behaves non-linearly, however, it can be modeled as a linear elastic material, which will be further investigated on later in section 6.1. The modulus of elasticity for interlayers can vary a lot depending on temperature, duration of load, and type of interlayers. The general mechanical properties of the PVB-interlayer are shown in Table 2.4.

Table 2.4: General Mechanical Properties of PVB-interlayer [14]

Modulus of elasticity	$E_{int} = 0.1\text{-}100 \text{ MPa}$
Poisson's ratio	$\nu_{int} = 0.45\text{-}0.50$

The interlayers have the same transparency as glass and come in many sizes and colors,

which is how laminated glass is made in different colors. PVB interlayers, for example, come in sizes starting from 0.38 mm as a simple layer, and increasing in multiples of 0.38 mm, such as 0.76 mm, 1.14 mm, 1.52 mm, 1.90 mm, 2.28 mm, etc. [15]. For example, two layers (0.76 mm), four layers (1.52 mm), or for special applications, six layers (2.28 mm) can be combined.

2.3.3 Insulated glass unit - IGU

Insulated glass units (IGUs) have multiple panes separated by a gas-filled space for thermal insulation. Coated glass includes low-emissivity (Low-E) glass, which improves energy efficiency, and reflective glass, which reduces glare and heat gain.

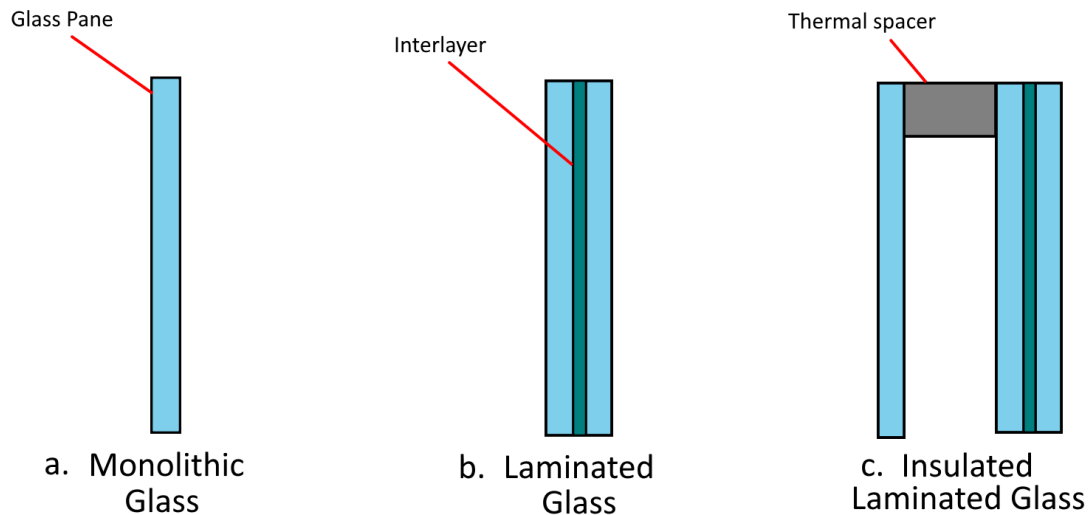


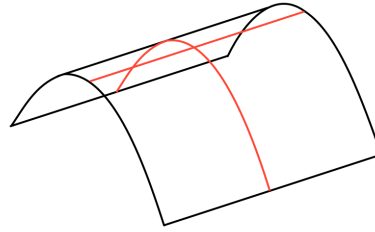
Figure 2.6: Cross-section comparison of (a) Monolithic Glass, (b) Laminated Glass with interlayer, and (c) Insulated Laminated Glass with thermal spacer [16].

2.4 Geometry of Curved Glass

2.4.1 Single Curved Glass (Uniaxial)

Single-curve or Monoclastic surfaces are defined by a single curve that causes a structure to bend in one direction, along one axis. This type of curvature forms a cylindrical surface, whereas curvatures in other directions remain unchanged. The term "mono" in Latin means one or single, referring to the single curvature, and "clastic" refers to its shape change.

Monoclastic



Monoclastic (or uniaxial) surfaces are single curved surfaces, characterised by only bending in one direction at a time.

Figure 2.7: Single Curved (Uniaxial) Glass Panel [17].

Single curve Monoclastic glass is popular and widely used, particularly in exterior windows and curtain walls, store and mall fronts, custom residential glazing and interior partitions, merchandise display cases, cylindrical elevator enclosures, skylights, even insulated, bullet resistant and security glazing can be curved [18].

This bending method is relatively easier and simpler to perform when it comes to calculations, time consumption and costs, when compared to more complex geometries. It can be achieved with either hot bending or cold bending, which will be expanded on later in the next subchapter.

However, there are some limitations. A curved glass panel typically exhibits greater stiffness along the direction of the curvature due to geometric stiffening, causing the structure to have weaker performance perpendicular to the curve [19]. It lacks geometric flexibility to match surfaces that have a curvature in two directions [20].

2.4.2 Double Curved Glass (Biaxial)

Double-curved, or biaxial, glass bending involves shaping the glass along two axes, creating curvature in two directions. This type of bending encompasses both synclastic and anticlastic forms, which differ in the relationship between their curvatures.

Derived from Greek, "syn" means "same" and "anti" means "opposite". A synclastic surface curves in the same direction along two principal axes, making the curvature is positive in both directions (positive Gaussian curvature). In contrast, an anticlastic surface curves in opposite directions, one axis curves upward, and the other curves downward (negative Gaussian curvature).

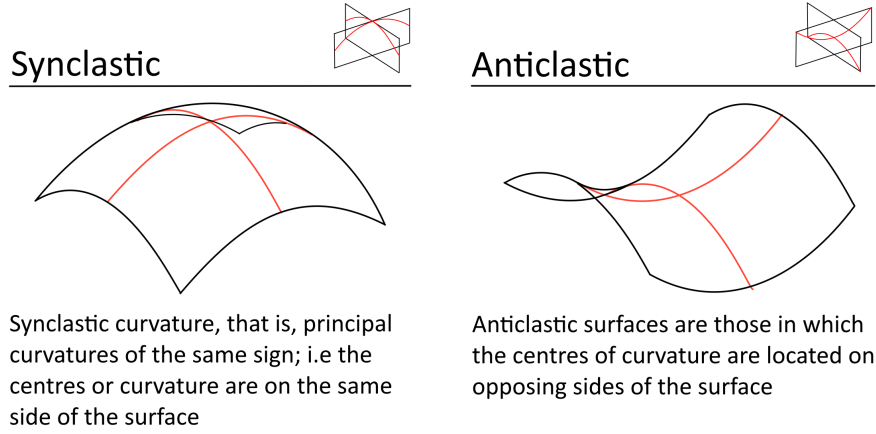


Figure 2.8: Double Curved (Biaxial) Glass Panel [17].

The Gaussian curvature K , defined as the product of the two principal curvatures κ_1 and κ_2 (i.e., $K = \kappa_1 \cdot \kappa_2$), can be either positive or negative. When the Gaussian curvature is negative, the surface is referred to as anticlastic, which forms hyperbolic paraboloids (saddle shapes). In contrast, if the curvature is positive, the surface is known as synclastic, typically represented by circular paraboloid shapes (dome shapes) [21].

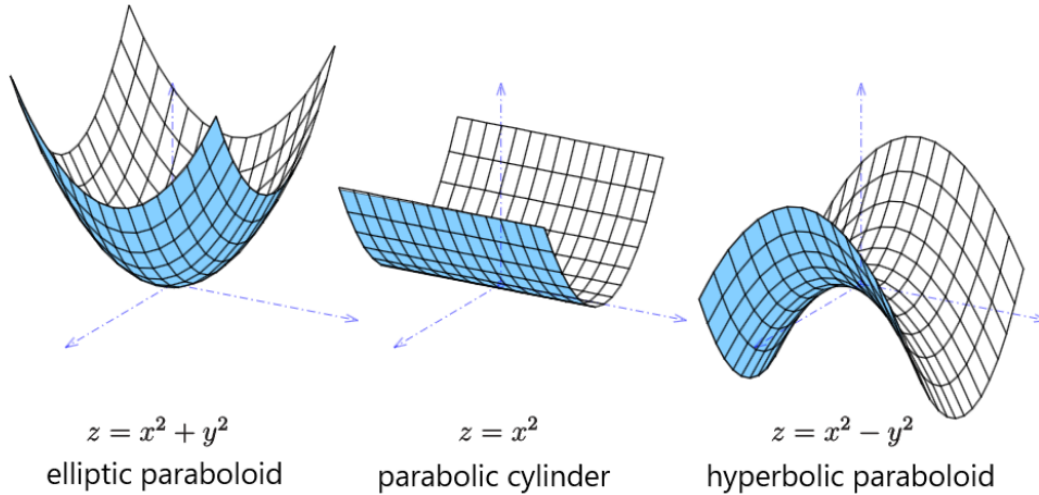


Figure 2.9: Schematics of different paraboloids [22].

Double curved glass pane can be achieved with hot bending. Double curved glass is mostly desired in glazing, which refers to glass panels used in buildings, particularly in windows, facades or architectural structures [23]. Double curved cold bent glass can be achieved by single curving the glass along the axis that goes from corner to corner, effectively by fixing one corner and bending from the other corner. However, this is still classified as a single curve bend, despite the glass being double curved. Double curved glass achieved by bending it along two separate axes is impossible to accomplish with cold bending.

In contrast to single-curve glass, double-curve glass has a better ability to distribute loads more evenly. Since a structure exhibits greater stiffness along the direction of a curvature, it would cause the structure to have a higher stiffness along both bending directions.

2.4.3 Free-form Glass

Free-forming of glass refers to the free curving and formation of glass into complex shapes instead of being limited to a single or double curve. The process involves hot bending, which will be touched on later in 2.5.1, where the glass sheets get heated to around 600°C until they became pliable. The glass gets then slumped into molds, shaping them to the desired geometry. After forming, the glass can be laminated, sometimes with colored interlayers to achieve both aesthetic and performance qualities. These techniques allow for greater design freedom, enabling the production of intricate and customized glass components.

Emporia, a landmark shopping center in Malmö's Hyllie district in Sweden, exemplifies the application of glass free-forming in contemporary architecture. Each of the 804 glass panes was uniquely shaped and custom-made, laminated with colored interlayers to achieve the desired hues and transparency. The supporting steel structures were assembled with tolerances within one millimeter to ensure a seamless integration of the glass panels.



Figure 2.10: The glass façade of Emporia shopping mall in Malmö, Sweden, exemplifies free-form glass architecture [24].

The free-form glass structure at Xujiahui Commercial Center in Shanghai is another example, featuring fluid curves that defy traditional architectural limits. Its dynamic design highlights the versatility of glass free-forming in modern construction.



Figure 2.11: Free-Form Glass Structure at Xujiahui Commercial Center in Shanghai, China [25].

2.5 Production of Curved Glass

2.5.1 Hot-bending

Hot bent glass is a popular method of curving glass that involves curving glass using heat, and is essential in our modern architectural design. It gives manufacturers more flexibility to create a wider range of shapes, allowing for non-cylindrical designs and tighter radius. It also enables free-forming without the downside of causing internal stresses that could weaken the glass [26]. The pane retains the precise shape of the mould and yields no inherent stress distribution [23].

Hot bending involves heating the glass (around 600-700 °C) until it becomes viscous, then shaping it using a mold or specialized bending equipment. Once formed, the glass can either be allowed to gradually cool, allowing the shape to set without enhancing its strength (gravity hot-bending) [27], or rapidly cooled down/quenched (heat-treated hot-bending)

Gravity Hot-Bending

Bending can be based solely on gravity, meaning its own self-weight (see Figure 2.12), or can also be assisted in which a mechanical bending press forces the glass into a target shape. The shape is then slowly cooled to avoid any residual tension build-up in the glass [26].

Hot bending allows producers to obtain a wider range of glass shapes, for example, a tighter radius and non-cylindrical shapes. However, this process does not add mechanical strength to the glass nor the ability to tolerate temperature variations [26].

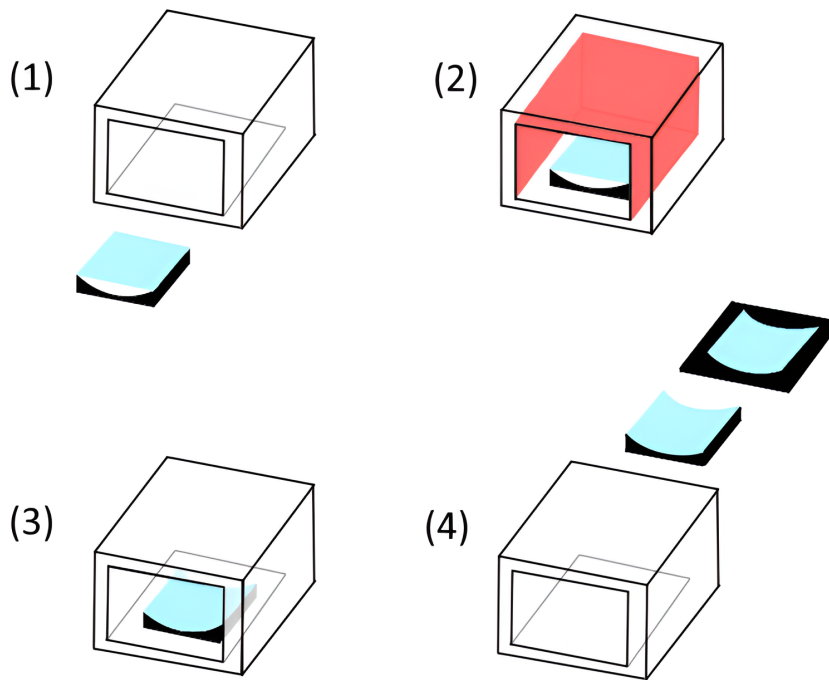


Figure 2.12: Stages of gravity-based hot bending of glass (1) Flat glass placed on mould, (2) Heated to 600°C, (3) Glass deforms into mould under gravity, (4) Curved glass cools gradually [28].

Heat-treated or Tempered Hot-Bending

Normally, annealed or heat-strengthened glass is desired. For this reason, we can conduct so-called heat-treated/tempered hot-bending glass. It involves a controlled cooling process that is carried out with a high temperature gradient (also known as rapid cooling) [21], which is similar to the process used for normal tempering or heat-strengthening of flat glass. The key difference in the tempering furnace is that there is a flexible area (a mold) that allows the glass to be shaped while it is being heated, before it is tempered by being quenched (rapidly cooled with high-pressure air) and set into its final form [28] (see Figure 2.13).

Meaning, the glass is bent during heat treatment in a furnace, and then later rapidly cooled down, which either fully tempers or heat-strengthens the glass at the same time.

Nowadays, the hot bending and rapid cooling process to create tempered hot-bent glass is carried out in the same furnace [21].

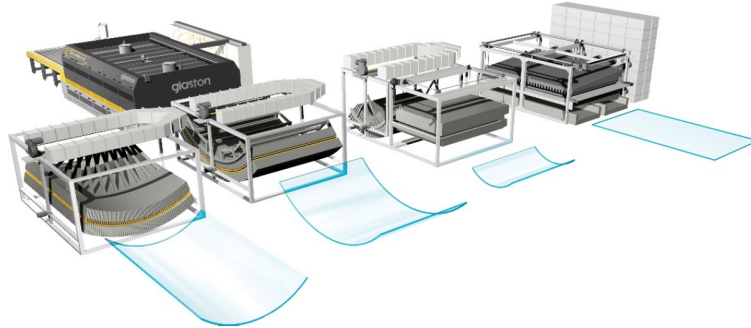


Figure 2.13: Multiple stages of the glass hot bending process, including heating, shaping, and quenching. Source: Glaston (www.glaston.net) [26].

It is far quicker than the gravity bending process, but it raises the challenge of potential optical distortions, typically created during the heating or rapid quenching/cooling stages. In addition, only concave and cylindrical shapes can be produced when certain coatings are used [28].

There are a few other drawbacks. Hot-bent glass is typically more expensive due to its demanding production process. Heating the glass past its transition temperature requires substantial energy as well as resources, since each unique shape for a sub-part requires a custom mold [23]. It also has reduced safety due to the larger and sharper shards it creates when broken. These issues may make it worthwhile to explore alternative options [29].

2.5.2 Cold-lamination

In contrast to hot bending, cold bending offers engineers two different approaches. Namely, cold lamination and plain elastic cold bending. Cold lamination is a process that involves gradually bending a flat glass panel into a curved shape while laminating them with a polymer interlayer under heat and pressure, which helps distribute stress and stabilize the curved shape. In prEN19100-2:2023, the lamination bending is described as a process in which glass is curved by cold bending and then laminated to retain the shape [30]. The glass will then retain its curved shape permanently without requiring external force. The key difference is that the glass itself is not thermally softened where it reaches a viscous state to be reshaped, as in hot bending. Instead, it is mechanically forced into shape and held there while the lamination process secures it in place [23]. The glass is cold bent and laminated in the same process, instead of cold bending an already laminated glass panel.

The process begins with stacking of polymer layers in between flat glass panes and then cold bent into shape using a bending device of some sort. While held in this curved

form, they are placed under autoclave conditions, where heat and pressure facilitate bonding between the glass and the polymer. After the polymer hardens, the glass retains its curved geometry, although a minor spring-back effect may occur overtime due to the elasticity of the polymer [23]. The process ends with a curved laminated safety glass as the final product.

As with hot-bent glass, cold-laminated curved glass must be transported in its final bent form, considering that it is prefabricated, resulting in higher transportation costs compared to standard flat glass. To avoid these costs, elastic cold bending can offer a more cost-effective option as well as an energy-effective option where no heating is required.

2.5.3 Cold-bending

In the context of cold bending, glass does not initially stand out as a suitable option. The general consensus is that glass is a weak and brittle material without any strength capabilities, giving the impression that it is not something that can be bent without instantly breaking. The claim that glass is a brittle material is correct; however, the perception of glass being weak is generally a misunderstanding. Glass is stronger than what is perceived as shown in figure 2.1, when compared to steel.

Over the last few decades, there has been an increasing amount of research and projects surrounding glass with many codes and standards emerging, establishing methods for determining the tensile bending strength of glass as shown in section 2.1, as well as FEM software, making investigating the boundaries of the material more accessible. [31].

The cold bending of glass is a process of elastically bending glass components at ambient temperatures to permanently achieve a desired shape. It is a relatively recent technique for creating curved glass plates [32, 30]. Cold bending is achieved by mechanically bending a glass panel and fixing it onto a curved frame substructure without heating or laminating. Whilst cold lamination holds the reaction forces through a lamination process, this approach maintains the glass in a constant state of elastic deformation, by being obliged to a supporting structure using clamps or strips to hold down the edges or corners in place as shown in figure 2.14, which induces continuous internal stresses.

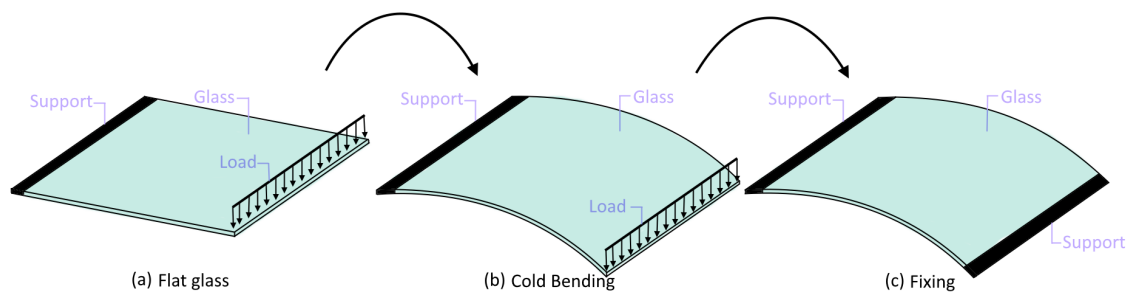


Figure 2.14: The process of cold bending glass [32].

A substructure is a structure that permanently supports the glass component, such as clamps, point fixing, line bearing, and the curved frame used for cold bending, ensuring the desired shape of the glass through mechanical constraints (point and / or linear support), which needs to handle the restraint forces induced by cold bending [30].

Cold lamination results in a more stable and low-stress final product, whereas elastic cold bending is more economical and energy efficient where transportation costs can be avoided by making it on site and with a small amount of equipment (see figure 2.14). It is also flexible since it can be used on flat glass (either monolithic or laminated safety glass) or an insulating glass unit, in contrast to cold lamination, which as the name suggests, is only applicable on laminated glass. The interlayer in laminated glass also helps absorb some of the stress, making the bending process more manageable [23]. Cold bending makes the glass more susceptible to extrinsic stresses. Extrinsic stresses are stresses within the glass that result from external loads and deflections other than cold bending, while intrinsic stresses result from cold bending [30].

Because cold bent glass experiences permanent intrinsic stresses, the use of tempered glass is therefore better suited than annealed or regular float glass because its residual compressive stresses counteract the internal tensile stresses introduced during cold bending, as shown in figure 2.15, increasing its safety and performance. In general, both cold bending and cold lamination use tempered and heat-strengthened glasses, which have undergone a heat treatment process that creates surface compression and internal tension. This makes them harder to bend compared to annealed glass or float glass; however, they still provide increased strength and safety benefits and are therefore still used in cold bending. During cold bending, the glass can be carefully curved within the elastic limit to prevent breakage, despite the surface compression making it more difficult to bend. When carefully controlled, it provides a more straightforward and efficient method for producing curved glass shapes while avoiding some of the challenges associated with traditional methods [23].

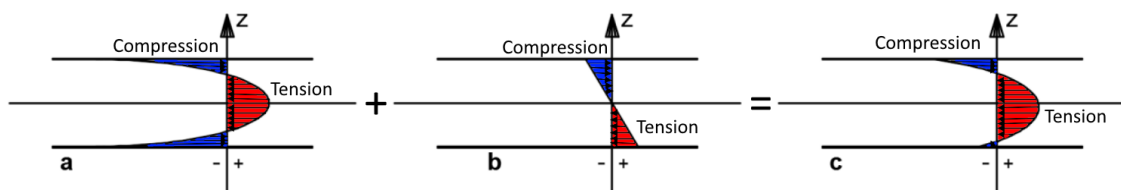


Figure 2.15: (a) Residual tempering stresses, (b) Cold bending stress, (c) Sum of (a) and (b) [21].

Not only is cold bending energy and cost efficient, it also does not affect the optical quality of the glass from its flat state because, unlike hot-bent glass, where local warping can occur and viscous flow is not required [32, 23].

Cold-bent glass is limited by geometric conditions, its bending strength, and the partial shear transfer or shear coupling effect of the interlayers in the case of laminated glass (see section 2.3.2). See Figures 2.16 and 2.17 for examples of real-life applications of glass cold bending.



Figure 2.16: IAC Headquarters in New York [33].



Figure 2.17: Strasbourg Ville station in France [34].

3 Numerical approach

3.1 The Finite Element Method

In engineering mechanics, most physical phenomena are described using differential equations. However, these problem are often too complex to be solved using traditional analytical approaches. The finite element method (FEM) offers a numerical approach for obtaining approximate solutions to such equations.

These differential equations apply to a specific region, which may be one-, two-, or three-dimensional. A fundamental aspect of FEM is that instead of trying to approximate the solution across the entire region at once, the region is divided into smaller, manageable sections called finite elements. The solution is then approximated within each of these smaller elements. For example even if a variable changes in a complex, non-linear way throughout the region, it may be reasonably approximated as changing linearly within each individual element. The group of all these elements forms what is known as the finite element mesh (see Figure 3.10) [35].

Once the type of approximation to be used in each element is chosen, the behavior of each element can be determined. This is feasible because of the simplicity of the assumed behavior within each element. After analyzing the elements individually, they are assembled using specific rules to represent the entire region. This process ultimately yields an approximate solution for the overall behavior of the system [35].

3.2 Abaqus

Abaqus is a Finite Element Analysis (FEA) software that is designed to assist engineers in simulating complex real-world problems for various industries, such as construction, and relies on it for advanced engineering models and simulations [36].

Abaqus provides a wide range of element and material models, enabling the simulation of nearly any geometry, regardless of complexity. It allows stress and deformation analysis for both isotropic and anisotropic materials under varying temperatures and strain rates. The software's material library includes:

- Metals and reinforced concrete
- Rubber and polymers (e.g., Polyvinyl butyral, PVB),
- Geotechnical materials like soil and rock
- Ceramics and crushable or resilient foam

Beyond the materials mentioned above, Abaqus also handles glass structures effectively, including laminated glass panels with their complex interlayer behavior. The software offers stress analysis which reliably models stress distributions and concentrations, making it well suited for analyzing how stresses develop in both monolithic and laminated glass components. Its capabilities will therefore prove useful for examining the mechanical behavior of cold-bent glass during deformation, as well as identifying critical stress zones.

Abaqus offers two main solvers for different types of simulations, Abaqus/Standard, for linear and nonlinear finite element analysis and Abaqus/Explicit for highly Nonlinear Transient Events [36].

Abaqus/Standard is a general-purpose implicit solver that uses matrix inversion and iterative methods, making it ideal for static or slow dynamic problems like structural bending, thermal stress analysis, and quasi-static nonlinear analyses. It is suitable for stress analysis of bent glass panels, laminated glass interlayer behavior, and long-duration creep studies.

In contrast, Abaqus/Explicit employs explicit time-step integration to handle high-speed dynamic events like impacts, blasts, or severe discontinuities (e.g., fracture). It would be suitable for simulating glass fracture from impacts or safety assessments of shattered laminated glass, for example. While Standard prioritizes accuracy for smooth, slow phenomena, Explicit specializes in transient, highly nonlinear events [36].

3.2.1 Model

The research focuses on performing stress analysis on a static model of cold bent glass panels. Therefore, Abaqus/Standard is the most suited solver where no dynamic events are involved.

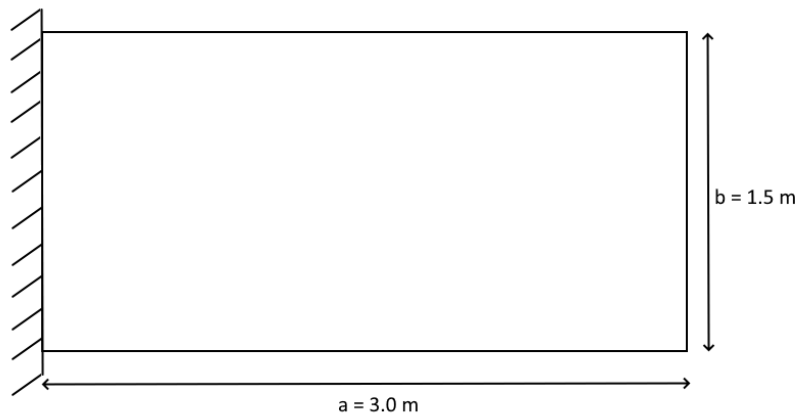


Figure 3.1: Schematic and boundary conditions of the model

Model Description

A cold bent glass unit usually consists of a glass panel, and a frame of some sort, usually a metal like aluminum or steel. For this study, a simple model of a glass panel measuring 3.0 m x 1.5 m (Figure 3.1) is used with varying thicknesses, where the panel is fixed on one of the short edges and cold bent uniaxially (single curve), from the other free short edge, resembling a cantilever beam, on top of a fixed, thin, and curved frame-like substructure with the cross-sectional area 2 mm x 2 mm, which stretches along the two long edges of the panel. The goal is to force the glass panel into the shape of the frame to match its curvature with a fixed radius as shown in Figure 3.2. Since deformations of the frame were not of interest during the analysis, it was modeled as a rigid body.

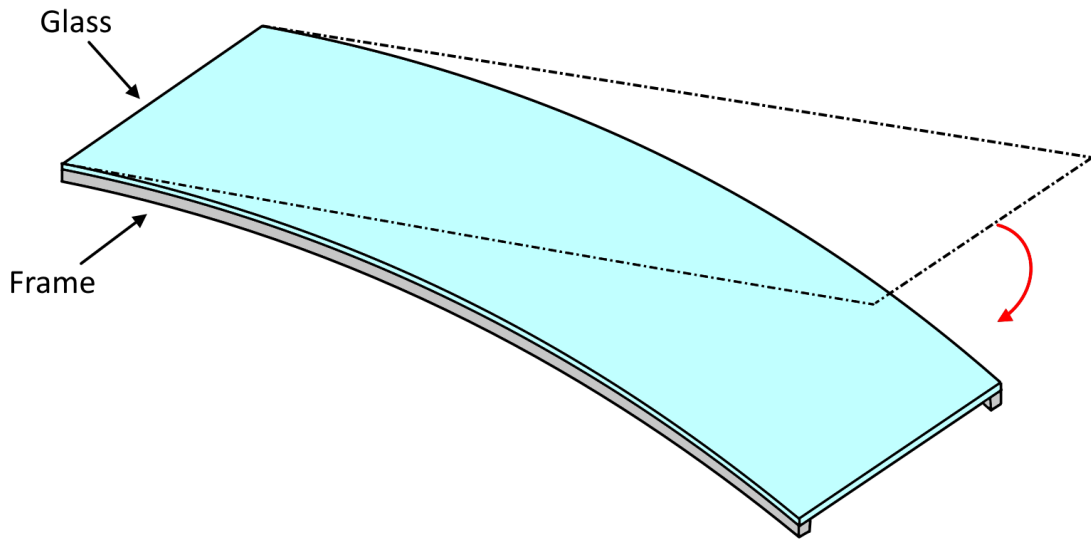


Figure 3.2: 3D Monoclastic Cold Bending Model

Loads and Boundary conditions

In order to simulate uniaxial cold bending, a displacement on one of the edges needs to be defined. However, the displacement should not be purely vertical (in the z -direction). The edge should follow a cylindrical path, as demonstrated in Section 4.4, by curving on top of a curved frame substructure.

To make this work properly in Abaqus, a cylindrical coordinate system was utilized, consisting of the parameters: angular displacement τ , radius R , and height Z , in contrast to classical Cartesian coordinates (x,y,z) (see Figure 3.3).

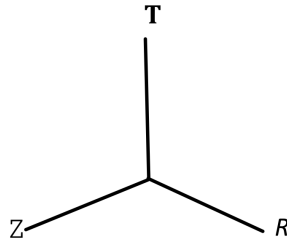


Figure 3.3: A Cylindrical coordinate system.

The displacements U1, U2, and U3 would then represent R , τ , and Z . The displacement boundary condition is applied to the angular displacement τ , which corresponds to the displacement U2 in Abaqus (see Figure 3.4).

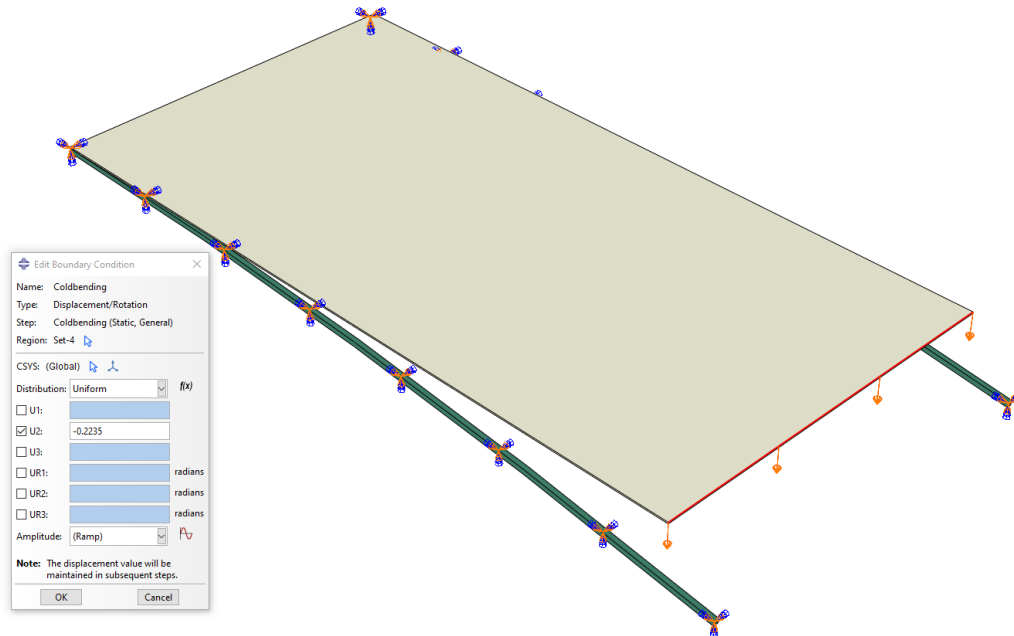


Figure 3.4: Displacement boundary condition applied in the U2 direction, corresponding to τ .

This will allow the displacement defined on the edge to stay perpendicular to the edge's

surface and follow along the cylindrical curve during the entire process. If you displace the edge purely straight down (Z -direction only) without accounting for the curved path that the glass will naturally follow, you artificially force in-plane stretching, which can create unrealistically high stresses. The cylindrical coordinates approach will ensure more accurate and realistic bending of the glass plate and will simulate the correct stresses. The angular displacements used for each radius are shown in Table 3.1.

Table 3.1: The angular displacement τ for a certain radius R

Radius R [m]	Angular displacement τ [radians]
10	0.443
15	0.298
20	0.224

Figure 3.5 showcases the glass panel's initial state, the curved frame, and the angular displacement.

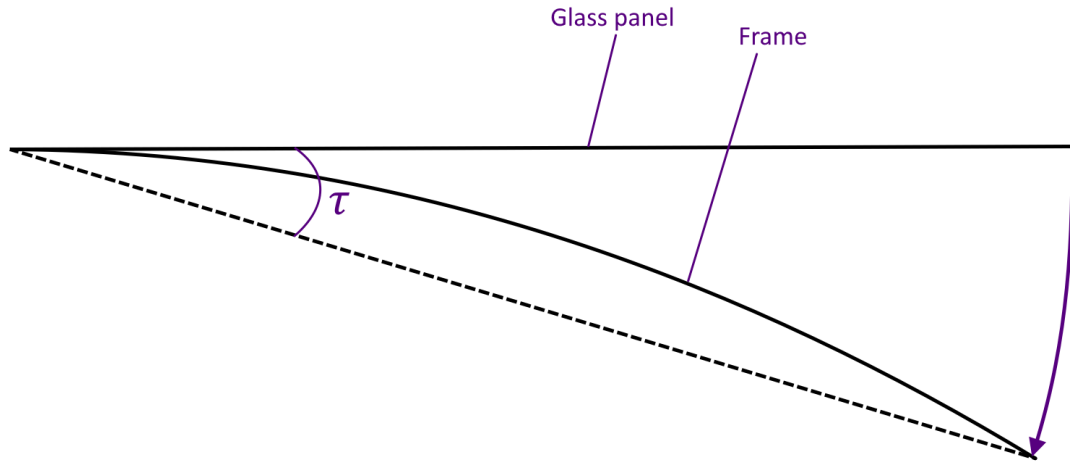
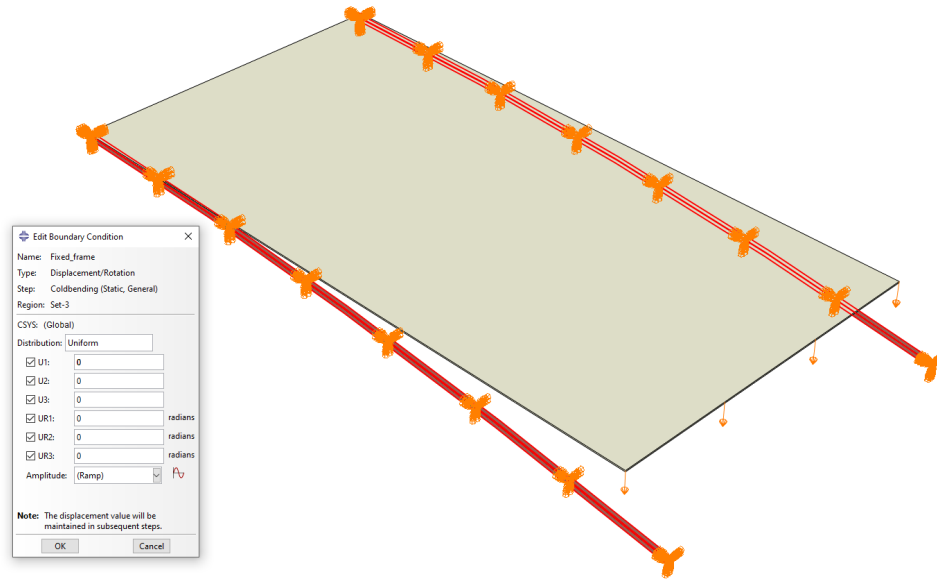
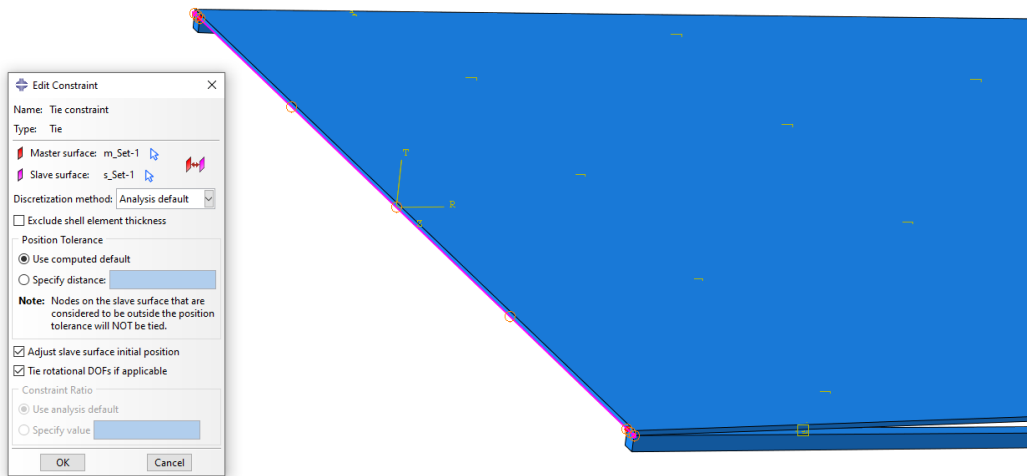


Figure 3.5: 2D showcase of the curvature τ .

While the cold bending displacement is on one of the short edges, the other short edge is tied to the frame substructure, which is fixed in place ($U_1, U_2, U_3, UR_1, UR_2, UR_3 = 0$), making the tied short edge clamped, as shown in Figure 3.6.



(a) Frame substructure boundary conditions



(b) Tie constraint between edge and frame.

Figure 3.6: Material properties of each part of the models.

Parts and Element Type

The glass and PVB were modeled as solid parts. Because glass and PVB have large differences in Young's moduli, bending in laminated glass creates sharp changes in stress in some regions, meaning highly discontinuous. The shell elements fail to capture these discontinuities in the stress distribution [9]. For the cold bending analysis of thin glass plates, the Continuum Solid Shell (CSS8) element type was chosen, which are first-order, 8-node elements. CSS8 elements are ideal for thin materials, including composites, such as laminated glass, when a full 3D stress-strain response is needed. They are more effective than standard 3D elements in bending situations with high aspect ratios [37]. Using continuum solid-shell elements to model shell-like solids also provides greater accuracy than conventional shell elements, which are limited to 2D plane stress behavior as described in "Shell elements: overview," Section 23.6.1 and 21.4.2 of the ABAQUS Analysis User's Manual [38, 39].

These elements use only displacement degrees of freedom and are fully compatible with regular solid elements, which were used in this thesis for better accuracy. They are good for modeling layered composite structures (laminated glass), by considering different material properties in each layer. They maintain full 3D constitutive laws, meaning that stress is correctly predicted across the thickness. Unlike full 3D solid models, which require many elements in the thickness direction, solid-shell elements only need one element per material layer but use multiple integration points inside each layer to capture variations in stress. This allows an advantage in computational efficiency, since one element per layer is needed, and still gives accurate predictions of stress distribution in glass bending, while being simpler to implement than full 3D models.

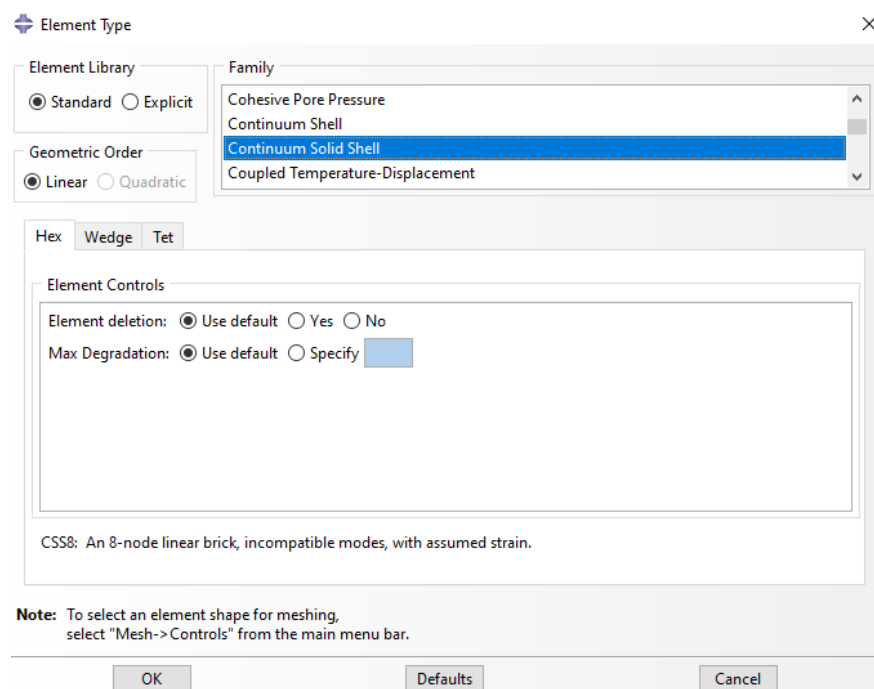


Figure 3.7: Continuum Solid Shell (CSS8) Element Type in Abaqus.

Material

All the materials are modeled as linear elastic, including the viscoelastic PVB Interlayer, as explained in section 6.1. The curved frame substructure is modeled as a steel material, with the material properties shown in Figure 3.2. It would also have been sufficient to model it as a rigid body and exclude it from the analysis as it is not covered in this study.

Table 3.2: Material Properties of Glass, PVB Interlayer, and Steel Frame

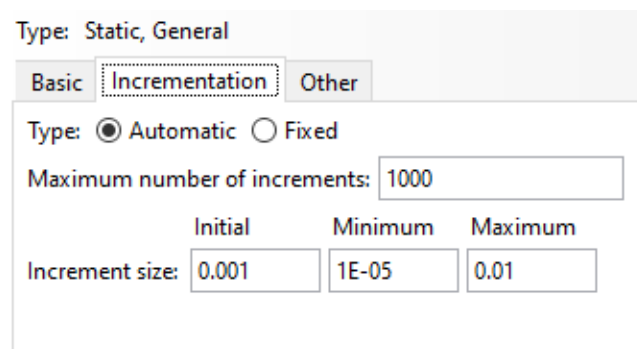
Material	Young's Modulus (Pa)	Poisson's Ratio
Glass	7.00×10^{10}	0.23
PVB Interlayer	2.98×10^5	0.49
Steel Frame	2.10×10^{11}	0.30

NLGEOM

According to prEN 19100-2:2023 D.4.1 General design principles, while analytical models can be used for simple and small deformation shapes, geometrically non-linear finite element (FE) models, should be used for more complex shapes and higher magnitudes of deformation [30]. In this study, NLGEOM = ON is used in Abaqus regardless of the magnitude of the deformation to ensure greater accuracy.

Increments

A Static, and general analysis step was used with an initial increment size of 0.001, a minimum of 1E-05, and a maximum of 0.01 to ensure gradual and accurate analysis. Up to 1000 increments were allowed, which is more than sufficient.



The image shows the 'Incrementation' tab of the 'Type: Static, General' dialog box in Abaqus. The 'Type' is set to 'Automatic' (selected with a radio button). The 'Maximum number of increments' is set to 1000. The 'Increment size' is defined by three input fields: 'Initial' (0.001), 'Minimum' (1E-05), and 'Maximum' (0.01).

Figure 3.8: Incrementation settings.

Mesh

A convergence analysis was conducted on a 1.5 x 3.0 m monolithic glass panel with a thickness of 6 mm curved with a radius of 15 m.

The mesh sizes used for the analysis are: 0.05, 0.075, 0.125, 0.15, and 0.25 m, with a reference line along the center of the plate to investigate the suitable mesh size. It is favorable to identify an appropriate mesh size beyond which further refinement does not significantly improve the accuracy of the results; this is called convergence analysis. This keeps the analysis both reliable and computationally efficient, avoiding unnecessary increases in computational time without meaningful gains in accuracy.

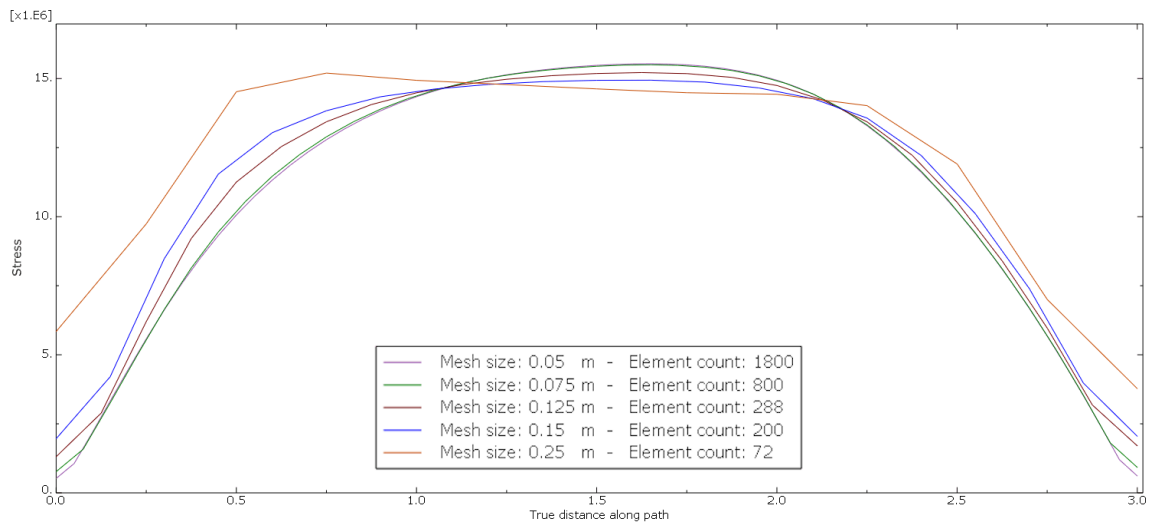
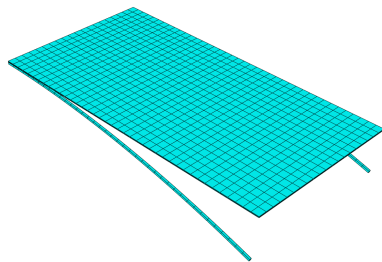
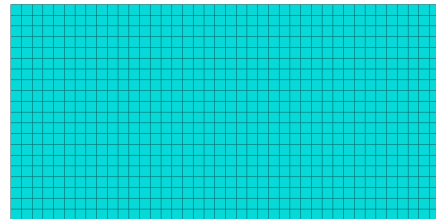


Figure 3.9: Convergence analysis for various mesh sizes and element count.

It was concluded that beyond the 0.075 m mesh size, there was no further improvement in accuracy, or in other words, convergence occurs. This is visualized in Figure 3.9, which showcases stress on the y-axis and distance along the center line path on the x-axis for various mesh sizes and their respective element count.



(a) Mesh of the entire model.



(b) Mesh of the glass plate model.

Figure 3.10: Showcase of model finite element mesh.

3.3 Principal Stresses in Cold Bending

When investigating the strength of the glass, it is important to observe the highest stresses, which would be the maximum principal stresses. The maximum principal stresses are the largest normal stresses acting on a material at a specific point, occurring along particular directions where shear stress is zero. They represent the maximum tensile or compressive stress the material experiences, and in this case the tensile stresses. The way it is obtained is by rotating the coordinate system so that only normal stresses remain, and all the shear stresses are zero. In this specific orientation, the stress vector aligns with the surface's normal vector, meaning that they point in the same direction. This direction is referred to as the principal stress direction, and the corresponding magnitude of the stress vector is also known as the principal stress value [40].

There are three principal stress values, as shown in Figure 3.11b, the first, second, and third principal stress, σ_1 , σ_2 , and σ_3 . These values are often called the Maximum, Intermediate, and Minimum Principal Stress, respectively [40].

The maximum principal stresses can be analytically calculated by first determining the angle of rotation φ , in radians, between the global and principal axes:

$$\varphi = \frac{1}{3} \cos^{-1} \left(\frac{2I_1^3 I_2 + 27I_3}{2(I_1^2 - 3I_2)^{3/2}} \right) \quad (3.1)$$

Where I_1 , I_2 , and I_3 are stress invariants, which are determined by the following equations [40]:

$$I_1 = \sigma_{xx} + \sigma_{yy} + \sigma_{zz} \quad (3.2)$$

$$I_2 = \sigma_{xx}\sigma_{yy} + \sigma_{yy}\sigma_{zz} + \sigma_{zz}\sigma_{xx} - \sigma_{xy}^2 - \sigma_{yz}^2 - \sigma_{zx}^2 \quad (3.3)$$

$$I_3 = \sigma_{xx}\sigma_{yy}\sigma_{zz} - \sigma_{xx}\sigma_{yz}^2 + \sigma_{zz}\sigma_{xx} - \sigma_{xy}^2 - \sigma_{yz}^2 - \sigma_{zx}^2 \quad (3.4)$$

Finally, the first principal stress, that is, the maximum principal stress, is determined by the following:

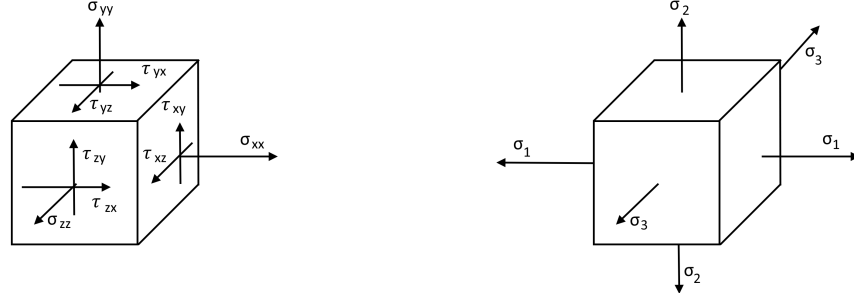
$$\sigma_1 = \frac{I_1}{3} + \frac{2}{3} (\sqrt{I_1^2 - 3I_2}) \cos(\varphi) \quad (3.5)$$

The glass panel in this study was single curved in the x-direction. This means that the largest tensile stresses induced by cold bending should occur in the x-direction too. This is realized by observing the results shown in Table 8.1.

In Abaqus, S11 represents the normal stress in the x-direction, denoted as σ_{xx} , and "Max. Principal" corresponds to the maximum principal stress, denoted as σ_1 .

The maximum principal stress will be very close to σ_{xx} (or S_{11}) provided that:

- The stress in the other directions (σ_{yy} , σ_{zz}) are much smaller.
- Shear stresses (τ_{xy} , τ_{xz} , τ_{yz}) are negligible or zero.



(a) Normal and shear stresses in 3D space

(b) The three principal stresses σ_1 , σ_2 , σ_3

Figure 3.11: Illustration of normal, shear and principal stresses.

If the stress state is predominantly uniaxial tension in the x-direction, then we can conclude that the maximum principal stress and S_{11} (or σ_{xx}) are nearly the same with slight deviation and, therefore, is a reasonable approximation:

$$\sigma_1 \approx \sigma_{xx} = S_{11} \approx \sigma_{cb,e/k}$$

However, since there is a slight deviation between the two, in this study, the component S_{11} (or σ_{xx}) will be the one compared to the analytical methods and to evaluate their precision. The maximum principal stress will still be used to investigate load combinations later on in chapter 7, and the approximation established in this section will be utilized.

4 Analytical approach

4.1 Assumptions

The Euler-Bernoulli beam theory and Kirchhoff-Love plate theory, are based on several simplifying assumptions to model the behavior of beams under bending loads [41, 42].

- Thin plates and no thickness changes: the in-plane plate dimensions are large compared to the thickness. The plate is also inextensible in the transverse direction, which means that, its thickness remains constant during deformation.
- Cross-section is infinitely rigid in its own plane: Loads that act transversely to the longitudinal axis and pass through the shear center eliminating any torsion or twist. This means that the cross-section does not deform significantly in its own plane under the applied loads, assuming it to be infinitely stiff and not undergo any warping or twisting.
- Cross-section remains plane and perpendicular to the longitudinal deformed beam / plate axis during bending.
- The material of the glass plate is linear elastic, homogeneous, and isotropic and has a constant Young's modulus in all directions in both compression and tension: This assumption means that the material behaves according to Hooke's law, meaning that stress is proportional to strain, and that the material's properties are uniform in all directions. It also assumes that the material is not subject to residual stresses or imperfections.
- Self-weight of the plate has been ignored and should be taken into account in practice.
- The neutral plane is subjected to zero axial stress and does not undergo any change in length.
- The response to strain is one-dimensional stress in the direction of bending.
- Deflections are assumed to be relatively small compared to the overall length of the beam.
- Membrane stresses and strains are neglected.
- Transverse shear is neglected: The theory assumes that shear stresses acting perpendicular to the plate's surface have negligible effects.

4.2 Euler-Bernoulli Beam Theory

Euler-Bernoulli beam theory (EBBT) is one of the most basic and elementary theories that describes the relationship between the beam's deflection and the applied load. It covers cases corresponding to small deflections or slopes of a beam that is subjected to lateral loads and provides a simplification of the linear theory of elasticity since it ignores the effects of shear deformation, rotatory inertia, and deformations in other directions other than the bending direction along the beam's length. The fundamental assumptions of the Euler-Bernoulli beam equation are as follows [35]:

- The beam section is infinitely rigid in its own plane. There is no deformation in the plane of the cross-section.
- The cross-section of the beam remains plane to the deformed axis of the beam
- The cross-section remains normal to the deformed axis of the beam

The Linear elasticity theory describes how solid materials deform under applied forces, assuming a linear relationship between stress and strain. It is based on Hooke's law, which states that stress is proportional to strain within the elastic limit of the material. This means that when a force is applied, the deformation is reversible, and the material returns to its original shape once the load is removed. The theory is valid for small deformations, where geometric changes are negligible, and for homogeneous, isotropic materials, where properties are uniform in all directions. Linear elasticity forms the basis for Euler-Bernoulli beam theory and, mathematically, it is expressed as [35]:

$$\sigma = E\varepsilon \tag{4.1}$$

A small infinitely small segment of a beam is considered with:

- Vertical shear force V
- Bending moment M
- Distributed load q

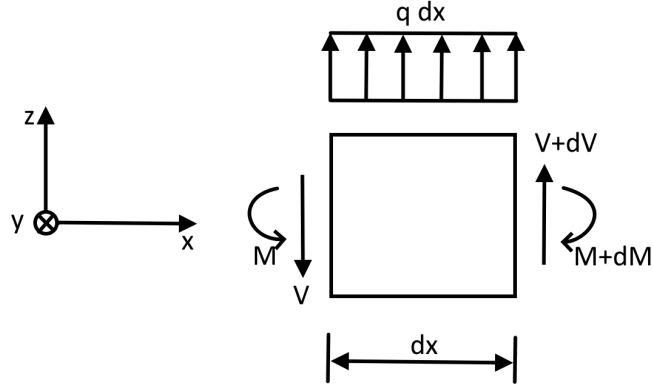


Figure 4.1: Infinitely small part of beam [35]

Vertical equilibrium in the undeformed state obtained from figure 4.1:

$$q dx - V + (V + dV) = 0$$

$$\frac{dV}{dx} = -q$$

Moment equilibrium about the left end:

$$M + q \frac{dx}{2} dx + (V + dV) dx - (M + dM) = 0$$

Since $q dx$ and dV are infinitesimal, they go to zero:

$$\frac{dM}{dx} = V$$

Combining vertical and moment equilibrium:

$$\frac{d^2 M}{dx^2} + q = 0$$

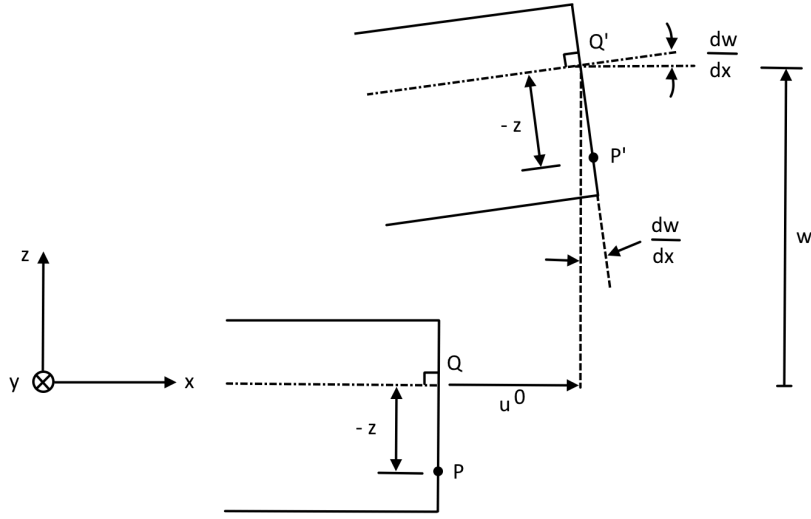


Figure 4.2: Deformation of Bernoulli beam [35]

Kinematic relations using deformation of a Bernoulli beam as shown in figure 4.2:

$$u_x = u^0 - z \frac{dw}{dx}$$

$$u_y = 0 \quad (\text{assumption, } u^0 = u^0(x) \text{ and } w = w(x), \text{ only depends on } x)$$

Strain relation:

$$\varepsilon_{xx} = \frac{du_x}{dx} = \frac{du^0}{dx} - z \frac{d^2w}{dx^2}$$

$$\varepsilon_{yy} = \varepsilon_{zz} = \gamma_{xy} = \gamma_{yz} = \gamma_{xz} = 0$$

Assuming Hooke's law, isotropic material, and note that the only nonzero strain is ε_{xx} , we get the following:

$$\begin{bmatrix} \sigma_{xx} \\ \sigma_{yy} \\ \sigma_{zz} \end{bmatrix} = \frac{E}{(1+\nu)(1-2\nu)} \begin{bmatrix} 1-\nu & \nu & \nu \\ \nu & 1-\nu & \nu \\ \nu & \nu & 1-\nu \end{bmatrix} \begin{bmatrix} \varepsilon_{xx} \\ 0 \\ 0 \end{bmatrix}$$

Since the cross-section is undeformed, $\nu = 0$, we get linear elasticity:

$$\sigma_{xx} = E\varepsilon_{xx} \tag{4.2}$$

Substituting the strain expression:

$$\sigma_{xx} = E \left(\frac{du^0}{dx} - z \frac{d^2w}{dx^2} \right)$$

Bending moment equation:

$$M = \int_A \sigma_{xx} z dA$$

Substituting σ_{xx} :

$$M = \int_A E z \left(\frac{du^0}{dx} - z \frac{d^2w}{dx^2} \right) dA$$

Choosing the vertical position of the x-axis so that:

$$\int_A E z dA = 0$$

$$M = -\frac{d^2w}{dx^2} \int_A E z^2 dA$$

If E is constant:

$$M = -\frac{d^2w}{dx^2} EI \tag{4.3}$$

Using the moment-equilibrium equation:

$$\frac{d^2M}{dx^2} + q = 0$$

Substituting M we get the Euler–Bernoulli equation:

$$-\frac{d^2}{dx^2} \left(EI \frac{d^2w}{dx^2} \right) - q = 0 \tag{4.4}$$

4.3 Kirchhoff-Love Plate Theory

Kirchhoff Love plate theory, also known as the classical plate theory (CPT), is a method used to analyze the behavior of thin plates under various loads. It simplifies

the three-dimensional plate analysis into two-dimensional, making it easier to solve. It relies on several key assumptions to simplify the analysis of thin plates. Essentially, it treats the plate as a two-dimensional surface element with a midplane and focuses on the bending behavior of the plate [43].

The fundamental assumptions of the Kirchhoff-Love plate equation are as follows [35, 42]:

- No thickness changes
- No transverse shear
- Linear in-plane stress distribution
- Parabolic transverse shear stress distribution
- Straight lines perpendicular to the mid-surface before deformation remain straight and normal after deformation

We begin with the general stress-strain relationship for an isotropic and homogeneous plate [35]:

$$\sigma = D\varepsilon - D\varepsilon_0$$

where ε_0 represents initial strains (e.g., thermal strains). In this case, we assume no initial strains $\varepsilon_0 = 0$ and thus, the equation simplifies to:

$$\sigma = D\varepsilon = zD\kappa = zD^*\nabla w$$

For an isotropic material, the stress-strain relationship in matrix form is:

$$\begin{bmatrix} \sigma_{xx} \\ \sigma_{yy} \\ \sigma_{xy} \end{bmatrix} = \frac{E}{1-\nu^2} \begin{bmatrix} 1 & \nu & 0 \\ \nu & 1 & 0 \\ 0 & 0 & \frac{1}{2}(1-\nu) \end{bmatrix} \begin{bmatrix} \varepsilon_{xx} \\ \varepsilon_{yy} \\ \varepsilon_{xy} \end{bmatrix}$$

Where:

$$\kappa = \nabla^* w \begin{bmatrix} \frac{\partial^2}{\partial x^2} \\ \frac{\partial^2}{\partial y^2} \\ 2\frac{\partial^2}{\partial x \partial y} \end{bmatrix}$$

And:

$$\varepsilon = z\kappa = z\nabla^* w \begin{bmatrix} \frac{\partial^2}{\partial x^2} \\ \frac{\partial^2}{\partial y^2} \\ 2\frac{\partial^2}{\partial x\partial y} \end{bmatrix}$$

We get that for small deformations, the strain-displacement relations are given by:

$$\varepsilon_{xx} = z\frac{\partial^2 w}{\partial x^2}, \quad \varepsilon_{yy} = z\frac{\partial^2 w}{\partial y^2}, \quad \varepsilon_{xy} = z\frac{\partial^2 w}{\partial x\partial y}$$

Substituting these into the stress equation:

$$\begin{bmatrix} \sigma_{xx} \\ \sigma_{yy} \\ \sigma_{xy} \end{bmatrix} = \frac{zE}{1-\nu^2} \begin{bmatrix} 1 & \nu & 0 \\ \nu & 1 & 0 \\ 0 & 0 & \frac{1}{2}(1-\nu) \end{bmatrix} \begin{bmatrix} \frac{\partial^2 w}{\partial x^2} \\ \frac{\partial^2 w}{\partial y^2} \\ \frac{\partial^2 w}{\partial x\partial y} \end{bmatrix}$$

To determine the maximum stress, we evaluate it at $z = \frac{h}{2}$. After performing the necessary matrix operations, we arrive at:

$$\begin{bmatrix} \sigma_{xx} \\ \sigma_{yy} \\ \sigma_{xy} \end{bmatrix} = \frac{Eh}{2(1-\nu^2)} \begin{bmatrix} \frac{\partial^2 w}{\partial x^2} + \nu\frac{\partial^2 w}{\partial y^2} \\ \nu\frac{\partial^2 w}{\partial x^2} + \frac{\partial^2 w}{\partial y^2} \\ (1-\nu)\frac{\partial^2 w}{\partial x\partial y} \end{bmatrix}$$

where h is the thickness of the plate.

Expression for σ_{xx} :

$$\sigma_{xx} = \frac{Eh}{2(1-\nu^2)} \left(\frac{\partial^2 w}{\partial x^2} + \nu\frac{\partial^2 w}{\partial y^2} \right)$$

Expression for σ_{yy} :

$$\sigma_{yy} = \frac{Eh}{2(1-\nu^2)} \left(\nu\frac{\partial^2 w}{\partial x^2} + \frac{\partial^2 w}{\partial y^2} \right)$$

This will be useful later on to derive the cold-bending stress equation.

4.4 Curvature

Curvature measures how much a curve or surface bends. It indicates the deviation from flatness, which means the deviation from a straight line (beam) for a 2D curve or a flat plane (plate) for a 3D surface. A straight line has zero curvature, while a tight bend has a high curvature.

In the context of beam and plate bending, the deflection $w(x)$ represents vertical displacement at any point x . Its first derivative, $\frac{dw}{dx}$, gives the slope at any point x , indicating how steep the curve is, which is the ratio of vertical change to horizontal change. The second derivative, $\frac{d^2w}{dx^2}$, represents the rate of change in slope, showing concavity. Curvature, denoted as $\kappa(x)$, measures how sharply the curve bends and is according to Ottosen and Petersson (1992), Introduction Finite Element Method [35], given by:

$$\kappa(x) = \frac{|w''(x)|}{(1 + (w'(x))^2)^{3/2}} = \frac{\frac{d^2w}{dx^2}}{\left[1 + \left(\frac{dw}{dx}\right)^2\right]^{3/2}} \quad (4.5)$$

which depends on both the slope and its rate of change. To obtain the curvature equation for a cold-bent glass, we first have to understand how these concepts tie together in the geometry of a circle and start with the circle's equation. A circle with a radius R centered at $(0,0)$ has the following equation:

$$x^2 + y^2 = R^2 \quad (4.6)$$

where R is the radius. Since y describes the vertical position or coordinates of a point on a circle, and in the case of a beam bending into a circular arc, this vertical position is equivalent to the deflection, it follows that y and w represent the same quantity in this context and therefore can be written as:

$$x^2 + w^2 = R^2.$$

Solving for $w(x)$ in the upper half of the circle, we get the following deflection equation:

$$w = \sqrt{R^2 - x^2}.$$

If we want to bend a glass panel into a circular shape, we need to position it so that its initial flat state aligns with the top of the desired arc. To achieve this, we imagine the glass panel starting as a horizontal line at $y = R$ in a circle, where one edge is fixed, and the other edge is free to move downward. The bending process forces the panel from the free edge to follow a circular (cylindrical) arc, which means that it deforms to match part of a larger circle.

The free edge follows the circular arc of the circle centered at $(0, R)$ and stops when the glass panel rests on the arc of the circle centered at $(0, 0)$ (see Figure 4.3).

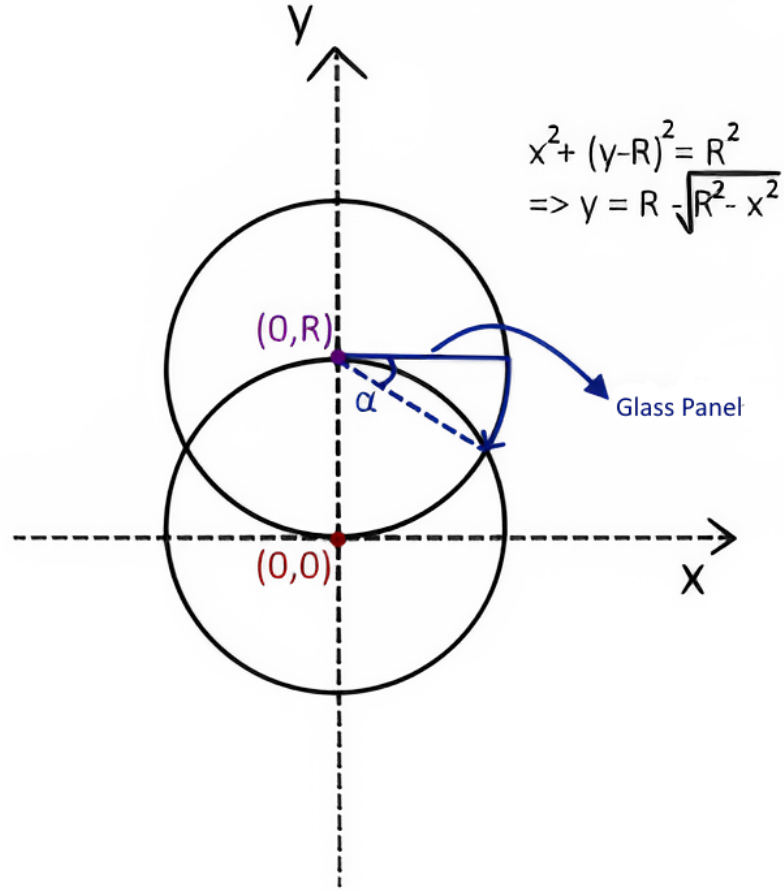


Figure 4.3: Demonstration of the circle equation.

The key to describing this mathematically is placing the center of this circle at $(0, R)$, ensuring that the curved shape naturally forms below this point. The equation of a circle with radius R centered on $(0, R)$ is the following:

$$x^2 + (y - R)^2 = R^2$$

Solving for y gives

$$y = R - \sqrt{R^2 - x^2}$$

which represents the new bent shape of the glass. Since we are interested in the deflection from the original flat position at $y = R$, we define the deflection function as

$$w(x) = R - \sqrt{R^2 - x^2}$$

This function describes deflection, how much the glass moves downward at any point along its length due to bending, following a smooth and continuous curve determined by the circular arc.

To find the slope, we take the first derivative ($\frac{dw}{dx}$), we get it by first differentiating both sides using the chain rule,

$$\frac{dw}{dx} = \frac{1}{2}(R^2 - x^2)^{-1/2} \cdot (-2x),$$

which simplifies to the slope equation:

$$\frac{dw}{dx} = -\frac{x}{\sqrt{R^2 - x^2}}. \quad (4.7)$$

Now we differentiate again to find the slope's rate of change by obtaining the second derivative of the deflection $w(x)$

$$\frac{d^2w}{dx^2} = \frac{d}{dx} \left(-\frac{x}{\sqrt{R^2 - x^2}} \right)$$

Using the quotient rule, where $f(x) = -x$ and $g(x) = \sqrt{R^2 - x^2}$, we get

$$\frac{d^2w}{dx^2} = \frac{(-1) \cdot \sqrt{R^2 - x^2} - (-x) \cdot \frac{-x}{\sqrt{R^2 - x^2}}}{(R^2 - x^2)}$$

Simplifying the numerator:

$$\frac{d^2w}{dx^2} = \frac{-\sqrt{R^2 - x^2} - \frac{x^2}{\sqrt{R^2 - x^2}}}{(R^2 - x^2)}$$

Factor out $\frac{1}{\sqrt{R^2 - x^2}}$ in the numerator:

$$\frac{d^2w}{dx^2} = \frac{-1}{(R^2 - x^2)} \cdot \left(\sqrt{R^2 - x^2} + \frac{x^2}{\sqrt{R^2 - x^2}} \right)$$

Rewriting the term in parentheses as a single fraction:

$$\sqrt{R^2 - x^2} + \frac{x^2}{\sqrt{R^2 - x^2}} = \frac{(R^2 - x^2) + x^2}{\sqrt{R^2 - x^2}}$$

Insert that term back in:

$$\frac{d^2w}{dx^2} = \frac{-1}{(R^2 - x^2)} \cdot \left(\sqrt{R^2 - x^2} + \frac{x^2}{\sqrt{R^2 - x^2}} \right) = \frac{-1}{(R^2 - x^2)} \cdot \frac{(R^2 - x^2) + x^2}{\sqrt{R^2 - x^2}}$$

Since $(R^2 - x^2) + x^2 = R^2$, we get

$$\frac{d^2w}{dx^2} = \frac{-1}{(R^2 - x^2)} \cdot \frac{(R^2 - x^2) + x^2}{\sqrt{R^2 - x^2}} = \frac{-1}{(R^2 - x^2)} \cdot \frac{R^2}{\sqrt{R^2 - x^2}} = \frac{-R^2}{(R^2 - x^2)\sqrt{R^2 - x^2}}$$

which simplifies to the change of slope equation:

$$\frac{d^2w}{dx^2} = -\frac{R^2}{(R^2 - x^2)^{3/2}} \quad (4.8)$$

Now finally, the curvature equation κ as previously mentioned is given by (3.1):

$$\kappa = \frac{\frac{d^2w}{dx^2}}{\left[1 + \left(\frac{dw}{dx} \right)^2 \right]^{3/2}}$$

Substituting $\frac{d^2w}{dx^2}$ and $\frac{dw}{dx}$ we get:

$$\kappa = \frac{\frac{R^2}{(R^2 - x^2)^{3/2}}}{\left(1 + \frac{x^2}{R^2 - x^2} \right)^{3/2}}$$

Rewriting the denominator inside the exponent:

$$1 + \frac{x^2}{R^2 - x^2} = \frac{R^2 - x^2}{R^2 - x^2} + \frac{x^2}{R^2 - x^2} = \frac{R^2}{R^2 - x^2}$$

Thus, the denominator simplifies to:

$$\left(\frac{R^2}{R^2 - x^2} \right)^{3/2} = \frac{R^3}{(R^2 - x^2)^{3/2}}$$

Now we compute κ :

$$\kappa = \frac{R^2}{(R^2 - x^2)^{3/2}} \cdot \frac{(R^2 - x^2)^{3/2}}{R^3} = \frac{R^2}{R^3}$$

which simplifies to the curvature equation:

$$\kappa = \frac{1}{R} \quad (4.9)$$

The curvature of a circle is simply $\kappa = \frac{1}{R}$, which is constant since a perfect circle bends uniformly.

As the slope dw/dx is assumed to be small (Bernoulli-Euler), meaning that when we have $(dw/dx)^2 \approx 0$, we obtain that the curvature is approximately equal to the second derivative of the deflection with respect to position (which will be useful later):

$$\frac{\frac{d^2w}{dx^2}}{\left[1 + \left(\frac{dw}{dx}\right)^2\right]^{3/2}} \approx \frac{d^2w}{dx^2}$$

$$\kappa = \frac{1}{R} \approx \frac{d^2w}{dx^2} \quad (4.10)$$

A different approach that leads to the same conclusion can be set up by first establishing the relation between curvature and beam deflection, we start with:

$$dx \approx ds = R d\theta \rightarrow \frac{d\theta}{dx} = \frac{1}{R}$$

We also know that for small displacements (Bernoulli-Euler) $\theta \approx \tan(\theta)$, meaning:

$$\theta \approx \tan(\theta) \approx \frac{dw}{dx}$$

This gives us the slope rate of change:

$$\frac{d^2w}{dx^2} = \frac{d\theta}{dx} = \frac{1}{R}$$

Here κ is also defined as $\frac{d\theta}{dx}$ and then we can conclude that for small displacements/slopes, we get the curvature:

$$\frac{1}{R} = \frac{d\theta}{dx} = \frac{d^2w}{dx^2} = \kappa \quad (4.11)$$

4.5 Stresses due to Cold-bending

Assumptions and geometry: - The glass plate is bent in a cylindrical shape with a radius of curvature R . - The plate has thickness t and the bending is assumed to be elastic. - Plane stress conditions apply (as the plate is thin).

4.5.1 Euler-Bernoulli Beam Approach

The Euler-Bernoulli beam theory can provide a simplified, analytical approach to estimating stress in cold bent glass, making it useful for comparison with numerical FEA analysis.

If the panel primarily undergoes bending in one direction (e.g., in the case of a long, narrow panel), the behavior can be approximated using beam theory. In cold bending, the primary deformation mode is often a simple curvature induced in one direction, monoclastic bending, meaning that stress distribution follows beam bending, specifically Euler's beam, principles somewhat well.

The Euler-Bernoulli beam theory assumes that cross-sections remain plane and normal to the neutral axis, which is valid if the panel is relatively slender (large aspect ratio) and if out-of-plane shear deformations are negligible.

Using Euler's theory as a baseline helps validate FEA results by offering a quick, simplified, approximate check against complex numerical models, ensuring that the calculated stresses are within the expected ranges.

If numerical simulations (e.g., finite element analysis) confirm that the principal stresses in the panel align with those predicted by beam theory, the assumption is validated for practical purposes.

Using the curvature definition, we have the following:

$$\frac{\partial^2 w}{\partial x^2} = \frac{1}{R}$$

Inserting it into the bending moment equation for an Euler beam, we obtain:

$$M = EI \frac{\partial^2 w}{\partial x^2} = EI \frac{1}{R} \quad (4.12)$$

When a beam is bending (Euler-Bernoulli Beam Theory), normal stress is given by:

$$\sigma = \frac{My}{I} \quad (4.13)$$

If we insert (4.12) into (4.13) we obtain the following:

$$\sigma = EI \frac{1}{R} \frac{y}{I}$$

This can be simplified and using $y = h/2$ it becomes the approximated cold-bending stress equation.

We could also obtain it using this approach:

$$\sigma_{xx} = E\varepsilon_{xx} = Ez \frac{d^2 w}{dx^2} = \frac{Eh}{2R}$$

Final Expressions For Euler-Bernoulli Cold-Bending Stress Equation

$$\sigma_{cb} = \frac{Eh}{2R} \quad (4.14)$$

This equation is derived from classical bending theory and assumes linear elastic behavior, small deformations, and uniform curvature, which aligns well with the initial deformation state of cold-bent glass.

4.5.2 Kirchhoff-Love Plate Approach

Kirchhoff's plate theory offers an analytical approach to estimate stress in cold bent glass while considering thin plate assumptions. Unlike Euler-Bernoulli beam theory, which strictly applies to bending in one direction, Kirchhoff's formulation is typically used for 2D plate bending. However, when the panel is predominantly bending in one direction, such as in the case of a thin plate with support along two long edges, the equations of plate theory can be simplified to match the behavior of a beam-like plate model.

Under this assumption, the secondary curvature in the y-direction is negligible, reducing the general equations of the plate to a form that resembles classical beam bending, but still retains key considerations of plate mechanics, such as Poisson effect of the material. This leads to a stress formulation that includes the $(1 - \nu^2)$ correction factor:

This approach should provide a more refined estimation than beam theory alone, as it acknowledges that the panel behaves as a thin plate rather than a pure beam. Kirchhoff's formulation, even in its simplified form, helps validate the FEA results by ensuring that the distribution of the bending stresses remains within the expected analytical limits, particularly for slender panels with minimal curvature in the y-direction.

If numerical simulations confirm that the stress distribution aligns with these plate bending principles, it supports the assumption that monoclastic bending dominates, validating the use of a simplified plate model over a full 2D bending analysis.

Using the definition of curvature and since the panel bends only in the x-direction \rightarrow we assume that curvature exists only in x, we have:

$$\frac{\partial^2 w}{\partial x^2} = \frac{1}{R}, \quad \frac{\partial^2 w}{\partial y^2} = 0$$

In monoclastic bending, the panel remains flat in the y-direction \rightarrow No bending curvature in y.

Finding σ_{xx} :

$$\sigma_{xx} = \frac{Eh}{2(1 - \nu^2)} \left(\frac{\partial^2 w}{\partial x^2} + \nu \frac{\partial^2 w}{\partial y^2} \right)$$

Substituting $\frac{\partial^2 w}{\partial x^2} = \frac{1}{R}$ and $\frac{\partial^2 w}{\partial y^2} = 0$:

$$\sigma_{xx} = \frac{Eh}{2(1-\nu^2)} \left(\frac{1}{R} + \nu \cdot 0 \right)$$

$$\sigma_{xx} = \frac{Eh}{2R(1-\nu^2)}$$

Finding σ_{yy} :

$$\sigma_{yy} = \frac{Eh}{2(1-\nu^2)} \left(\nu \frac{\partial^2 w}{\partial x^2} + \frac{\partial^2 w}{\partial y^2} \right)$$

Substituting the same curvature assumptions:

$$\sigma_{yy} = \frac{Eh}{2(1-\nu^2)} \left(\nu \frac{1}{R} + 0 \right)$$

$$\sigma_{yy} = \frac{Eh\nu}{2R(1-\nu^2)}$$

Final Expressions For Kirchhoff-Love Cold Bending Stress Equation

$$\sigma_{xx} = \frac{Eh}{2R(1-\nu^2)} \tag{4.15}$$

$$\sigma_{yy} = \frac{Eh\nu}{2R(1-\nu^2)} \tag{4.16}$$

Note: σ_{yy} is reduced due to the Poisson ratio effect but is still present.

5 Cold Bending of Monolithic Glass

Monolithic glass thicknesses commonly used for cold bending include 6-19 mm. Thicker glass allows for larger bending radii and better structural performance, but requires more force to bend.

5.1 Influence of plate dimensions

It was concluded from chapter 4, that theoretically with simplified assumptions, the length and width of the glass panel has no effect on the cold bending stresses. However, this has limitations, which will be investigated in this section. In order for the assumptions to be valid, certain conditions have to be met within the model.

The test was carried out on a 10 mm monolithic glass panel, cold bent with a radius of 20 m in Abaqus with the model shown in 3.2. It was conducted on 3 panels, with the dimensions shown in figure 5.1.

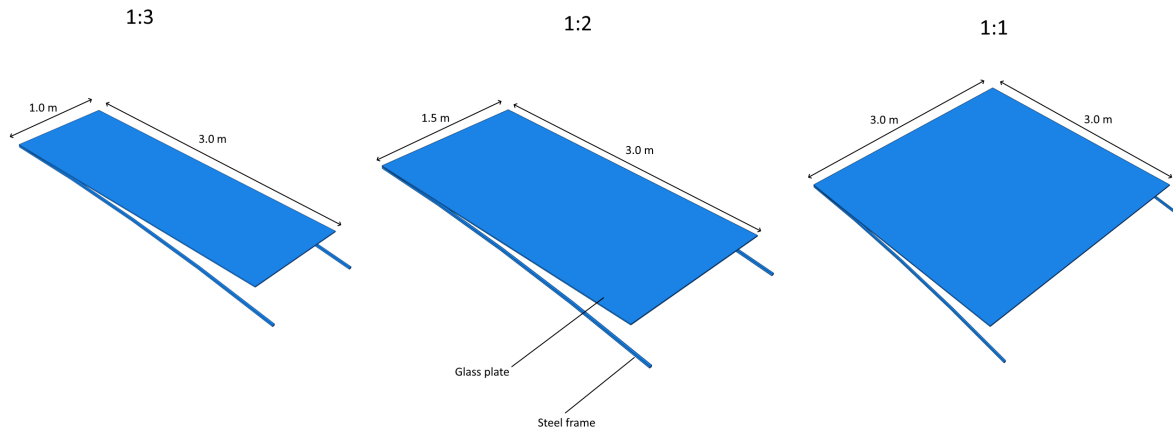
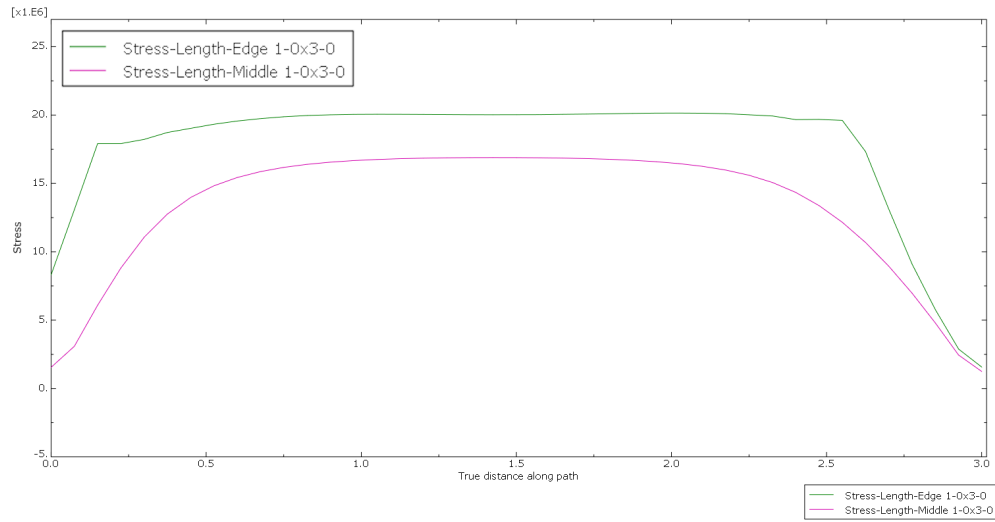
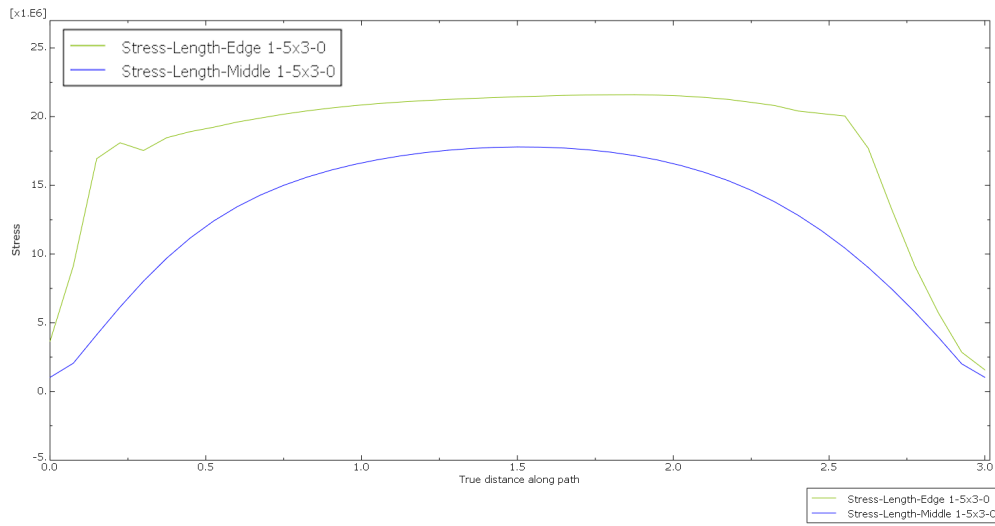


Figure 5.1: Cold-bent glass models with three different dimensions.

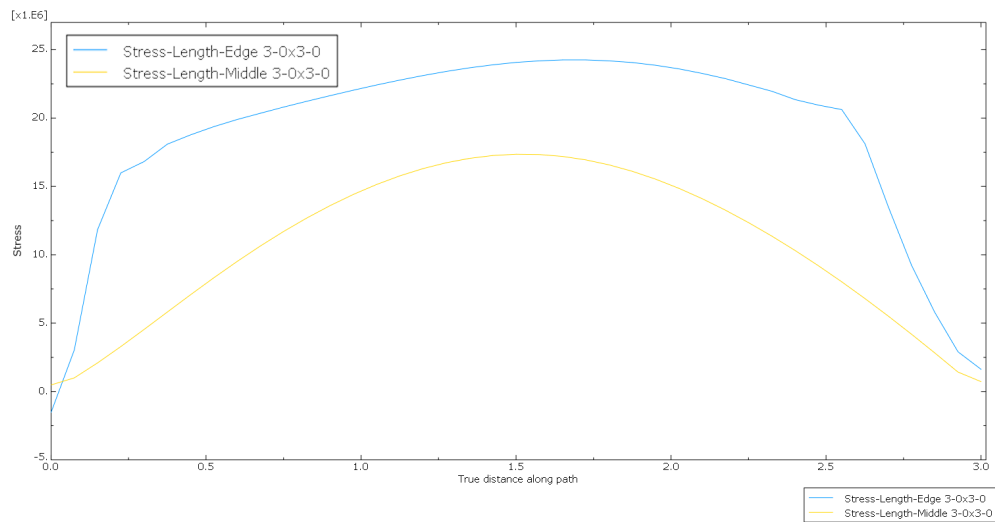
The panel is kept in shape along the two longitudinal edges. In the middle of the plate, in between these two edges, the panel is unconstrained. The results show a very minor difference in the pure bending stresses that occur in the middle of the plate due to cold bending. However, there appear to be some edge effects that play into hand with a magnitude depending on the width of the plate. The wider the plate, the higher these edge effects are, which are shown by the difference between the stresses induced in the middle of the plate and near the edges where the glass gets in contact with the frame. This is visualized in figure 5.2.



(a) 1.0 x 3.0



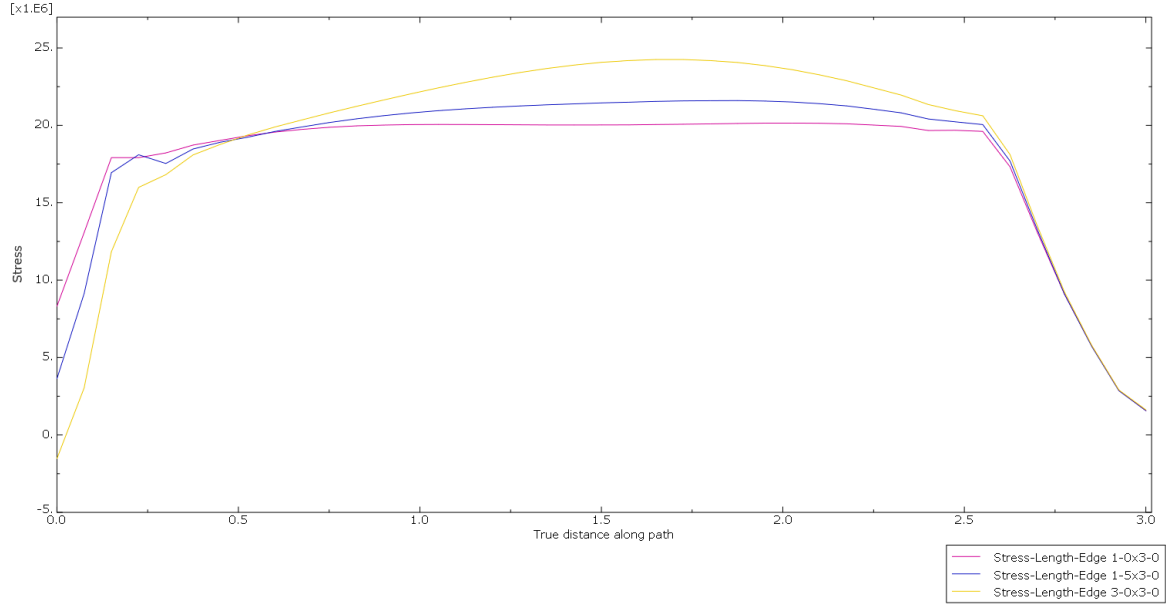
(b) 1.5 x 3.0



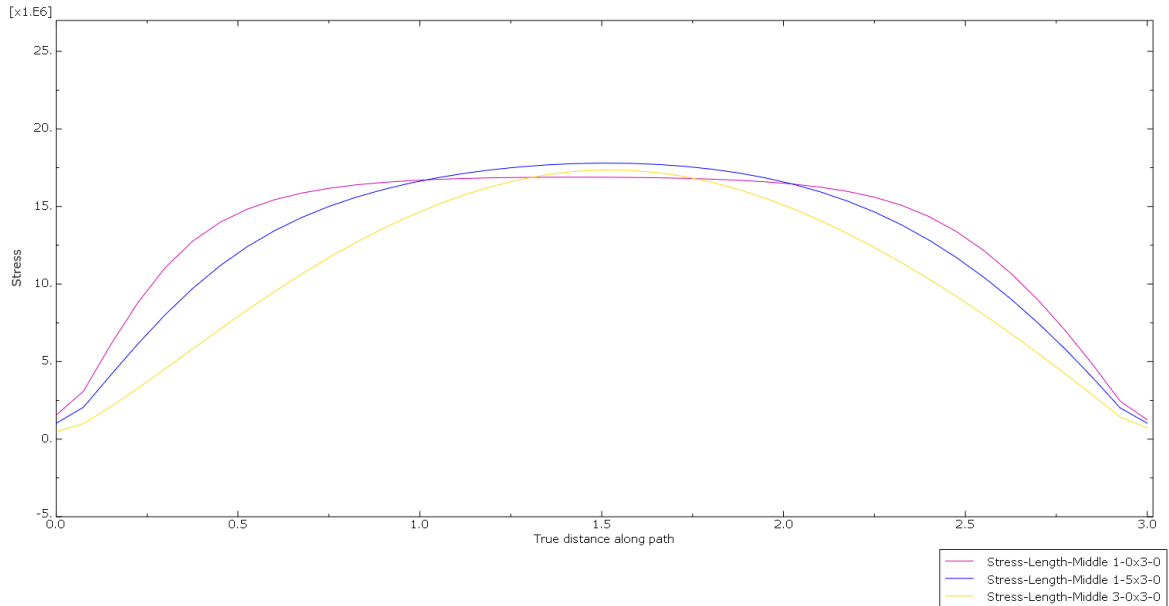
(c) 3.0 x 3.0

Figure 5.2: Plots illustrating the differences in cold-bending stresses between the plate's edges and center.

The stress plots along the length of the plates in Figure 5.3b show consistency in the stresses that occur in the center line of the plate where the effects of pure bending apply. In contrast, the stress plots along the length of the plate at the edges show some variation with increasing width followed by increasing stresses, as shown in Figure 5.3a.



(a) Difference between edge stresses depending on the width.



(b) Difference between center stresses depending on the width.

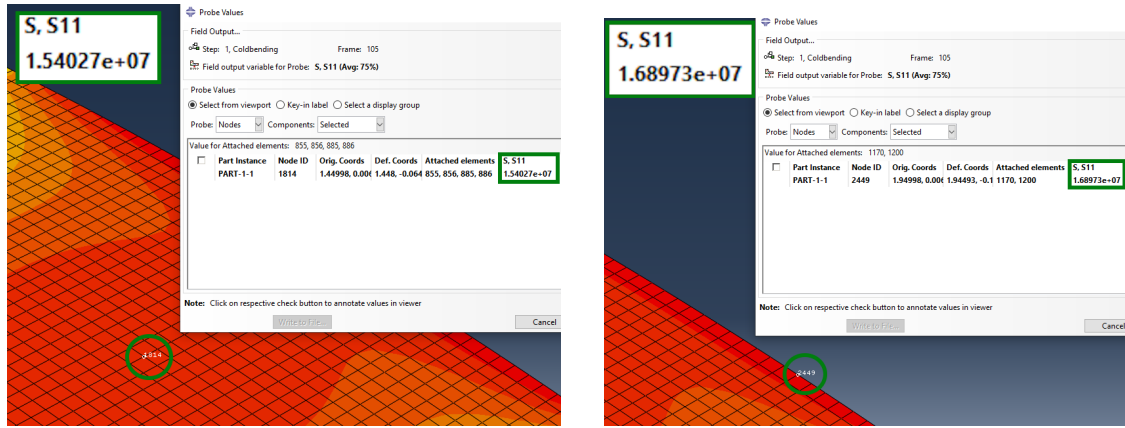
Figure 5.3: Plots illustrating the differences in cold-bending stresses between the models in the center and on the edges.

This agrees well with the pure bending beam and plate theories, where when pure bending is assumed, the width/length ratio of the plate will be irrelevant as the edge effects are neglected in this study.

The exact boundary between acceptable and unacceptable width/length ratios when

taking into account edge effects is difficult to determine. An acceptable and practical guideline can be a width/length ratio of 1/2 such as shown in the 1.5 x 3 model and as was chosen in chapter 3.2.1 and showcased in figure 3.1.

The higher stresses are near the long edges of the glass panel where the frame sub-structure is located, which is caused by the effects of the edges and the constraints. This happens because the panel is not super narrow, thus edge constraints will matter more. If the short edge is fully clamped and the curvature is enforced via side rails, stress concentrations near corners will be bound to occur as shown in figure 5.4b.



(a) Maximum cold bending stresses from pure bending. (b) Demonstration of the higher stress concentrations near edges due to edge effects.

Figure 5.4: Plots illustrating the differences in cold-bending stresses between the models in the center and on the edges.

5.2 Cold-Bending Stresses

Euler-Bernoulli beam cold bending stress approximation:

$$\sigma_{cb,e} = \frac{Eh}{2R} \quad (5.1)$$

Kirchhoff–Love plate cold bending stress approximation:

$$\sigma_{cb,k} = \frac{Eh}{2R(1 - \nu^2)} \quad (5.2)$$

In Abaqus, S11 represents the normal stress in the x-direction, denoted as σ_{xx} , and "Max. Principal" corresponds to the maximum principal stress, denoted as σ_1 .

Table 5.1: Values used for analytical approach

Parameters	Value
Elasticity modulus	$E = 70 \text{ GPa}$
Poisson's ratio	$\nu = 0.23$
Radius	$R = 10, 12 \text{ m}$
Thickness	$h = 6, 8, 10, 12 \text{ mm}$

The tables 5.2, 5.3, and 5.4, present the results of the cold bending stress of both numerical and analytical methods for various radii and configurations of monolithic glass shown in table 5.1. Additionally, tables 5.5 and 5.6, present the deviation between the analytical and numerical stresses.

Table 5.2: Comparison of Numerical and Analytical approach to calculate cold bending stresses for radius 10 m.

Method	Cold Bending Stresses σ_{cb} for various Glass Thicknesses h [MPa] and Radius of 10 m:			
	6 mm	8 mm	10 mm	12 mm
σ_1	23.60	31.45	38.92	45.98
σ_{xx}	22.89	30.63	37.98	44.90
$\sigma_{cb,k}$	22.17	29.56	36.95	44.35
$\sigma_{cb,e}$	21.0	28.0	35.0	42.0
$\frac{h}{R}$	0.6	0.8	1.0	1.2

Table 5.3: Comparison of Numerical and Analytical approach to calculate cold bending stresses for radius 15 m.

Method	Cold Bending Stresses σ_{cb} for various Glass Thicknesses h [MPa] and Radius of 15 m:			
	6 mm	8 mm	10 mm	12 mm
σ_1	15.69	20.49	24.94	29.16
σ_{xx}	15.51	20.26	24.67	28.85
$\sigma_{cb,k}$	14.78	19.71	24.64	29.56
$\sigma_{cb,e}$	14.0	18.7	23.3	28.0
$\frac{h}{R}$	0.4	0.533	0.667	0.8

Table 5.4: Comparison of Numerical and Analytical approach to calculate cold bending stresses for radius 20 m.

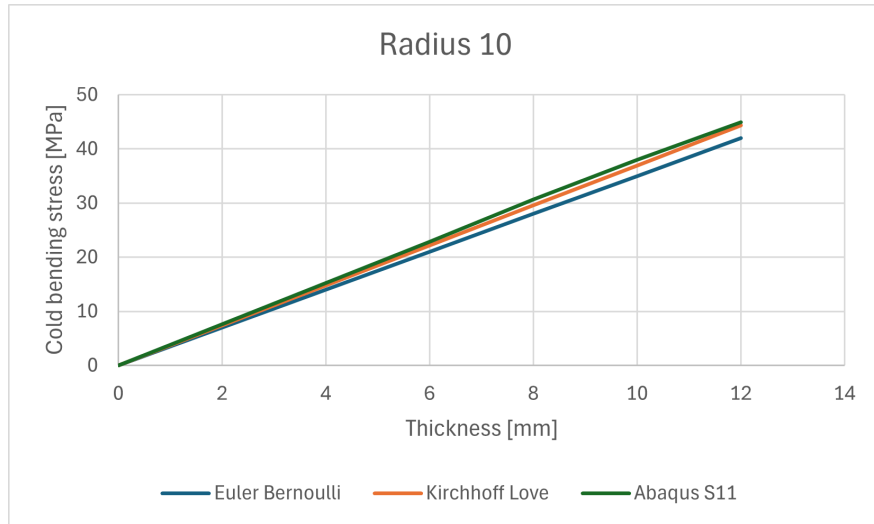
Method	Cold Bending Stresses σ_{cb} for various Glass Thicknesses h [MPa] and Radius of 20 m:			
	6 mm	8 mm	10 mm	12 mm
σ_1	11.49	14.80	17.90	20.92
σ_{xx}	11.42	14.70	17.80	20.81
$\sigma_{cb,k}$	11.09	14.78	18.48	22.17
$\sigma_{cb,e}$	10.5	14.0	17.50	21.0
$\frac{h}{R}$	0.3	0.4	0.5	0.6

Table 5.5: Differences between the normal stresses in the x-direction and the stresses calculated using Euler Bernoulli's theory

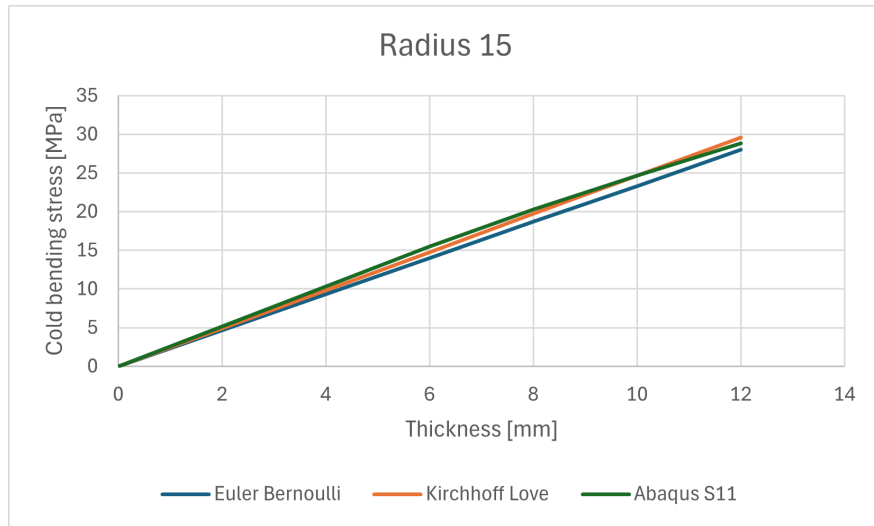
Radius	$\sigma_{xx} - \sigma_{cb,e}$			
	6 mm	8 mm	10 mm	12 mm
10 m	1.89 (8.3%)	2.63 (8.6%)	2.98 (7.8%)	2.90 (6.4%)
15 m	1.51 (9.7%)	1.56 (7.7%)	1.37 (5.5%)	0.85 (2.9%)
20 m	0.92 (8.0%)	0.70 (4.7%)	0.30 (1.7%)	-0.19 (-0.9%)

Table 5.6: Differences between the normal stresses in the x-direction and the stresses calculated using Kirchhoff's Love theory.

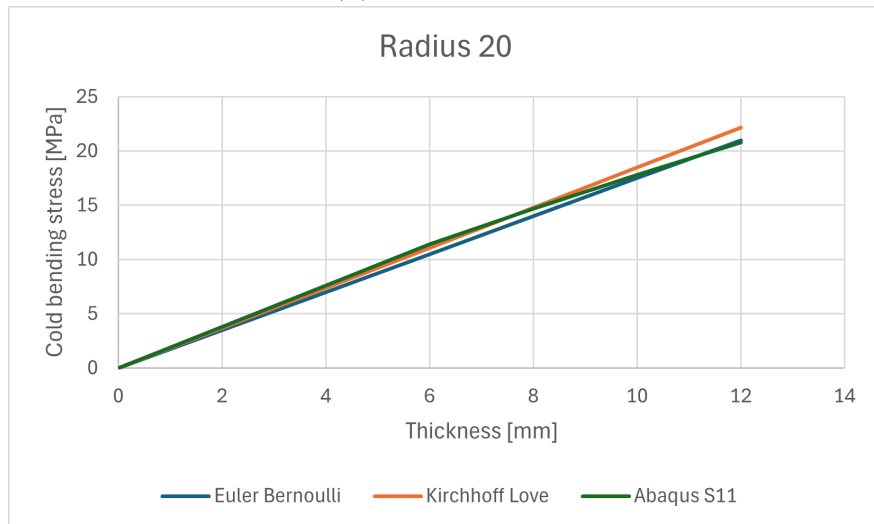
Radius	$\sigma_{xx} - \sigma_{cb,k}$			
	6 mm	8 mm	10 mm	12 mm
10 m	0.72 (3.1%)	1.07 (3.4%)	1.03 (2.7%)	0.55 (1.2%)
15 m	0.73 (4.7%)	0.55 (2.7%)	0.03 (0.1%)	-0.71 (-2.4%)
20 m	0.33 (2.9%)	-0.08 (-0.5%)	-0.68 (-3.8%)	-1.36 (-6.5%)



(a) Radius = 10 m



(b) Radius = 15 m



(c) Radius = 20 m

Figure 5.5: Plots illustrating the differences in cold-bending stresses between numerical and analytical approach.

6 Cold Bending of Laminated Glass

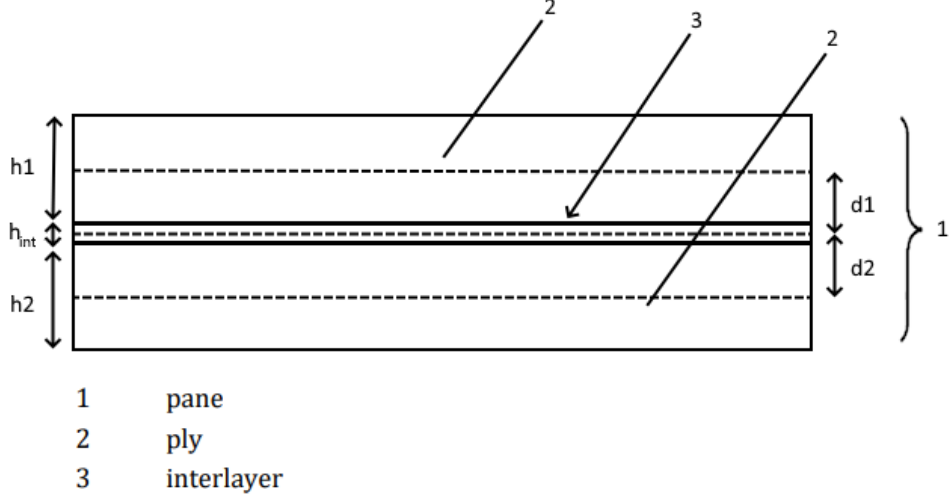


Figure 6.1: Two Ply Laminated Glass Panel

6.1 Mechanical Properties of the Interlayer (PVB)

According to prEN 16613:2019 [14], the commonly used interlayers, such as PVBs, are generally isotropic materials. The interlayer shear or Young's modulus can be converted into each other using the formula:

$$G_{int} = \frac{E_{int}}{2(1 + \nu_{int})} \quad (6.1)$$

Where G_{int} and E_{int} are the shear and Young's modulus, and ν_{int} is the Poisson's number of the interlayer and can be approximated to 0.49 and therefore:

$$E_{int} = 2G_{int}(1 + \nu_{int}) \approx 3G_{int} \quad (6.2)$$

The PVB interlayer is a highly viscoelastic material. Viscoelasticity is normally accounted for by implementing the so-called Prony series. A Prony series, also known as a Prony decomposition or a relaxation modulus series, is a way to account for the time-dependent behavior of a viscoelastic material. It is a mathematical model, derived from the generalized Maxwell model, that describes the viscoelastic behavior of a material, such as the ability to deform under stress and recover over time using a series of exponential terms, effectively simplifying or breaking down the complex

viscoelastic behavior into more manageable components. It is a series consisting of a sum of exponential terms, each with its own time constant and weight [44, 45, 46].

The time dependent variables $G(t)$ and $E(t)$ are calculated from [47]:

$$G(t) = G_0(1 - g_i(1 - e^{-\frac{t}{\tau_i}})) \quad (6.3)$$

$$E(t) = E_0(1 - k_i(1 - e^{-\frac{t}{\tau_i}})) \quad (6.4)$$

where G_0 and E_0 are the instantaneous shear and elastic moduli [47].

For simplification purposes, in this study, the glass is modeled as a linear elastic material. This is possible because the viscoelastic interlayer, while inherently time-dependent, can also be approximated as a linear elastic material by choosing a significantly reduced modulus of elasticity to reflect its long-term behavior under constant loading and temperature. It is a commonly accepted simplification to assume that the polymer is linear elastic, with proper secant elastic moduli that account for environmental temperature and load duration [48].

This simplification is based on the fact that, over time, viscoelastic materials exhibit creep, gradually deforming under constant stress, making it possible for the interlayer to be treated as if it has already undergone this long-term deformation, effectively representing a 'fully crept' state by choosing a reduced modulus of elasticity that the material would have reached after relaxation. This approach allows for long-term flexibility of the interlayer to be captured using a static analysis. It provides a practical and computationally efficient means of simulating its behavior under permanent loading conditions such as cold bending.

For the shear modulus, G_∞ is used, which is the relaxed shear modulus with the infinity sign referring to permanent loading, to represent the shear modulus of the interlayer G_{int} after long-term loading. It effectively represents the equilibrium modulus in which the material settles after all time-dependent effects (such as creep or stress relaxation) have occurred.

For cold bent or permanently loaded laminated glass, the interlayer material (such as PVB) undergoes creep, slowly deforming under sustained stress. Over time, the shear stiffness of the interlayer reduces, and the material approaches a stable, relaxed state, which is represented by G_∞ . This long-term behavior is key when modeling the performance of laminated glass under permanent loading conditions.

To clarify the terminology:

G_0 the initial shear modulus (short-term or instantaneous response).

$G(t)$ the time-dependent shear modulus (viscoelastic behavior).

G_∞ the long-term or relaxed shear modulus (constant load).

G_{int} the effective shear modulus used in Eurocode for laminated glass.

There are various commercial polymeric films, such as polyvinyl butyral (PVB), ethyl-

ene vinyl acetate (EVA), and sentry glass (SG) [48]. Depending on the type of polymer, the temperature T and the duration of the load t_0 , the secant shear modulus of the interlayer can vary from 0.01 MPa (PVB at $T = +60^\circ\text{C}$ under permanent load) up to 300 MPa (SG at $T = 0^\circ\text{C}$ and $t_0 = 1\text{ s}$) [48].

For PVB, a temperature of 20°C and a permanent load, numerous studies support the use of shear modulus values as low as 0.05 – 0.2 MPa, to capture long-term effects such as creep [49, 50, 51, 52, 53]. Based on these references and the general consensus in the literature, a value of $G_\infty = 0.1\text{ MPa}$ for the long-term shear modulus of PVB and a temperature of 20°C , can be considered a safe and conservative estimate for cold-bent laminated glass panels. This approximation provides a realistic lower-bound stiffness, ensuring that viscoelastic effects are adequately represented in structural analyses.

Looking at figure 2.5, specifically the monolithic configuration (c), we observe that laminated glass is considered monolithic glass with a thickness equal to the sum of the thicknesses of the glass plies; glass plies are considered as absolutely bonded together and the shear modulus tends to infinity $G_{int,\infty} = \infty$. This happens when you assume full shear transfer or full coupling. In our case, with the permanent load duration from cold bending, we are looking at the layered configuration (a), where the shear modulus $G_{int,\infty} \approx 0$, which means little or no shear transfer (no coupling effect). We do this to predict the long-term creep behavior of the interlayer. When looking at layered or laminated configurations, we cannot use the actual thickness of the interlayer as for a monolithic configuration. An effective thickness calculation is required; see the next Section 6.2.

The Young's modulus used in the numerical study was obtained from the following:

$$G_{int,\infty} = 0.1$$

$$E_{int} = 2G_{int}(1 + \nu_{int}) = 2 \cdot 0.1(1 + 0.49) = 0.298 \approx 0.3\text{ MPa}$$

6.2 Effective Thickness of Laminated Glass

Determination of the effective thickness according the enhanced effective thickness approach (EET) according to prEN 19100-2:2023

The effective thickness for a laminated glass panel deflection calculation is calculated using Formula (A.1):

$$h_{ef,w} = \sqrt[3]{\frac{1}{\frac{\eta}{\sum_{i=1}^n h_i^3 + 12 \cdot \sum_{i=1}^n (h_i \cdot d_i^2)} + \frac{1-\eta}{\sum_{i=1}^n h_i^3}}} \quad (6.5)$$

Where $h_{ef,w}$ is the effective thickness of a laminated glass to calculate out-of-plane bending deflection.

The effective thickness of the ply 'i' of the laminated glass for stress calculation should be calculated from Formula (A.2):

$$h_{\text{ef},o,i} = \sqrt{\frac{1}{\frac{2 \cdot \eta \cdot |d_i|}{\sum_{i=1}^n h_i^3 + 12 \cdot \sum_{i=1}^n (h_i \cdot d_i^2)} + \frac{h_i}{h_{\text{ef},w}^3}}} \quad (6.6)$$

Where $h_{\text{ef},o,i}$ is the effective thickness of a laminated glass for calculating out-of-plane bending stress of ply i.

For a laminated glass pane made of 2 plies, the coupling parameter η_{p2} is calculated using Formula (A.3):

$$\eta_{p,2} = \frac{1}{1 + \frac{h_{\text{int}} \cdot E}{G_{\text{int}} \cdot (1 - \nu^2)} \cdot \frac{D_{\text{abs}}}{D_{\text{full}}} \cdot \frac{h_1 \cdot h_2}{(h_1 + h_2)} \cdot \Psi_p}$$

The boundary coefficient for a plate fixed at one end and bent from the free end:

$$\begin{aligned} a &= 3 \text{ m} \\ b &= 1.5 \text{ m} \\ \lambda &= \frac{a}{b} = \frac{3}{1.5} = 2.0 \end{aligned}$$

Table 6.1: Ψ_b [10^6 mm^{-2}] coefficients for different loading and boundary conditions from prEN 19100-2:2023 table A.1 [30].

$\lambda=a/b$ b [mm]	1.667	2.50
1500	5.03983	4.74433

Interpolation:

$$\begin{aligned} \Psi_b &= 5.03983 + \left(\frac{2 - 1.667}{2.5 - 1.667} \right) \cdot (4.74433 - 5.03983) \\ \Psi_b &= 4.9217 \cdot 10^6 \text{ mm}^{-2} = 4.9217 \text{ m}^{-2} \end{aligned}$$

Flexural stiffness at the layered limit according to Formula (A.4):

$$D_{\text{abs}} = \sum_{i=1}^n D_i = \frac{E \cdot \sum_{i=1}^n h_i^3}{12(1 - \nu^2)}$$

Flexural stiffness at the monolithic limit according to Formula (A.5):

$$D_{\text{full}} = D_{\text{abs}} + \frac{E \cdot \sum_{i=1}^n (h_i \cdot d_i^2)}{(1 - \nu^2)}$$

Table 6.2: Equivalent Thickness for various Laminated Glass Thicknesses for interlayer thickness 0.76 mm

Glass Thickness [mm]	Equivalent Thickness $h_{ef,\sigma,i}$ [mm]
$3 + 0.76 + 3$	5.27
$4 + 0.76 + 4$	6.68
$5 + 0.76 + 5$	8.10
$6 + 0.76 + 6$	9.52

Table 6.3: Equivalent Thickness for various Laminated Glass Thicknesses for interlayer thickness 1.52 mm

Laminated Glass Thickness [mm]	Equivalent Thickness $h_{ef,\sigma,i}$ [mm]
$3 + 1.52 + 3$	5.18
$4 + 1.52 + 4$	6.51
$5 + 1.52 + 5$	7.86
$6 + 1.52 + 6$	9.23

A thicker, more flexible interlayer results in laminated glass that bends more easily, as the layers can move independently.

6.3 Cold-Bending Stresses

To investigate the behavior of laminated glass panels that are subjected to cold bending, the same model and conditions used for monolithic glass will be adopted to ensure a consistent method. Using the same modeling approach is important to separate the effects of lamination from those of other factors. This ensures that any differences in structural behavior are due to the material setup itself, not because of changes in how the simulation was done.

Euler-Bernoulli beam cold bending stress approximation:

$$\sigma_{cb,e} = \frac{Eh}{2R} \quad (6.7)$$

Kirchhoff–Love plate cold bending stress approximation:

$$\sigma_{cb,k} = \frac{Eh}{2R(1 - \nu^2)} \quad (6.8)$$

6.3.1 Interlayer thickness 0.76 mm

The tables 6.4, 6.5, and 6.6, present the results of the cold bending stress of both numerical and analytical methods for various radii and configurations of laminated glass with a PVB thickness of 0.76 mm. Additionally, tables 6.7 and 6.8, present the deviation between the analytical and numerical stresses.

Table 6.4: Comparison of Numerical and Analytical approach to calculate cold bending stresses for laminated glass with a radius 10 m and interlayer thickness 0.76.

Method	Cold Bending Stresses σ_{cb} [MPa] for various Glass Thicknesses [mm] and Radius of 10 m:			
	3+0.76+3 $h_{eff}=5.27$	4+0.76+4 $h_{eff}=6.68$	5+0.76+5 $h_{eff}=8.10$	6+0.76+6 $h_{eff}=9.51$
σ_1	19.55	24.40	28.99	33.31
σ_{xx}	19.05	23.71	28.21	32.43
$\sigma_{cb,k}$	19.48	24.69	29.93	35.18
$\sigma_{cb,e}$	18.45	23.38	28.35	33.32
$\frac{h}{R}$	0.527	0.668	0.810	0.952

Table 6.5: Comparison of Numerical and Analytical approach to calculate cold bending stresses for laminated glass with a radius 15 m and interlayer thickness 0.76.

Method	Cold Bending Stresses σ_{cb} [MPa] for various Glass Thicknesses h [mm] and Radius of 15 m:			
	3+0.76+3 $h_{eff}=5.27$	4+0.76+4 $h_{eff}=6.68$	5+0.76+5 $h_{eff}=8.10$	6+0.76+6 $h_{eff}=9.51$
σ_1	13.27	16.44	19.24	21.95
σ_{xx}	13.10	16.23	19.09	21.69
$\sigma_{cb,k}$	12.98	16.46	19.96	23.45
$\sigma_{cb,e}$	12.30	15.59	18.90	22.21
$\frac{h}{R}$	0.351	0.445	0.54	0.634

Table 6.6: Comparison of Numerical and Analytical approach to calculate cold bending stresses for laminated glass with a radius 20 m and interlayer thickness 0.76.

Method	Cold Bending Stresses σ_{cb} [MPa] for various Glass Thicknesses h [mm] and Radius of 20 m:			
	3+0.76+3 $h_{eff}=5.27$	4+0.76+4 $h_{eff}=6.68$	5+0.76+5 $h_{eff}=8.10$	6+0.76+6 $h_{eff}=9.51$
σ_1	9.94	12.15	14.08	15.89
σ_{xx}	9.87	12.07	14.02	15.79
$\sigma_{cb,k}$	9.74	12.34	14.97	17.57
$\sigma_{cb,e}$	9.22	11.69	14.18	16.64
$\frac{h}{R}$	0.351	0.445	0.54	0.634

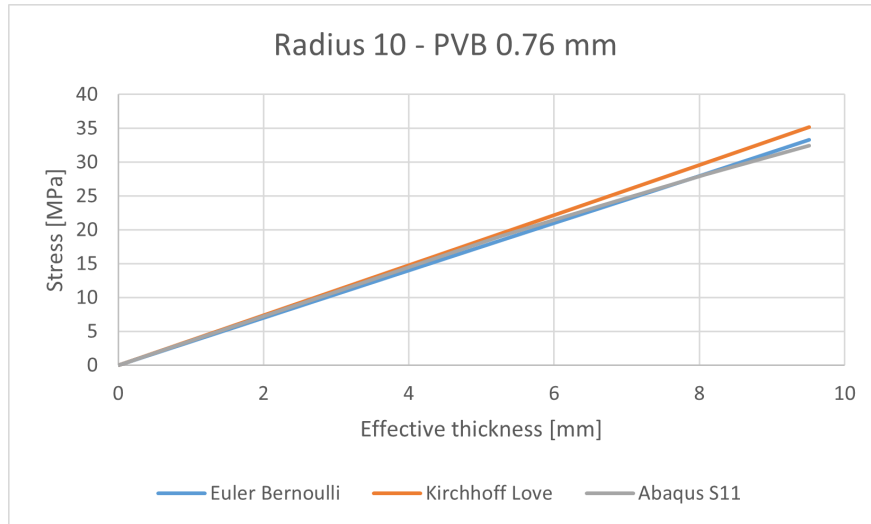
Table 6.7: Differences between the normal stresses in the x-direction and the stresses calculated using Euler Bernoulli's theory

Radius	$\sigma_{xx} - \sigma_{cb,e}$			
	3+0.76+3 $h_{eff}=5.27$	4+0.76+4 $h_{eff}=6.68$	5+0.76+5 $h_{eff}=8.10$	6+0.76+6 $h_{eff}=9.52$
10	0.6 (3.1%)	0.33 (1.3%)	-0.14 (-0.4%)	-0.89 (-2.7%)
15	0.8 (6.1%)	0.64 (3.9%)	0.19 (0.9%)	-0.52 (-2.3%)
20	0.65 (6.6%)	0.38 (4.1%)	-0.16 (-1.1%)	-0.85 (-5.4%)

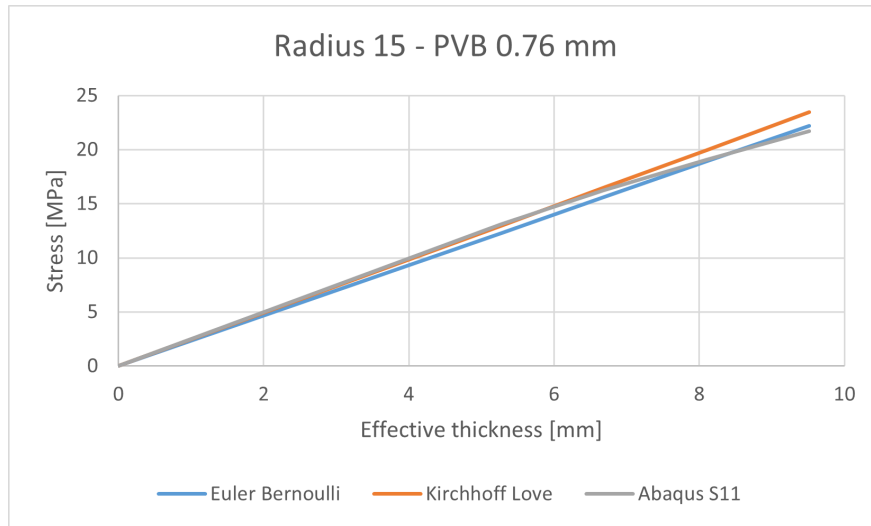
Table 6.8: Differences between the normal stresses in the x-direction and the stresses calculated using Kirchhoff's Love theory.

Radius	$\sigma_{xx} - \sigma_{cb,k}$			
	3+0.76+3 $h_{eff}=5.27$	4+0.76+4 $h_{eff}=6.68$	5+0.76+5 $h_{eff}=8.10$	6+0.76+6 $h_{eff}=9.52$
10	-0.43 (-2.2%)	-0.98 (-4.1%)	-1.72 (-6.1%)	-2.75 (-8.5%)
15	0.12 (0.9%)	-0.23(-1.4%)	-0.87(-4.6%)	-1.76 (-8.1%)
20	0.13 (1.3%)	-0.27 (-2.2%)	-0.95 (-6.8%)	-2.0 (-12.8%)

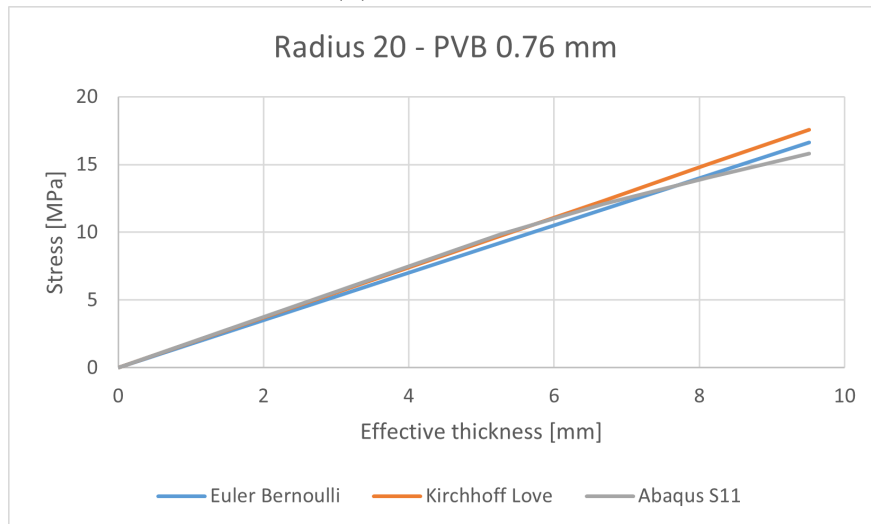
The results confirm that the analytical results are reliable with a slight overprediction in approximating the numerical results. The overprediction is probably attributed to the complex nonlinear behavior of the PVB interlayer. More on that in the discussion in chapter 8.



(a) Radius = 10 m



(b) Radius = 15 m



(c) Radius = 20 m

Figure 6.2: Plots illustrating the differences in cold-bending stresses between numerical and analytical approach for laminated glass with a PVB thickness 0.76 mm.

6.3.2 Interlayer thickness 1.52 mm

The tables 6.9, 6.10, and 6.11, present the results of the cold bending stress of both numerical and analytical methods for various radii and configurations of laminated glass with a PVB thickness of 1.52 mm. Additionally, tables 6.12 and 6.13, present the deviation between the analytical and numerical stresses.

The results ends up confirming the same conclusion as the configuration of 0.76 mm PVB interlayer, that the analytical results are reliable with a slight overprediction in approximating the numerical results. However, with a 1.52 mm PVB interlayer, the overprediction has shown to be slightly bigger. This is attributed to the fact that PVB interlayers are soft which means, when they are thicker, they soften up the whole laminated glass structure, reducing the cold bending stresses by redistributing them more effectively. This behavior is complex and nonlinear, which makes it hard to capture using linear models. The thicker the PVB interlayer is, the more nonlinear the behavior is.

Table 6.9: Comparison of Numerical and Analytical approach to calculate cold bending stresses for laminated glass with a radius 10 m and interlayer thickness 1.52.

Method	Cold Bending Stresses σ_{cb} [MPa] for various Glass Thicknesses h [mm] and Radius of 10 m:			
	3+1.52+3 $h_{eff}=5.18$	4+1.52+4 $h_{eff}=6.51$	5+1.52+5 $h_{eff}=7.86$	6+1.52+6 $h_{eff}=9.23$
σ_1	17.95	22.26	26.36	30.36
σ_{xx}	17.61	21.56	25.59	29.49
$\sigma_{cb,k}$	19.14	24.06	29.05	34.11
$\sigma_{cb,e}$	18.13	22.79	27.51	32.31
$\frac{h}{R}$	0.518	0.651	0.786	0.923

Table 6.10: Comparison of Numerical and Analytical approach to calculate cold bending stresses for laminated glass with a radius 15 m and interlayer thickness 1.52.

Method	Cold Bending Stresses σ_{cb} [MPa] for various Glass Thicknesses h [mm] and Radius of 15 m:			
	3+1.52+3 $h_{eff}=5.18$	4+1.52+4 $h_{eff}=6.51$	5+1.52+5 $h_{eff}=7.86$	6+1.52+6 $h_{eff}=9.23$
σ_1	12.27	14.98	17.55	19.97
σ_{xx}	12.12	14.79	17.34	19.74
$\sigma_{cb,k}$	12.76	16.04	19.36	22.74
$\sigma_{cb,e}$	12.09	15.19	18.34	21.54
$\frac{h}{R}$	0.345	0.434	0.524	0.615

Table 6.11: Comparison of Numerical and Analytical approach to calculate cold bending stresses for laminated glass with a radius 20 m and interlayer thickness 1.52.

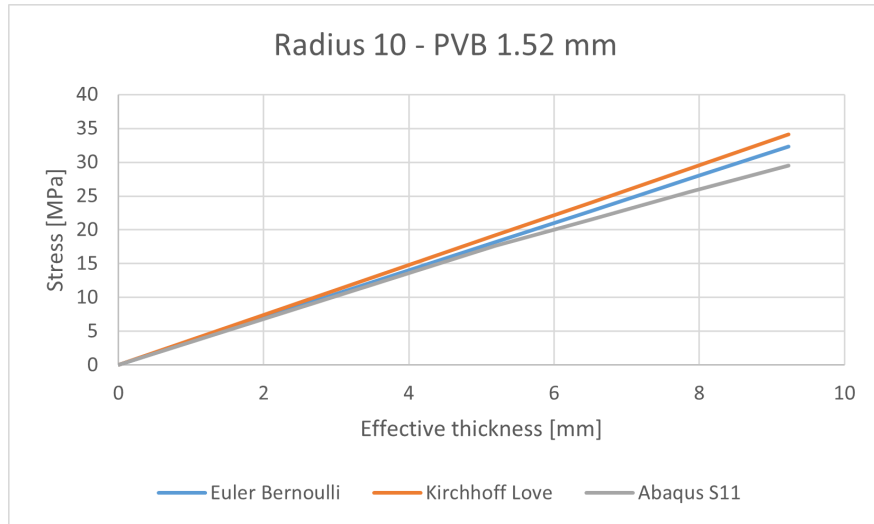
Method	Cold Bending Stresses σ_{cb} [MPa] for various Glass Thicknesses h [mm] and Radius of 20 m:			
	3+1.52+3 $h_{eff}=5.18$	4+1.52+4 $h_{eff}=6.51$	5+1.52+5 $h_{eff}=7.86$	6+1.52+6 $h_{eff}=9.23$
σ_1	9.20	11.08	12.81	14.48
σ_{xx}	9.13	11.01	12.75	14.39
$\sigma_{cb,k}$	9.57	12.03	14.52	17.05
$\sigma_{cb,e}$	9.07	11.39	13.76	16.15
$\frac{h}{R}$	0.518	0.651	0.786	0.923

Table 6.12: Differences between the normal stresses in the x-direction and the stresses calculated using Euler Bernoulli's theory

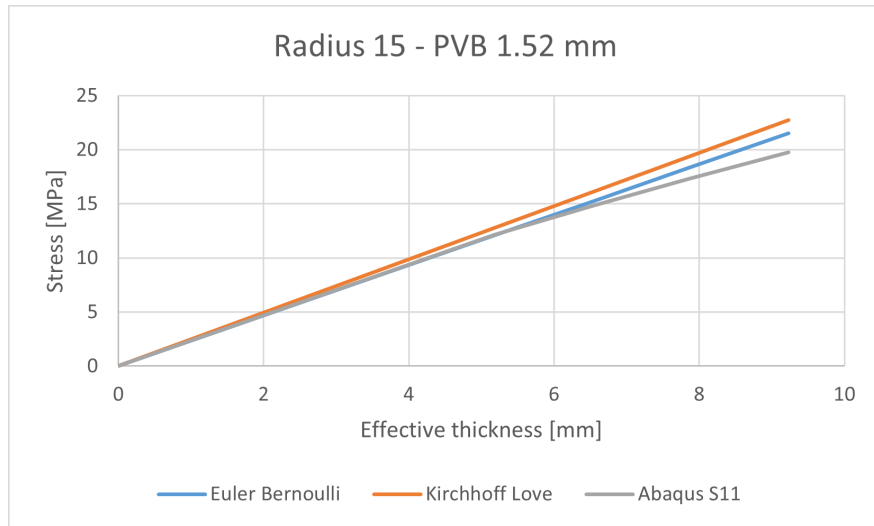
Radius	$\sigma_{xx} - \sigma_{cb,e}$			
	3+1.52+3 $h_{eff}=5.18$	4+1.52+4 $h_{eff}=6.51$	5+1.52+5 $h_{eff}=7.86$	6+1.52+6 $h_{eff}=9.23$
10	-0.52 (-3.0%)	-1.23 (-5.7%)	-1.92 (-7.5%)	-2.82 (-9.6%)
15	0.03 (0.2%)	-0.4 (-2.2%)	-1.0 (-5.8%)	-1.8 (-9.1%)
20	0.06 (0.6%)	-0.38 (-3.5%)	-1.01 (-7.9%)	-1.76 (-12.2%)

Table 6.13: Differences between the normal stresses in the x-direction and the stresses calculated using Kirchhoff's Love theory.

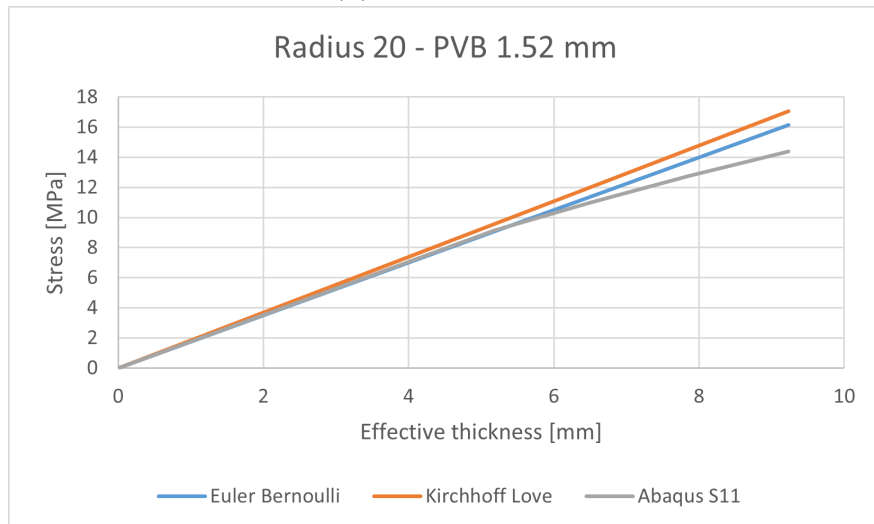
Radius	$\sigma_{xx} - \sigma_{cb,k}$			
	3+1.52+3 $h_{eff}=5.18$	4+1.52+4 $h_{eff}=6.51$	5+1.52+5 $h_{eff}=7.86$	6+1.52+6 $h_{eff}=9.23$
10	-1.53 (-8.7%)	-2.5 (-11.6%)	-3.46 (-13.5%)	-4.62 (-15.7%)
15	-0.64 (-5.3%)	-1.25 (-8.5%)	-2.02 (-11.6%)	-3.0 (-15.2%)
20	-0.44 (-4.8%)	-1.02 (-9.3%)	-1.77 (-13.9%)	-2.66 (-18.5%)



(a) Radius = 10 m



(b) Radius = 15 m



(c) Radius = 20 m

Figure 6.3: Plots illustrating the differences in cold-bending stresses between numerical and analytical approach for laminated glass with a PVB thickness 1.52 mm.

7 Load combinations

Cold bent glass components are subject to a range of effects induced by both external loads, such as wind, snow, and temperature changes, and internal loads induced by the cold bending process itself. Understanding the load combinations for internal and external loads in cold-bent glass structures is crucial to ensuring their structural integrity and performance. The effects of external loads and whether they are possible to superpose with cold bending effects are studied in this chapter.

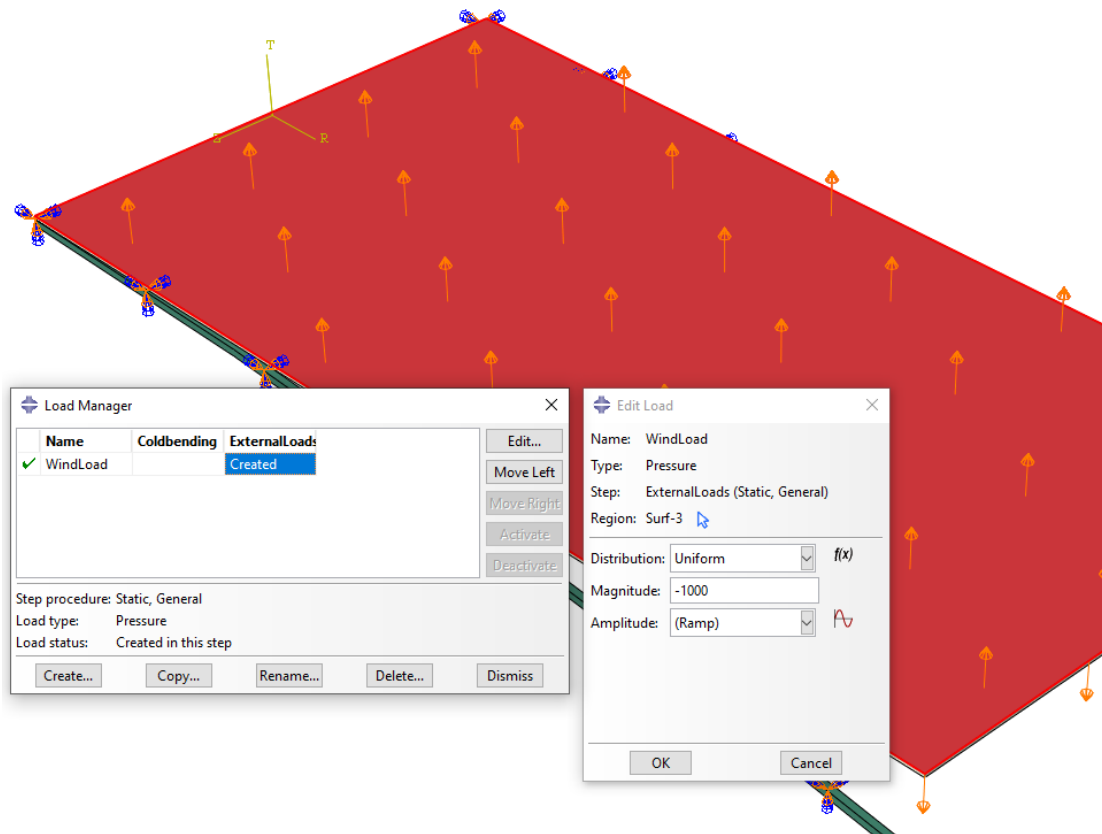
External loads, such as wind loads, will not induce stresses primarily in one direction, as cold bending would do. The external load stresses will be distributed differently and therefore we would need to look at the maximum principal stresses σ_1 . The maximum tensile bending stresses in the x -direction σ_{xx} cannot be superposed with maximum principal stresses because they are not the same. Unless they give approximately the same values, and that would be the case if the stress state is predominantly uniaxial tension in the x -direction, then we can conclude that the maximum principal stress and σ_{xx} are nearly the same. An approximate expression for the principal stress induced by cold bending can then be estimated using tensile stresses in the bending direction σ_{xx} , with little deviation, and can be estimated from classical bending theories that are given by the derived Euler and Kirchhoff formulas. Since tensile bending stresses are typically dominant in cold bent configurations, they align with the direction of the maximum principal stress. Therefore, these derived expressions provide a conservative and practical estimate of the maximum principal tensile stress in the absence of additional loads or complex boundary conditions. However, this works better the lower the cold bending stresses are, e.g. bigger radii (smaller deflection). Therefore, in order to approximate the maximum principal stress with good accuracy using the derived formulas, a small deflection is favored.

The radius was chosen large enough to leave room for superimposed stress from both internal and external stresses. The thicker a glass panel is, the higher the cold bending stresses become, on the contrary, the thinner it is, the less durable it is against external loads.

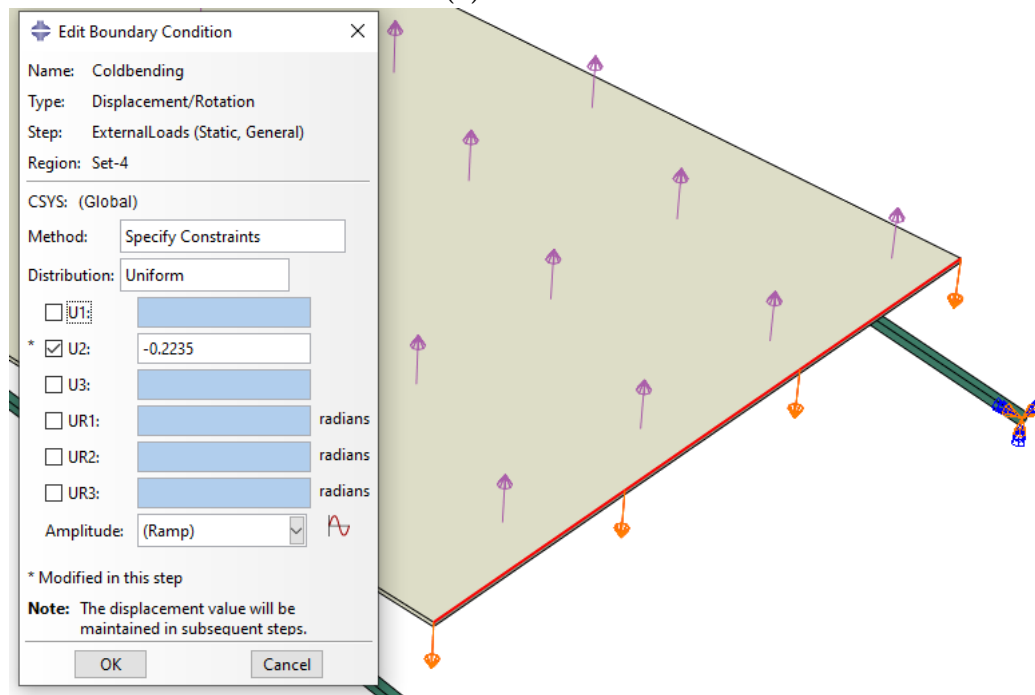
Because cold bending takes place first and then loads are applied later, and because glass stays mostly elastic (linear material behavior) up to failure, the principle of superposition should be approximately valid.

The investigation is carried out with an assumed external load $F_d = 1000$ Pa to simulate possible wind loads.

Firstly, whether superposing cold bending and external loads is possible was tested on a 10 mm glass panel, cold bent with a radius of 20 m. The curvature τ for a radius of 20 has a value of 0.2335 radians, as shown in figure 7.1b.



(a) Wind Load



(b) Cold Bending Displacement

Figure 7.1: Loads and displacement of the model.

The cold bending stresses alone gave about 17.90 MPa principal stresses in the middle of the plate where pure bending stresses are shown, see figure 7.2.

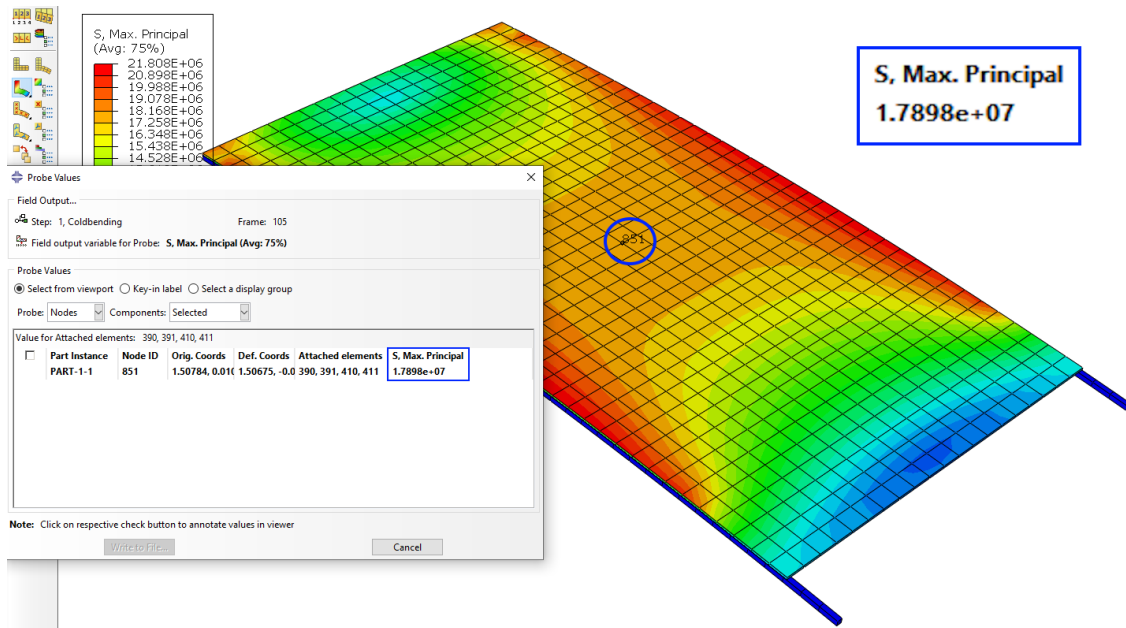


Figure 7.2: Maximum principal stresses caused by Cold Bending a 10 mm glass plate with a radius of 20 m

Afterwards, a similar model was created of an already curved glass geometry that would resemble the cold bent glass panel but without the stresses it induces, and was used to measure external load effects. A 1000 Pa wind load was added on top of the geometry as a "pressure" load in Abaqus and aimed upward to simulate the wind-suction effect as shown in Figure 7.1a.

To simulate that the glass will be glued to the frame after cold bending, the long edges were modeled to be restricted from vertical displacement by adjusting the interaction property between the glass and the frame in Abaqus to be set as "Normal behavior" and then disallow separation after contact, that is, after the cold bending process is done (see Figure 7.3).

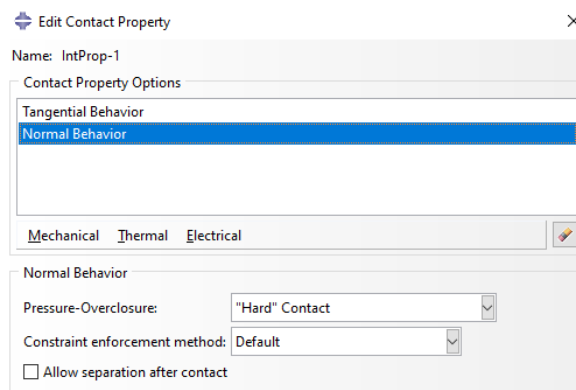


Figure 7.3: Interaction Property Settings.

The simulation gave a maximum principal stress of 3.64 MPa in the middle of the plate, as shown in figure 7.4.

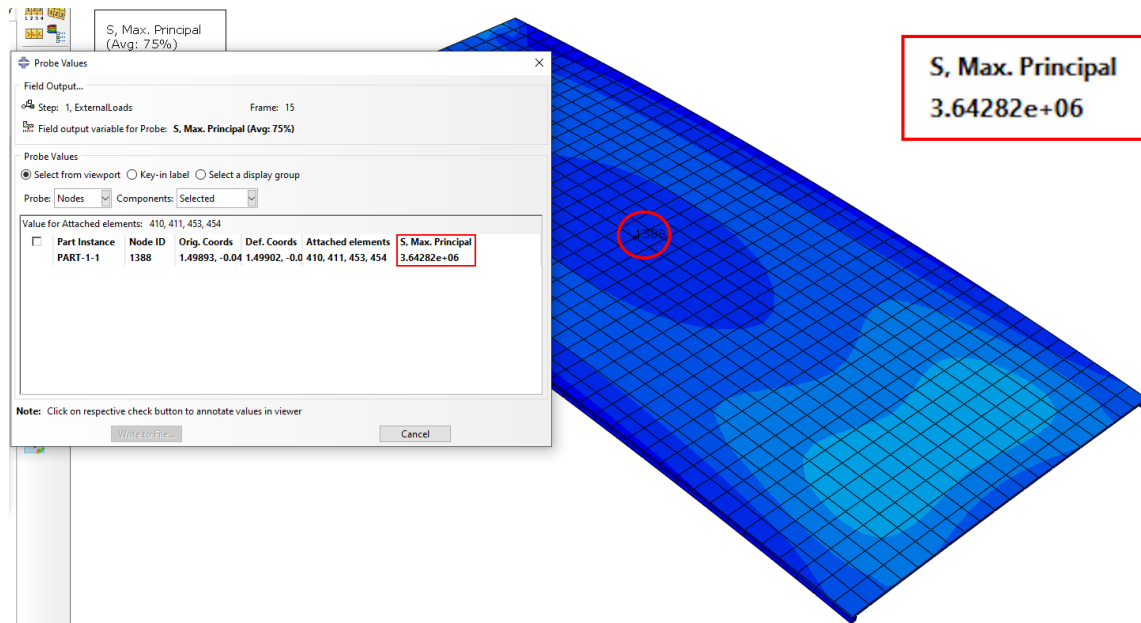


Figure 7.4: Maximum principal stress in the middle of the curved plate caused by external loads alone

To test whether superposing is possible, a combined model was created. The wind load was added on top of the plate in the cold bent glass model in Figure 7.2, the long edges were modeled to not separate after contact by changing the interaction property in Abaqus to "normal behavior" and unchecking the box that allows separation after contact. This will cause the plate to remain intact with the frame after initiating contact after cold bending the glass. Then a wind load of 1000 Pa was added and the combined maximum principal stresses measured up to 21.71 MPa, as seen in figure 7.5. If we try to combine the separate loads analytically, $3.64 + 17.90$, we get 21.54, which is very close to 21.71 MPa.

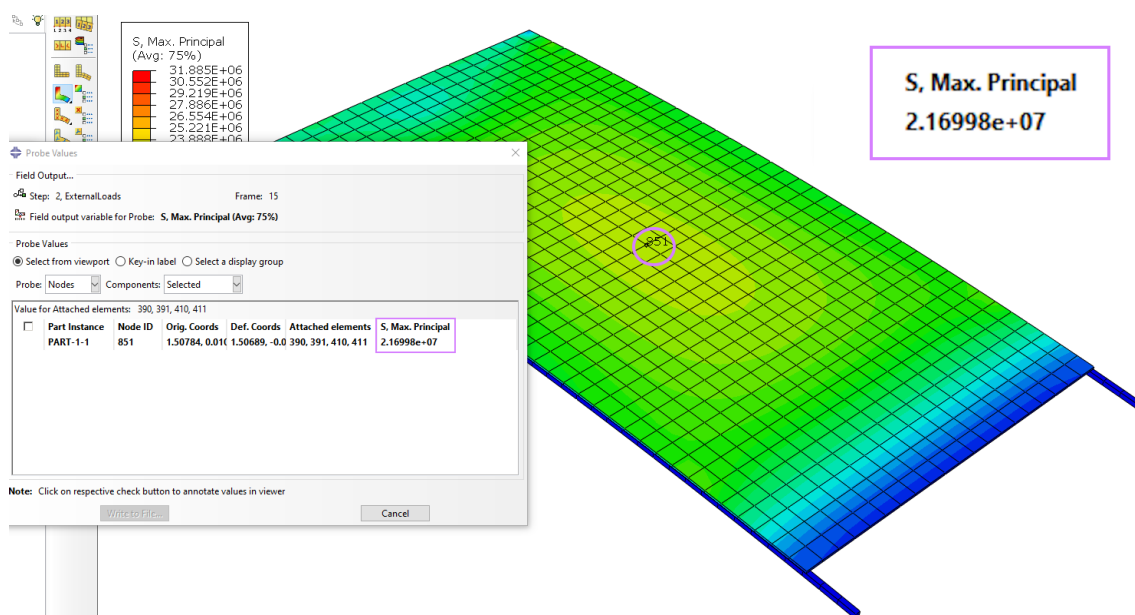


Figure 7.5: The combined loads analysis of cold bending and wind load.

The cold bending stress can be calculated using analytical methods, Euler-Bernoulli and Kirchhoff-Love, gave 17.50 and 18.48 MPa, which are very close approximations. To calculate the external loads with hand calculations, it is reasonable to try and simplify the model by trying to calculate it on a flat (non- initially curved panel) to see if we can simplify it by assuming it is a rectangular pane supported on all edges, for simplification purposes, and add the wind load on top and see if it gives the same 3.64 MPa stress.

To calculate the maximum tensile bending stress for large deflections of rectangular panes supported on all edges, which is the maximum principal stress, the formula (B.1) from SS-EN 16612:2019 [6] will be used:

$$\sigma_{max} = k_1 \frac{a^2}{h^2} F_d$$

Where $h = h_{eq;\sigma}$ for laminated glass.

The coefficient k_1 is obtained from Table B.1 by first calculating p^* and $\lambda = a/b$

$$p^* = \left(\frac{A}{4h^2}\right)^2 \frac{F_d}{E_{glass}} = \left(\frac{3 \cdot 1.5}{4 \cdot (10e-3)^2}\right)^2 \frac{1e3}{70e9} = 1.81$$

$$\lambda = a/b = 1.5/3 = 0.5$$

At $\lambda = 0.5$, the table values are 0.595 for $p^* = 1$ and 0.580 for $p^* = 2$.

We now interpolate for $p^* = 1.81$ using the correct values.

$$k_1 = 0.595 + \left(\frac{1.81-1}{2-1}\right) \cdot (0.580 - 0.595) = 0.58285$$

Which gives the maximum tensile stress:

$$\sigma_{max} = 0.58285 \cdot \frac{1.5^2}{(10e-3)^2} \cdot 1000 = 13.1 \text{ MPa}$$

To verify this analytical value, it was investigated in Abaqus by modeling the flat rectangular pane supported on all edges. Which gave a maximum principal value of 11.39 MPa as shown in 7.6.

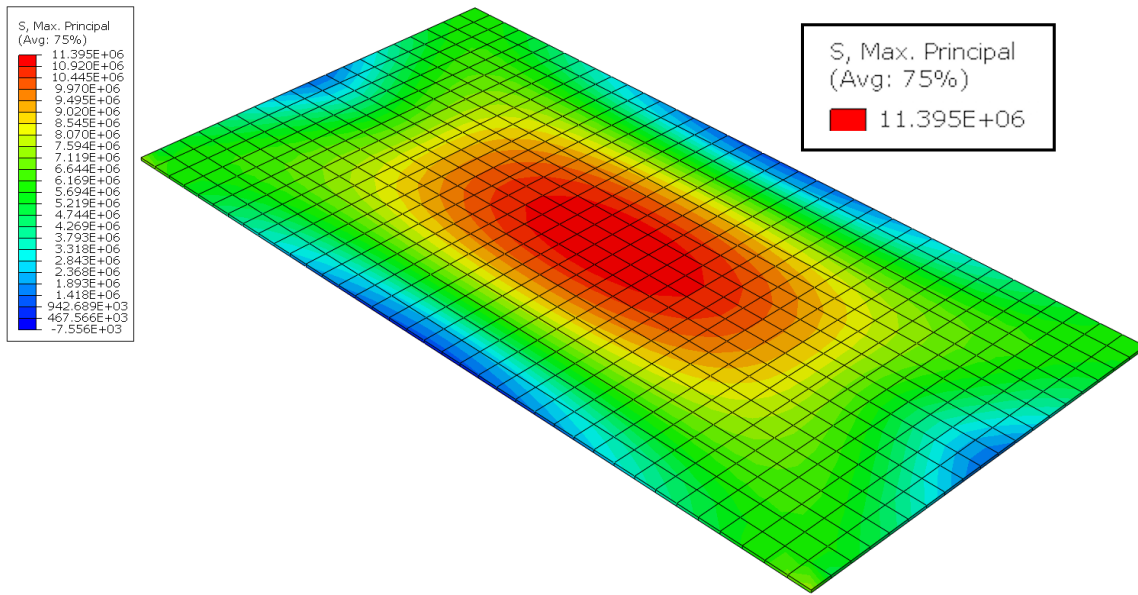


Figure 7.6: Numerical stress analysis of a rectangular panes supported on all edges.

The variation could likely be due to the formula being made for large deflections. A different method was tested and table 7.7 was used:

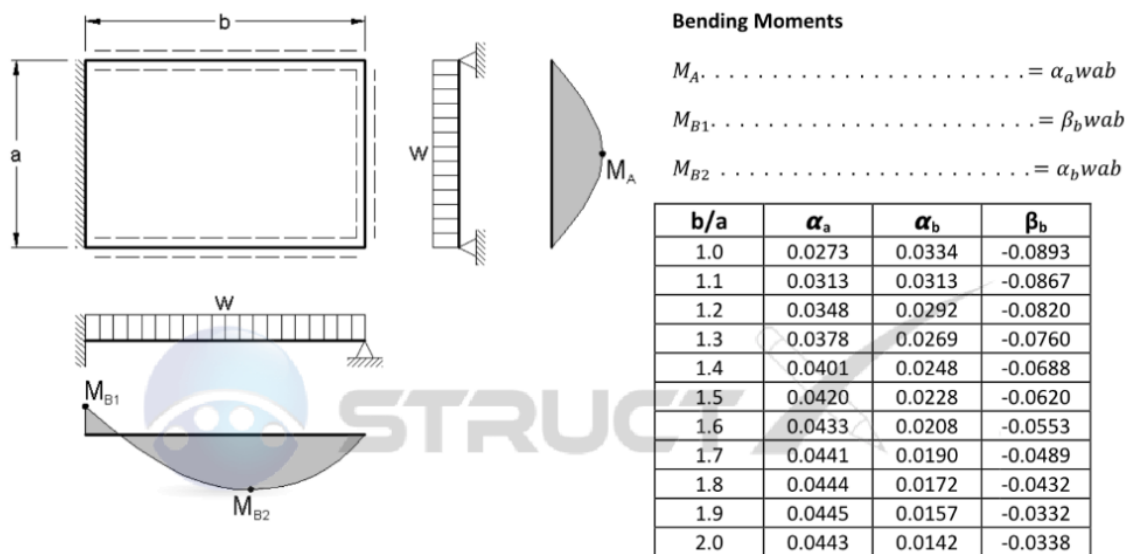


Figure 7.7: Moment calculation for a simply supported plate on three Edges and one fixed with UDL [54]

For $b/a = 3/1.5 = 2.0$, the following coefficients are obtained:

α_a	α_b	β_b
0.0443	0.0142	-0.0338

To obtain the maximum principal stress, the most critical moment should be calculated. Therefore, the biggest coefficient will be used to calculate M_A

$$M_A = \alpha_a q a b = 0.0443 \cdot 1000 \cdot 1.5 \cdot 3.0 = 199.35 \text{ Nm}$$

Finally, the stress is calculated using:

$$\sigma = \frac{M y}{I} = \frac{199.35 \cdot \frac{0.01}{2}}{\frac{0.013}{12}} = 11.961 \text{ MPa}, \text{ which aligns well with the 11.39 MPa result obtained from Abaqus on the flat rectangular glass model.}$$

However, it does not appear to match with the curved surfaces as the maximum principal stress is around 3.64 MPa in the middle of the plate and higher in other areas with values ranging from 5-10 MPa, as shown in Figure 7.4 & 7.8. Then compared with the rectangular flat model in figure 7.6.

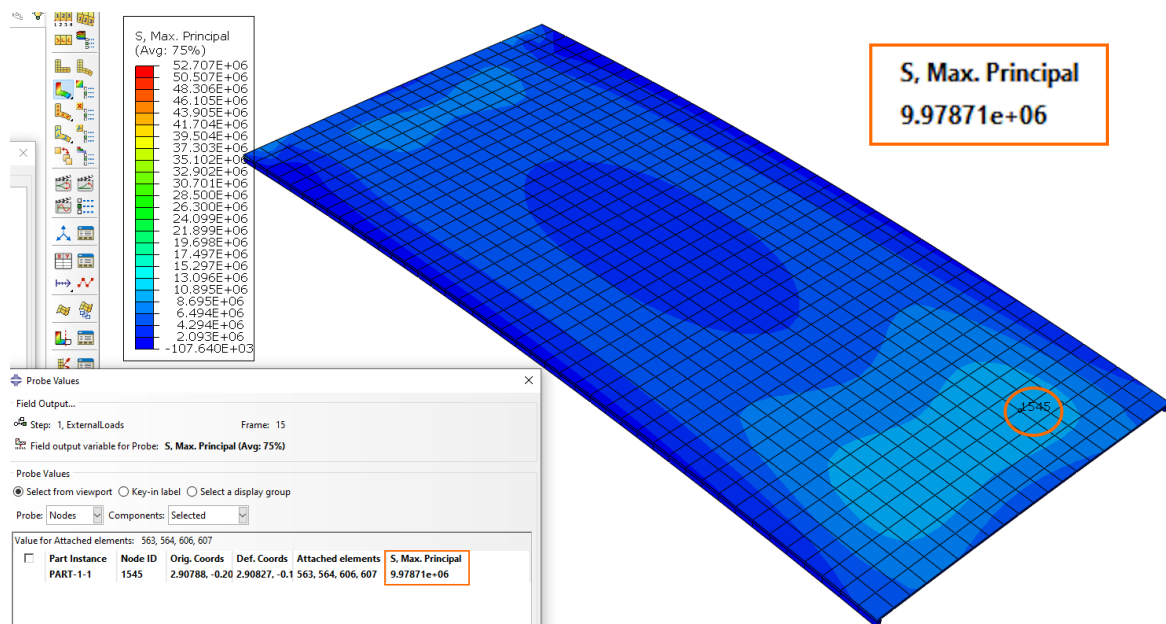


Figure 7.8: Maximum principal stress in other areas of the curved plate caused by external loads alone

This means that it is probably not possible to assume that the already curved geometry to behave the same as a flat rectangular simply supported plate for simplification purposes when compared to Figure 7.6.

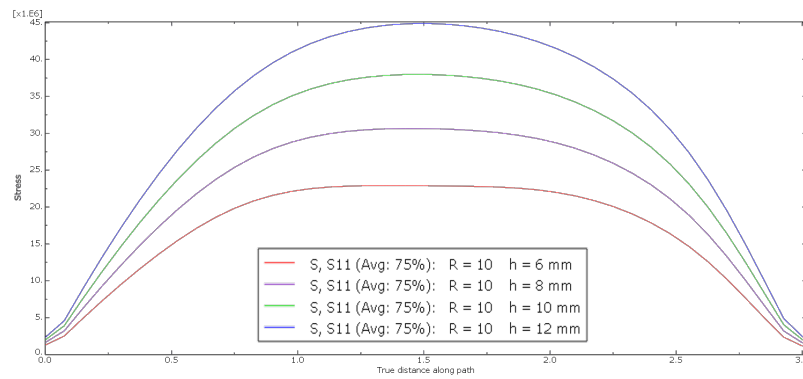
8 Discussion

8.1 Monolithic Glass

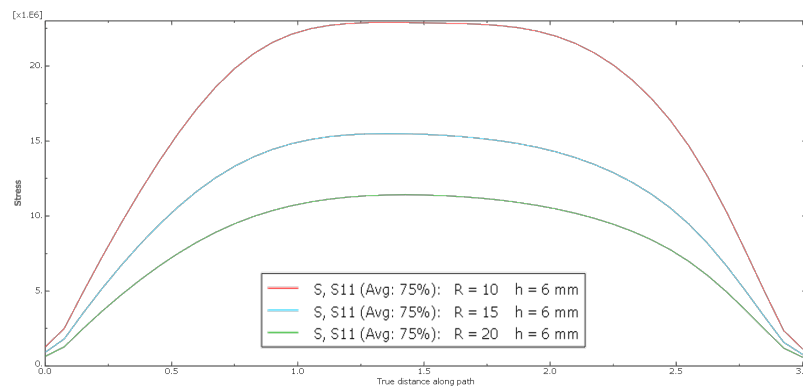
8.1.1 Analysis of Monolithic glass cold bending behavior

Numerical cold bending stresses

Looking at the stress results in tables 5.2 & 5.3 & 5.4, it is apparent that thinner plates and lower curvatures are favorable for cold bending of glass panels, as illustrated in figure 8.1. The bending strength of tempered glass is around 86.6 MPa as calculated in section 2.1.



(a) Stress distribution along center line for different thicknesses h of monolithic glass (6 mm to 12 mm) showing increased stress with greater thickness.



(b) Stress distribution along center line for different radii R of monolithic glass (10 m to 20 m) showing increased stress with smaller radii (i.e., bigger curvature).

Figure 8.1: Stress distribution plots comparing varying glass thickness and curvature in monolithic glass.

For the glass to be able to withstand cold bending with potential external loads on top,

it is favorable for the cold bending stresses to be as low as possible. Load combinations are discussed in chapter 7.

Numerical vs Analytical cold bending stresses

Overall, the analytical methods have shown to be very promising in predicting these cold bending stresses of the glass panel. This is realized by observing the plots in figure 5.5.

Table 5.5 presents the differences between the normal stresses in the x-direction σ_{xx} obtained from Abaqus simulations and the theoretical stresses calculated using Euler-Bernoulli beam theory $\sigma_{cb,e}$.

The results show that the deviation decreases with increasing radius, indicating improved agreement with Euler-Bernoulli theory for larger curvature radii and a more linear behavior. This is consistent with the underlying assumptions of the theory, which is derived under the condition of small curvature ($R = 20$ m).

At a radius of 20 m and thicknesses above 10 mm, the differences start becoming negative, suggesting a slight overestimation by the theoretical model; this will apply to the other radii if we had kept increasing their thicknesses, the matching point or the turning point where it goes from underestimation to overestimation differs depending on which radius and seems to occur at lower thicknesses for the higher radii. That is because at higher radii, or in other words, smaller curvature, stress is distributed better, making it more likely for analytical methods to overestimate the actual stresses. These findings highlight the limitations of Euler-Bernoulli theory in accurately capturing stress distributions, and they underscore the necessity of using higher-order theories or finite element methods in such cases.

While the theoretical stress calculated from Euler-Bernoulli theory scales linearly with thickness and radius (h/R ratio), the Abaqus simulations incorporate geometric nonlinearities, including shear deformation and out-of-plane effects, which are not accounted for in the classical beam theory. These additional factors contribute to the observed discrepancies, especially at lower radii, where the limitations of the Euler-Bernoulli assumptions become more pronounced.

Table 5.6 highlights how Kirchhoff Love's plate theory does better at approximating the cold bending normal stresses in general but also particularly for larger curvatures meaning a large deflection with a smaller radius than Euler Bernoulli's beam theory, which is expected given that the plate theory correction factor $1 - \nu^2$ is taken into account; it accounts for Poisson's ratio influence in plates. It is also realized here that the discrepancies decrease with increasing radii, effectively a smaller curvature.

8.1.2 Analytical limitations (h/R)

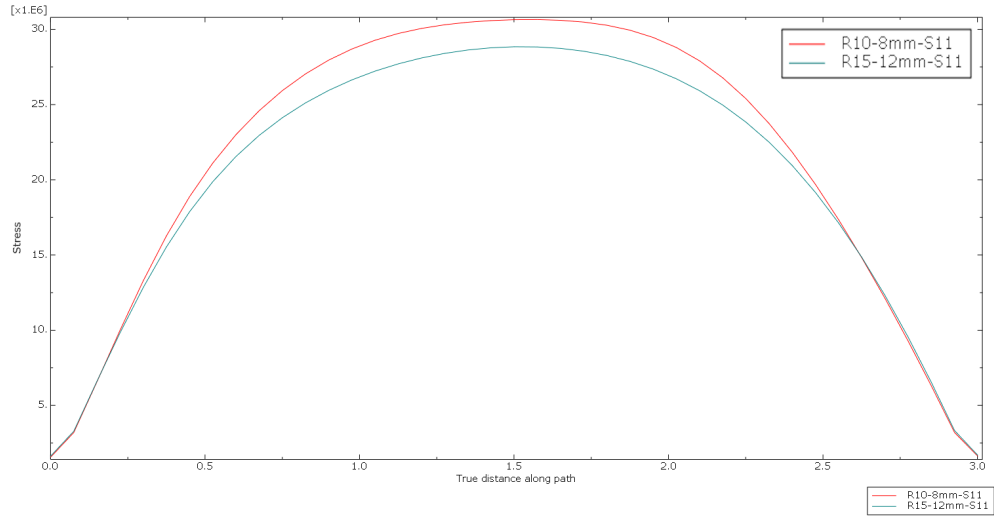
In the analytical approach, using the derived formulas, the stress is completely dependent on the h/R ratio.

$$\sigma_{cb,e} = \frac{Eh}{2R}, \quad \sigma_{cb,k} = \frac{Eh}{2R(1 - \nu^2)}$$

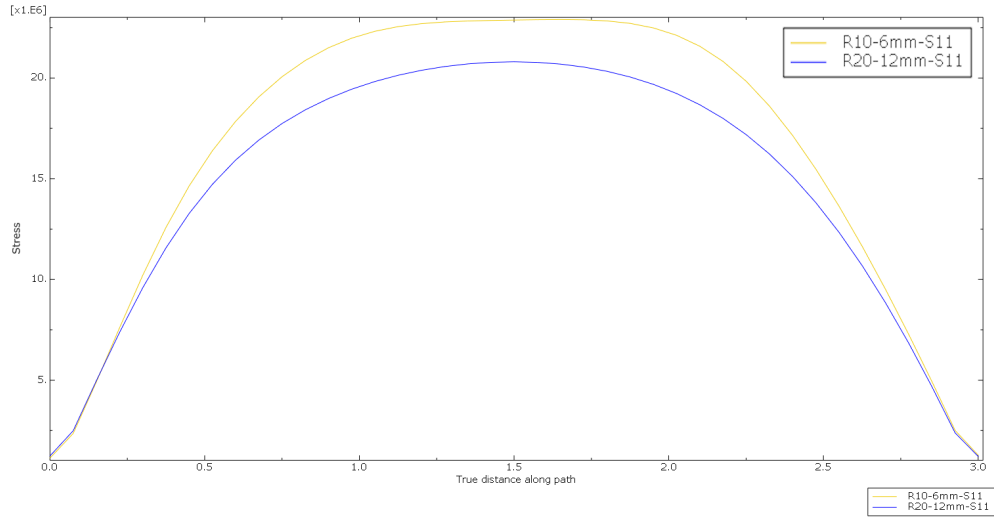
For example, a 8 mm & $R = 10$ m, gives the same bending stresses as a 12 mm & $R = 15$ mm, as shown in figure 8.2a, where for both cases, $h/R = 0.8$. However, in real scenarios, where non-linearity and other effects play a role, the stresses obtained from the numerical analysis in Abaqus, for both of these, are close but not exactly identical.

The same can be found when observing a 6 mm, $R = 10$ m, which gives the same results as 12 mm, $R = 20$ m in the analytical approach, a h/R ratio of 0.6, but it differs numerically, as demonstrated in figure 8.2b.

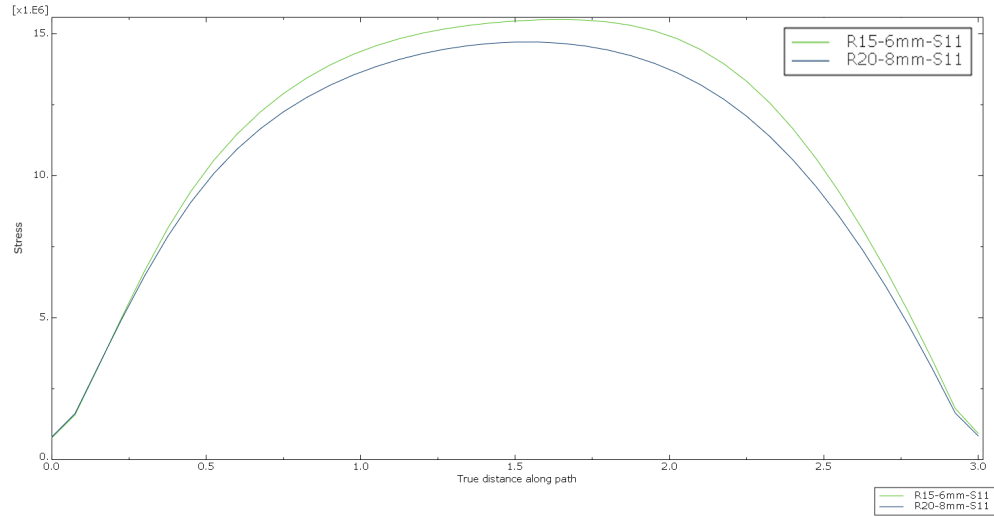
The numerical data show lower stresses for a larger radius despite having a constant h/R ratio. This concludes that having a larger radius in cold bending is more favorable than decreasing the thickness of the plate, to obtain lower cold bending stresses.



(a) $R = 10$ & $h = 8$ mm and $R = 15$ & $h = 12$ mm



(b) $R = 10$ & $h = 6$ mm and $R = 20$ & $h = 12$ mm



(c) $R = 15$ & $h = 6$ mm and $R = 20$ & $h = 8$ mm

Figure 8.2: Plots illustrating stress differences between two models with the same h/R ratio.

8.1.3 Maximum Principal Stress

Looking at table 8.1, it can be observed that the difference between normal stresses in the x-direction and maximum principal stresses decreases with decreasing thickness or increasing radius, resulting in a more uniform and uniaxial stress state. Thinner plates are more flexible and thus can be bent with less resistance. This reduces overall cold-bending stresses, which in itself indirectly reduces the development of significant stresses in other directions than the primary direction. Similarly, a larger bending radius corresponds to a gentler curvature, resulting in lower bending stresses in all directions. The smaller the curvature, the closer the stress state is to pure in-plane tension in one direction, where shear and transverse stresses are negligible.

The difference in stress between maximum principal stress and tensile stresses in the bending direction gets smaller with thinner thicknesses, and dramatically decreases with a larger radius. A larger radius has a larger impact than a thinner plate. This is utilized in chapter 7.

Table 8.1: Differences between the normal stresses in the x-direction and the maximum principal stresses.

Radius	$\sigma_1 - \sigma_{xx}$			
	6 mm	8 mm	10 mm	12 mm
10	0.71 (3.0%)	0.82 (2.6%)	0.94 (2.4%)	1.08 (2.3%)
15	0.08 (0.5%)	0.23 (1.1%)	0.27 (1.1%)	0.31 (1.1%)
20	0.07 (0.6%)	0.10 (0.7%)	0.10 (0.6%)	0.11 (0.5%)

8.2 Laminated Glass

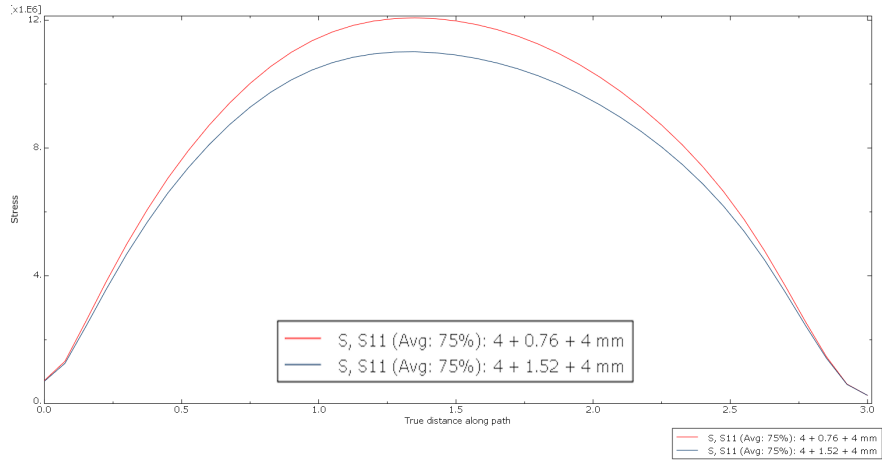
8.2.1 Analysis of Laminated glass cold bending behavior

The investigation of cold bending stresses was carried on laminated glass with various glass thicknesses and two main interlayer thicknesses, namely, 0.76 mm and 1.52 mm, which are popular interlayer thicknesses and corresponds to two and four layers of PVB with a thickness of 0.38 mm.

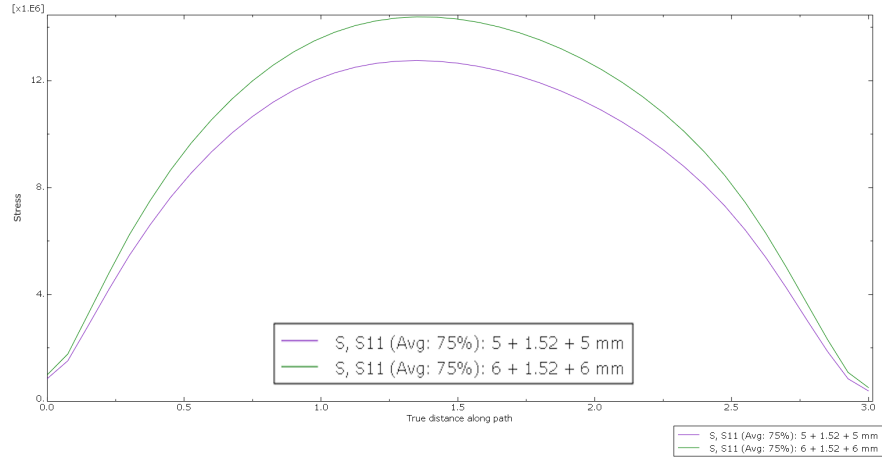
Numerical cold bending stresses

It is apparent, as for monolithic glass, that thinner plates and lower curvatures (higher bending radii) are favorable for cold bending of laminated glass panels. Laminated glass with a PVB thickness of 1.52 mm exhibited lower stresses than that of which had a PVB thickness of 0.76 mm, as shown in figure 8.3a. The thicker interlayer increases overall flexibility, making the laminated glass panel softer and easier to bend. This added compliance allows the glass layers to deform more uniformly and absorb strain

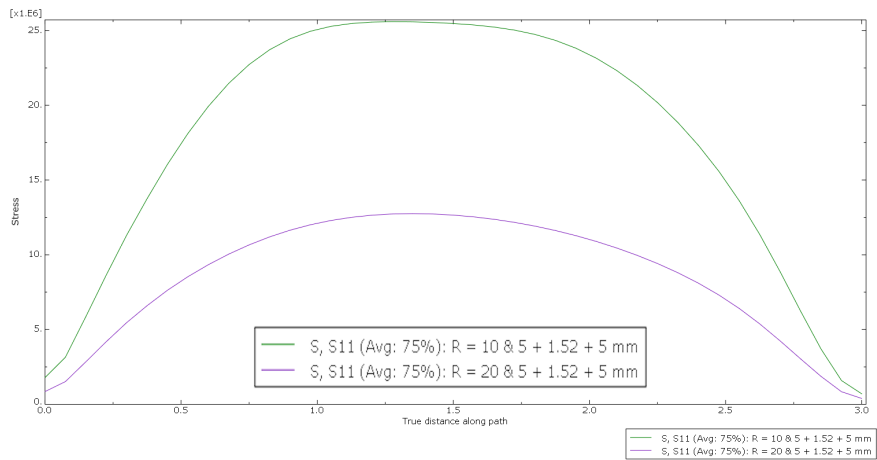
more effectively, reducing peak stress concentrations in the glass and distributing the stresses more effectively during bending.



(a) Stress distribution comparison along the center line for laminated glass with 0.76 mm vs. 1.52 mm PVB interlayer thickness.



(b) Stress distribution comparison along the center line for laminated glass with 5 mm vs. 6 mm glass ply thickness.



(c) Stress distribution comparison along the center line for laminated glass with a radius of 10 m vs. 20 m for

Figure 8.3: Stress distribution plots comparing varying glass, interlayer thickness and curvature.

This concludes that cold bending stresses decreases with:

- Thinner glass plates h_i (e.g. 6+1.52+6 mm \rightarrow 5+1.52+5 mm)
- Smaller curvatures κ (e.g. R = 10 m \rightarrow R = 20 m)
- Thicker PVB interlayer h_{int} (e.g. 4+0.76+4 mm \rightarrow 4+1.52+4 mm), which effectively is the same as a thinner laminate effective thickness (e.g. h_{eff} =6.68 mm \rightarrow h_{eff} =6.51 mm). That is because it was established in Section 6.2, from tables 6.2 & 6.3, that for the same glass ply thickness h_i but a thicker interlayer, the effective thickness h_{eff} decreases, making the laminate softer and therefore corresponds to a thinner monolithic glass plate.

Numerical vs Analytical cold bending stresses

The data, as in an earlier chapter, compare normal stresses in the x-direction σ_{xx} from Abaqus (S11) with analytical predictions from the Euler-Bernoulli $\sigma_{cb,e} = \frac{Eh}{2R}$ and Kirchhoff-Love $\sigma_{cb,k} = \frac{Eh}{2R(1-\nu^2)}$ theories, which is shown in tables 6.4 & 6.5 & 6.6 for interlayer thickness of 0.76 mm and tables 6.9 & 6.10 & 6.11 for interlayer thickness of 1.52 mm.

Both theories do a good job at predicting the cold bending stresses when compared to the numerical results from Abaqus, as observed from tables 6.7, 6.8 for 0.76 mm interlayer & 6.12, 6.13 for 1.52 mm interlayer, with errors increasing as the effective thickness h_{eff} increases and radius decreases (i.e., higher curvature). The deviations are plotted in figures 6.2 and 6.3.

This indicates that classical analytical models are valid only for thin, low-curvature plates, while finite element methods like Abaqus are necessary for more accurate stress prediction in complex geometries. However, both theories tend to overpredict the cold bending stresses, up to the 18% discrepancy. This is because even though an effective thickness is calculated for the laminates, the analytical methods like Euler-Bernoulli and Kirchhoff-Love, still assume perfect bonding and linear elastic behavior across the full thickness. These models cannot fully capture the viscoelastic and compliant nature of the PVB interlayer. The effective thickness has helped get an approximate prediction, but it is still an approximation that tends to behave more like a stiffer monolithic section than the actual softer laminated system. As a result, the models will overpredict the stresses because they do not account for the partial shear transfer or time-dependent behavior of the interlayer, but also do not account for geometrical nonlinearities.

The overprediction of the cold bending stresses given by the analytical approach could be an advantage in terms of safely designing glass structures. That is because it introduces a conservative safety margin. Since glass is brittle and prone to sudden failure, overestimating stresses ensures that the structure is not underdesigned. This makes simplified methods safer for preliminary design, as they reduce the risk of unexpected failure by encouraging more robust solutions.

8.2.2 Maximum Principal Stress

In the previous chapter it was concluded that if the stress state is a predominantly uniaxial tension in the x-direction, then we can conclude that the maximum principal stress and S_{11} (or σ_{xx}) are nearly the same. This would still apply for laminated glass panels as it is independent on what kind of glass it is and more on what type of bending is taking place, which in this case is uniaxial bending in the x-direction.

Observing tables 8.2 & 8.3, we notice the same behavior from monolithic glass as for laminated glass, where the difference between normal stresses in the x-direction and maximum principal stresses decreases with decreasing thickness or increasing radius, resulting in a more uniform and uniaxial stress state.

Thinner plates are more flexible and thus can be bent with less resistance. This reduces overall cold-bending stresses, which in itself indirectly reduces the development of significant stresses in other directions than the primary direction. Similarly, a larger bending radius corresponds to a gentler curvature, resulting in lower bending stresses in all directions. The smaller the curvature, the closer the stress state is to pure in-plane tension in one direction, where shear and transverse stresses are negligible.

The difference in stress between maximum principal stress and the normal tensile stresses in the bending direction decreases with thinner plates, and dramatically decreases with a larger radius. Larger radii tend to have a stronger impact.

Table 8.2: Differences between the normal stresses in the x-direction and the maximum principal stresses for laminated glass with the interlayer thickness 0.76 mm.

Radius	$\sigma_1 - \sigma_{xx}$			
	3+0.76+3 $h_{eff}=5.27$	4+0.76+4 $h_{eff}=6.68$	5+0.76+5 $h_{eff}=8.10$	6+0.76+6 $h_{eff}=9.52$
10	0.5 (2.6%)	0.69 (2.8%)	0.78 (2.7%)	0.88 (2.6%)
15	0.17 (1.3%)	0.21 (1.3%)	0.15 (0.7%)	0.26 (1.2%)
20	0.07 (0.7%)	0.08 (0.7%)	0.06 (0.4%)	0.1 (0.6%)

Table 8.3: Differences between the normal stresses in the x-direction and the maximum principal stresses for laminated glass with the interlayer thickness 1.52 mm.

Radius	$\sigma_1 - \sigma_{xx}$			
	3+1.52+3 $h_{eff}=5.18$	4+1.52+4 $h_{eff}=6.51$	5+1.52+5 $h_{eff}=7.86$	6+1.52+6 $h_{eff}=9.23$
10	0.34 (1.9%)	0.7 (0.3%)	0.77 (0.3%)	0.87 (2.9%)
15	0.15 (1.2%)	0.19 (1.2%)	0.21 (1.2%)	0.23 (1.2%)
20	0.07 (0.8%)	0.07 (0.6%)	0.06 (0.5%)	0.09 (0.6%)

8.3 Load Combinations

It was also found that using the S11 stress component (i.e., σ_{xx}) as an approximation for the maximum principal stress remains valid in most cases, particularly when bending is uniaxial. Across the simulations, the difference between σ_{xx} and σ_1 remained below 3%, suggesting that simplified evaluations using σ_{xx} can be considered safe and efficient in practice, especially for preliminary assessments, without requiring complete 3D stress evaluations and complex calculations.

The analysis of load combinations in cold bent glass has shown the feasibility of superposing intrinsic and extrinsic stresses induced by cold bending and external loads such as wind loads. The results of numerical simulation showed that these stresses can be reliably added together with great accuracy, supported by almost an exact match between the results of the combined model and the sum of individual cases. For example, in the case of a 6 mm monolithic glass panel with a cold bending radius of 20 m, the maximum principal stress due to cold bending alone was 17.90 MPa, while wind loading alone induced a maximum principal stress of 3.64 MPa. When both loads were applied simultaneously, the resulting principal stress was 21.71 MPa, demonstrating a close match with the sum of the individual cases ($17.90 + 3.64 = 21.54$ MPa), with only a deviation of 0.17 MPa, a difference less than 1%. This validates the assumption, that because of the elastic behavior of the glass, the principle of superposition holds reasonably well for typical and simple loading scenarios.

However, attempts to apply simplified analytical models, such as those assuming flat, four-edge simply supported panels, proved to be not quite accurate in predicting the behavior of curved geometries under external loads.

Although cold bending stresses could be approximated using the Euler-Bernoulli or Kirchhoff-Love theories, external loads applied to an already curved geometry do not behave the same as in flat panels. Analytical estimates based on flat, simply supported on four edges configurations did not produce the same stress distribution or magnitude as in the numerically curved structures on top of a frame models, indicating that the curvature, as well as the boundary conditions, significantly affect structural response under external loading. When the wind load was analytically estimated on a flat, simply supported glass pane on four edges using EN 16612, the stress was 13.1 MPa, while the numerical result from a finite element model of the same flat configuration was 11.39 MPa, still far above the 3.64 MPa observed in the curved configuration. This increase in stress when using flat-panel approximations highlights the critical role of initial curvature, as well as boundary conditions, which redistributes load and reduces local stresses differently.

In summary, the study confirms that while stress superposition is valid and practical in numerical analysis, reliance on analytical expressions derived for flat plates can pose a challenge under combined loading scenarios. Numerical simulations remain essential for accurate prediction when geometric nonlinearity, material properties, and complex boundary conditions are present.

9 Conclusion

9.1 The goal of the study

Looking back at the issues and research questions of this study:

- How can cold-bent glass be modeled?
- What parameters and conditions are crucial?
- Is it possible to develop simplified models that maintain sufficient accuracy for practical use?
- How should other loads be combined with the bending stresses that arise during cold bending of glass?

1. Glass is a linear elastic material and can be modeled as such. While the PVB interlayer in laminated glass is inherently a time- and temperature-dependent viscoelastic material, it was proven to be possible to model it as linear elastic by assigning it a very low shear and elasticity modulus that would account for its long-term relaxation and creep for simplification purposes of avoiding complex viscoelastic evaluations. Cold bent glass can be modeled by creating a flat rectangular glass plate in Abaqus, then adding a cylindrical displacement on one of the edges, bending it down on top of a curved substructure with a fixed radius that would act as a shaping frame made out of steel or aluminum. The other edge would be tied to the frame with a tie-constraint, which is fixed, and a surface-to-surface contact property applied to the surfaces.

2. Through numerical and analytical methods, cold bent glass has been shown to exhibit lower stresses with thinner glass plates and larger radii. In laminated glass, it has also been shown that PVB played a role in distributing these stresses because of the interlayer's softening abilities; it creates a softer glass configuration, making thicker interlayers more favorable to reducing cold bending stresses. The boundary conditions had a notable impact on the stress concentrations, particularly near the edges that interacted with the supporting frame, leading to the detection of elevated stress levels which are unfavorable and should be taken into account. In short, the most important parameters and the most crucial are the thickness of the glass panel h or h_{eff} for laminated glass, the curvature determined by the radius of the frame substructure R , the thickness of the interlayer in laminated glass h_{int} , as well as the constraints. To cold bend glass, you simply fix it on one edge and deform it cylindrically on the other edge, on top of a frame substructure with a fixed radius, on which the glass will rest on top of. The influence of the cold bending curvature on the cold bending stress is the largest, followed by the thickness of the glass panes, and the influence of the interlayer thickness is small. Less predictable are the results of the variation of width, but the edge effects increase with increasing width. In laminated glass, the

overprediction could be beneficial because it introduces a conservative safety margin by ensuring that the structure is not underdesigned. This makes simplified methods safer for preliminary design, as they reduce the risk of unexpected failure by encouraging more robust solutions.

3. This study has concluded that it is possible to develop simplified models to predict the stresses in glass induced by cold bending while maintaining sufficient precision for practical use. Two models were evaluated. Namely, the Euler-Bernoulli method and the Kirchhoff-Love method. These methods are based on classical beam and plate theories that were found to be suitable for approximating cold bending stresses in thin glass plates. The models have proven to be effective and reliable methods compared to numerical methods, with slight deviations highlighting the limitations of these methods. The analytical approach is limited to predicting linear elastic pure bending behavior in thin plates with small deformations. It cannot account for edge effects, large deformations and curvatures, thick plates, geometrical nonlinearities, and heterogeneity and anisotropy. The Kirchhoff-Love plate theory has shown to be slightly more accurate in predicting cold bending stresses, but overall it was not too big of an improvement. In laminated glass, the methods have been shown to consistently overpredict the cold bending stresses, not by a large margin, but considerable enough to mention. This is speculated to be because of the complex behavior of the PVB interlayer, which is hard to fully capture despite having attempted to account for it by implementing an effective thickness method.

4. Numerically, it has been shown that it is possible to superpose external loads such as stresses induced by wind with cold bending stresses by, for example, simulating a suction load in a direction opposite to the direction of the cold bending, resembling the behavior to that of wind. When simulating cold bending alone, the wind loads alone, then superposing these stresses, they have matched up to great accuracy with the combined model simulation. The challenge was to approximate the wind loads on a curved structure with given constraints from the model, as simplifying the model by assuming it is a flat, rectangular pane and supported on all edges did not give the same results. In short, it is possible to superpose cold bending stresses with external load stresses, but finding a simplified method to approximate the external load stresses remains unclear.

9.2 Additional notes

1. The cold bending stress of both monolithic glass and PVB laminated tempered glass panes has given maximum stresses near edges due to edge effects, which should be accounted for using numerical methods.
2. The thickness of the PVB interlayer has shown little impact on the cold bending stresses. Although it may be beneficial to bearing capacity, its effect can be ignored in cold bending.
3. When the glass thickness is large, the curvature is large and the interlayer thickness is small, meaning the cold bending stresses are large, the bearing capacity of the glass panes would then be controlled by the cold bending stresses and not external loads. External loads such as wind are more crucial when the glass panel is thin, which would impact the bearing capacity of the glass. The glass should not be too thin or thick, and a smaller curvature is always favorable.
4. When laminated glass is used, the effects on the mechanical and visual properties of the interlayer due to cold bending should be investigated.
5. The use of continuum solid-shell elements to model shell-like solids instead of conventional shell elements should be investigated.

Bibliography

- [1] Mehran Arbab and James J Finley. ‘Glass in architecture’. In: *International Journal of Applied Glass Science* 1.1 (2010), pp. 118–129.
- [2] Rudolf F Graf. *Modern dictionary of electronics*. Elsevier, 1999.
- [3] Wikipedia contributors. *Soda–lime glass — Wikipedia, The Free Encyclopedia*. 2025.
- [4] Rubieyat Bin Ali, Md Mofizul Islam and Moushtakim Billah. ‘Sophisticated developments and advanced applications of glass structure: summary of recent research’. In: *World Scientific News* 124.1 (2019).
- [5] CEN. *Eurocode 10 — Design of glass structures — Part 1: General rules*. prEN 19100-1:2023. 2023.
- [6] CEN. *Glass in building – Laminated glass and laminated safety glass – Determination of interlayer viscoelastic properties*. prEN 16612:2019. 2019.
- [7] David Z Yankelevsky. ‘Strength prediction of annealed glass plates–A new model’. In: *Engineering structures* 79 (2014), pp. 244–255.
- [8] Dragon Glass. *FAQ: Heat Strengthened Glass vs Toughened Glass*. Accessed: 2025-04-23. n.d. URL: <https://szdragonglass.com/faq-heat-strengthened-glass-vs-toughened-glass/>.
- [9] Jens Malmborg. ‘A finite element based design tool for point fixed laminated glass’. MA thesis. Lund’s University, 2006.
- [10] Mathieu Hubert and Peter J Lezzi. ‘Glass: Annealing and tempering’. In: (2021).
- [11] Maximilian Laurs, Benjamin Schaaf, Pietro Di Biase and Markus Feldmann. ‘Determination of prestress profiles in chemically toughened glass by means of photoelasticity’. In: *GPD Glass Performance Days* (2019), pp. 145–49.
- [12] GlassOnWeb. ‘The Influence of the Distribution of Residual Stress on Strength Tests’. In: *GlassOnWeb* (2024). URL: <https://www.glassonweb.com/article/influence-distribution-residual-stress-strength-tests>.
- [13] Wikipedia contributors. *Laminated glass — Wikipedia, The Free Encyclopedia*. 2024. URL: https://en.wikipedia.org/wiki/Laminated_glass#:~:text=Laminated%20glass%20was%20invented%20in,did%20not%20break%20into%20pieces..
- [14] CEN. *Glass in building – Laminated glass and laminated safety glass – Determination of interlayer viscoelastic properties*. prEN 16613:2019. 2019.
- [15] Qingdao Laurel Glass Technology Co., Ltd. *Clear PVB/SGP Laminated Glass For Modern Design Glass Building*. 2025. URL: <https://www.laurelglasstech.com/safety-glass/laminated-glass/clear-pvb-sgp-laminated-glass-for-modern.html>.
- [16] Glazing Centre. *Why and When to Use Laminated Glass*. n.d. URL: <https://glazingcentre.co.uk/why-and-when-to-use-laminated-glass/>.

- [17] We Want to Learn. *Posts tagged "Anticlastic" – We Want to Learn*. 2025. URL: <https://wewanttorearn.wordpress.com/tag/anticlastic/>.
- [18] Pulp Studio. *Bent Glass – Pulp Studio*. 2025. URL: https://www.pulpstudio.com/bent-glass/?utm_source=chatgpt.com.
- [19] Jan Wurm. *Glass structures: design and construction of self-supporting skins*. De Gruyter, 2007.
- [20] Helmut Pottmann, Michael Eigensatz, Amir Vaxman and Johannes Wallner. ‘Architectural geometry’. In: *Computers & graphics* 47 (2015), pp. 145–164.
- [21] Franz Pölzl. ‘Mechanical behavior of cold-bent insulating glass units’. PhD thesis. Graz University of Technology, 2017.
- [22] Wikipedia contributors. *Paraboloid — Wikipedia, The Free Encyclopedia*. 2025. URL: <https://en.wikipedia.org/wiki/Paraboloid>.
- [23] Maximilian Laurs. ‘Numerical and Experimental Investigations on the Inherent Stress State of Cold-bent Glass’. In: *Challenging Glass Conference Proceedings*. Vol. 7. 2020.
- [24] John Hill. *Emporia’s Double-Curved Glass*. Accessed: 2025-05-14. 2014. URL: <https://www.world-architects.com/it/pages/products/emporia-double-curved-glass>.
- [25] Dlubal Software. *Xujiahui Commercial Center, Shanghai, China*. Customer project reference on glass free-form structure design. Accessed 2024. URL: <https://www.dlubal.com/en/downloads-and-information/references/customer-projects/001105>.
- [26] Glastory. *Curved Glass – An Obstacle or an Opportunity in Glass Architecture?* 2025. URL: <https://www.glastory.net/curved-glass-an-obstacle-or-an-opportunity-in-glass-architecture/>.
- [27] Glass Manufacturer. *Hot Bent Glass*. 2025. URL: <http://glass-manufacturer.com/11-1-hot-bent-glass.html>.
- [28] Gujarat Guardian Glass. *Curved Facades - Glass for Facades - Applications of Glass*. n.d.
- [29] VSOM Glass. *Hot Bending Glass vs. Tempered Curved Glass: What’s the Difference and Which One is Right for Your Project?* 2023.
- [30] CEN. *Eurocode 10 — Design of glass structures — Part 2: Out-of-plane loaded glass components*. prEN 19100-2:2023. 2023.
- [31] Mark Feijen, Ivo Vrouwe and Peter Thun. ‘Cold-bent single curved glass; opportunities and challenges in freeform facades’. In: *Challenging Glass 3* (2012).
- [32] Kyriaki Corinna Datsiou. ‘Design and performance of cold bent glass’. In: (2017).
- [33] Wikipedia contributors. *IAC Building*. https://en.wikipedia.org/wiki/IAC_Building. Accessed: 2025-05-26. 2024. URL: https://en.wikipedia.org/wiki/IAC_Building.
- [34] Wikipedia contributors. *Strasbourg-Ville station*. https://en.wikipedia.org/wiki/Strasbourg-Ville_station. Accessed: 2025-05-26. 2024. URL: https://en.wikipedia.org/wiki/Strasbourg-Ville_station.

- [35] Niels Ottosen and Hans Petersson. *Introduction to the Finite Element Method*. English. Pocket edition. Englewood Cliffs, NJ: Prentice Hall, 1992.
- [36] Dassault Systèmes. *Abaqus Unified FEA*. Accessed: 2024-03-01. 2023. URL: <https://www.3ds.com/products/simulia/abaqus>.
- [37] Dassault Systèmes. *Abaqus 2023 Documentation: Solid Element Library*. 2023.
- [38] ABAQUS Inc. *ABAQUS User's Manual Version 6.6*. Accessed on May 30, 2025. Dassault Systèmes. 2006. URL: <http://classes.engineering.wustl.edu/2009/spring/mase5513/abaqus/docs/v6.6/books/usi/default.htm?startat=pt04ch21s04s02.html>.
- [39] *User Subroutines Reference Guide — Abaqus Documentation, Version 6.6*. <https://classes.engineering.wustl.edu/2009/spring/mase5513/abaqus/docs/v6.6/books/usi/default.htm?startat=pt04ch21s04s02.html>. Accessed: 2025-05-30. 2009. URL: <https://classes.engineering.wustl.edu/2009/spring/mase5513/abaqus/docs/v6.6/books/usi/default.htm?startat=pt04ch21s04s02.html>.
- [40] Autodesk. *Fusion Help — Principal Stress Calculations*. 2025. URL: <https://help.autodesk.com/view/fusion360/ENU/?guid=SIM-PRINCIPAL-STRESS-EQ-CONCEPT>.
- [41] Thomas Richter. *Fluid-structure interactions: models, analysis and finite elements*. Vol. 118. Springer, 2017.
- [42] CM Wang, Junuthula Narasimha Reddy and KH Lee. *Shear deformable beams and plates: Relationships with classical solutions*. Elsevier, 2000.
- [43] Wikipedia contributors. *Kirchhoff–Love plate theory — Wikipedia, The Free Encyclopedia*. 2025. URL: https://en.wikipedia.org/wiki/Kirchhoff%E2%80%9393Love_plate_theory.
- [44] Rong Luo, Huijie Lv and Hanqi Liu. ‘Development of Prony series models based on continuous relaxation spectrums for relaxation moduli determined using creep tests’. In: *Construction and Building Materials* 168 (2018), pp. 758–770.
- [45] SW Park and RA0942 Schapery. ‘Methods of interconversion between linear viscoelastic material functions. Part I—A numerical method based on Prony series’. In: *International journal of solids and structures* 36.11 (1999), pp. 1653–1675.
- [46] Chen Tzikang. *Determining a Prony series for a viscoelastic material from time varying strain data*. Tech. rep. 2000.
- [47] Camilla Fors. ‘Mechanical properties of interlayers in laminated glass’. In: *Experimental and numerical evaluation (Thesis of Master of Science), Lund University, Sweden* (2014).
- [48] Laura Galuppi and Gianni Royer-Carfagni. ‘The effective thickness of laminated glass plates’. In: *Journal of Mechanics of Materials and Structures* 7.4 (2012), pp. 375–400.
- [49] Tomáš Hána, Miroslav Vokáč, Martina Eliášová, Zdeněk Sokol and Klára V Machalická. ‘Four-point bending tests of PVB double laminated glass panels—experiments and numerical analysis’. In: *Challenging Glass Conference Proceedings*. Vol. 7. 2020.

- [50] Wim Stevels and Pol D’Haene. ‘Determination and verification of PVB interlayer modulus properties’. In: (2020).
- [51] PA Hooper, BRK Blackman and JP Dear. ‘The mechanical behaviour of poly (vinyl butyral) at different strain magnitudes and strain rates’. In: *Journal of Materials Science* 47 (2012), pp. 3564–3576.
- [52] Laura Galuppi and Gianni Royer-Carfagni. ‘Cold-lamination-bending of glass: Sinusoidal is better than circular’. In: *Composites Part B: Engineering* 79 (2015), pp. 285–300.
- [53] Laura Galuppi and Gianni Royer-Carfagni. ‘Optimal cold bending of laminated glass’. In: *International Journal of Solids and Structures* 67 (2015), pp. 231–243.
- [54] StructX. *Plates - StructX*. Accessed: 2025-05-19. 2024. URL: <https://structx.com/plates.html>.

Appendix A

Enhanced effective thickness (EET)

MATLab code for calculating effective thickness of laminated glass:

```
G_int = 0.1e6;
Psi = 4.9217;
L = 3;
h1 = 5e-3;
h2 = 5e-3;
h_int = 1.52e-3;
d1 = (h1/2)+(h_int/2);
d2 = (h2/2)+(h_int/2);
v_glass = 0.23;
E_glass = 70e9;
D_abs = E_glass*(h1^3+h2^3)/(12*(1-v_glass^2));
D_full = D_abs+E_glass*(h1*d1^2+h2*d2^2)/(1-v_glass^2);
Eta_p2 = 1/(1+((h_int*E_glass)/
(G_int*(1-v_glass^2)))*(D_abs/D_full)*((h1*h2)/(h1+h2))*Psi);

%Effective Thickness for deflection calculation:
h_ef_w = (1/((Eta_p2/
(h1^3+h2^3+12*(h1*d1^2+h2*d2^2)))+(1-Eta_p2)/(h1^3+h2^3)))^(1/3));

%Effective Thickness for stress analysis:
h_ef_sig = (1/(((2*Eta_p2*d1)/
((h1^3+h2^3)+12*(h1*d1^2+h2*d2^2)))+(h1/h_ef_w^3)))^(1/2)

%-----%
Radius=15;
Euler_metod = (E_glass*h_ef_sig)/(2*Radius)
Kirchoff_metod = (E_glass*h_ef_sig)/(2*Radius*(1-v_glass^2))
```